Order Number 8805138

Investigation of the catalytic behavior and chemical nature of alkali promoted copper and copper-cobalt-chromium oxide catalysts for the conversion of synthesis gas to methanol and higher alcohols

Sheffer, Gordon R., Ph.D.

Iowa State University, 1987

U·M·I
300 N. Zeeb Rd.
Ann Arbor, MI 48106

PLEASE NOTE:

In all cases this material has been filmed in the best possible way from the available copy. Problems encountered with this document have been identified here with a check mark ✓.

1. Glossy photographs or pages ✓
2. Colored illustrations, paper or print _____
3. Photographs with dark background ✓
4. Illustrations are poor copy _____
5. Pages with black marks, not original copy _____
6. Print shows through as there is text on both sides of page _____
7. Indistinct, broken or small print on several pages _____
8. Print exceeds margin requirements _____
9. Tightly bound copy with print lost in spine _____
10. Computer printout pages with indistinct print _____
11. Page(s) _____ lacking when material received, and not available from school or author.
12. Page(s) _____ seem to be missing in numbering only as text follows.
13. Two pages numbered _____. Text follows.
14. Curling and wrinkled pages _____
15. Dissertation contains pages with print at a slant, filmed as received _____
16. Other _____

_____

_____

Investigation of the catalytic behavior and chemical nature of alkali promoted copper and copper-cobalt-chromium oxide catalysts for the conversion of synthesis gas to methanol and higher alcohols

by

Gordon R. Sheffer

A Dissertation Submitted to the
Graduate Faculty in Partial Fulfillment of the
Requirements for the Degree of
DOCTOR OF PHILOSOPHY

Major: Chemical Engineering

Approved:

Signature was redacted for privacy.
In Charge of Major Work

Signature was redacted for privacy.
For the Major Department

Signature was redacted for privacy.
For the Graduate College

Iowa State University
Ames, Iowa

1987

TABLE OF CONTENTS

	Page
DEDICATION	vi
SECTION I: EXPLANATION OF WORK COMPLETED FOR DISSERTATION	1
INTRODUCTION	2
Explanation of Dissertation Format	7
LITERATURE REVIEW	8
Thermodynamics	8
Higher Alcohol Catalysts	9
The IFP Catalyst	16
Other Investigations of the IFP Catalyst	22
RESEARCH OBJECTIVES	25
REVIEW OF PAPERS WRITTEN	28
GENERAL CONCLUSIONS	31
RECOMMENDATIONS FOR FUTURE WORK	34
REFERENCES	35
ACKNOWLEDGEMENTS	39
APPENDIX	40
Flory Product Distributions	40
REFERENCES	43
SECTION II: PARAMETRIC STUDY OF THE PREPARATION OF POTASSIUM PROMOTED COPPER-COBALT-CHROMIUM CATALYSTS FOR THE PRODUCTION OF HIGHER ALCOHOLS	44
ABSTRACT	45
INTRODUCTION	46

EXPERIMENTAL 48

RESULTS AND DISCUSSION 51

Effect of Choice of Metal Salts 51

Effect of Feed Gas Composition 55

Effect of Amount of Citric Acid Added 57

Effect of Potassium Loading 59

Effect of Calcination Temperature 62

SUMMARY 66

REFERENCES 68

ACKNOWLEDGEMENTS 70

SECTION III: INVESTIGATION OF THE CHEMICAL NATURE OF ALKALI PROMOTED COPPER-COBALT-CHROMIUM HIGHER ALCOHOL CATALYSTS AS A FUNCTION OF CALCINATION TEMPERATURE 71

ABSTRACT 72

INTRODUCTION 73

EXPERIMENTAL 76

RESULTS 79

X-ray Diffraction 79

X-ray Photoelectron Spectroscopy 86

Mono- and Bimetallic Catalysts 89

Reactor studies 89
X-ray diffraction 93

DISCUSSION 98

SUMMARY 107

REFERENCES 109

ACKNOWLEDGEMENTS 112

SECTION IV: INVESTIGATION OF THE PROMOTIONAL EFFECT OF POTASSIUM ON UNSUPPORTED COPPER CATALYSTS FOR METHANOL SYNTHESIS 113

ABSTRACT 114

INTRODUCTION 115

EXPERIMENTAL 117

RESULTS 122

Reactor Studies 122

X-ray Diffraction 125

X-ray Photoelectron Spectroscopy 127

Comparison of Alternate Preparations 130

DISCUSSION 138

SUMMARY 142

REFERENCES 143

ACKNOWLEDGEMENTS 144

SECTION V: DIFFERENCES IN THE PROMOTIONAL EFFECT OF THE GROUP 1A ELEMENTS ON UNSUPPORTED COPPER CATALYSTS FOR CARBON MONOXIDE HYDROGENATION 145

ABSTRACT 146

INTRODUCTION 147

EXPERIMENTAL 149

RESULTS 152

Catalytic Behavior of Copper-Alkali Catalyst 152

Characterization of Copper-Alkali Catalysts 155

Preparation and Characterization of LiCuO 160

DISCUSSION 164

SUMMARY 168

REFERENCES 170

ACKNOWLEDGEMENTS 172

DEDICATION

To my wife, Toni, my daughter, Kimberly, and my son, Gregory, for their love and the many personal sacrifices they have willingly made in helping me to realize this goal.

SECTION I: EXPLANATION OF WORK COMPLETED FOR DISSERTATION

INTRODUCTION

Currently 95% of the world's chemical production is based on petroleum and natural gas. However, these resources account for only 20% of the world's fossil fuel reserves. It is anticipated that by the end of this century oil and gas demand will exceed production capability and that reserves will be exhausted by the end of the next century (1). The development of other sources of carbon for the chemical industry is the challenge of the immediate decades.

Coal represents an alternative source of carbon for chemical feedstocks. Reserves are sufficient for several centuries. In particular the indirect liquefaction of coal may become a major source of liquid fuels and chemical intermediates. In this approach coal is first converted to synthesis gas, a mixture of carbon monoxide and hydrogen, which is subsequently catalytically converted to more valuable compounds.

Synthesis gas can be manufactured by the partial oxidation of coal:

$$2CH_x + O_2 \rightarrow 2CO + xH_2$$

Coal has relatively low amounts of hydrogen ($x \cong 0.8$) and a typical coal gasifier produces a synthesis gas composed of 30% H_2, 60% CO, and 10% CO_2. The hydrogen concentration can be increased through the water-gas shift reaction:

$$CO + H_2O \xrightarrow[\text{or}\ Cu/ZnO/Al_2O_3,\ 523\ K]{Fe_3O_4,\ 723\ K} CO_2 + H_2$$

Until coal becomes more economically attractive, synthesis gas may also be manufactured from natural gas or other hydrocarbons by a process called steam reforming:

$$C_nH_m + nH_2O \xrightarrow[1173\ K]{Ni/\alpha\text{-}Al_2O_3} nCO + (n + m/2)H_2$$

Since this reaction is in equilibrium with the water-gas shift reaction, high temperatures and excess water are required to favor the formation of CO and H_2. A typical steam reformer using natural gas as the feed produces a synthesis gas composed of 76% H_2, 16% CO, and 8% CO_2.

Currently only two commercial processes involving the direct conversion of synthesis gas have been realized. The first process synthesizes methanol using copper-zinc-alumina oxide catalysts operating at 523-573 K and 5-10 MPa. All of the methanol produced in the world today is manufactured in this way. The majority of the synthesis gas used for this process comes from steam reforming of natural gas. The second industrial process is the production of liquid hydrocarbon fuels and a small amount of oxygenated chemicals via the Fischer-Tropsch synthesis. Iron catalysts are used at typical operating conditions of 548-598 K and 2-3 MPa. The hydrocarbon distribution is quite broad ranging from methane to waxes. South Africa is the only country currently utilizing this technology. Coal gasification is the most economical method of synthesis gas manufacture in South Africa because of a natural abundance of coal deposits and absence of petroleum reserves.

A recently invented process which may be economically attractive is the conversion of synthesis gas to normal alcohols. This process is

similar to the Fischer-Tropsch synthesis outlined above except that instead of producing linear hydrocarbons in a broad molecular weight distribution, linear alcohols are produced. A mixture of the C_1 to C_8 normal alcohols may be commercially exploited in two ways. First, without separation, the alcohols could be used as fuel extenders. A blend of normal alcohols with gasoline results in several advantages as compared to methanol or ethanol alone (2). These are:

1. decreased volatility
2. improved hydrocarbon solubility
3. improved water tolerance
4. higher volumetric heats of combustion
5. improved drivability.

Second, with separation the chemical value of the alcohols as solvents, additives, and intermediates may be exploited. The current methods of production (3, 4), uses (3, 4), and prices (5) of the C_3 to C_8 normal alcohols are presented in Table 1.

The work presented in this thesis has examined the conversion of synthesis gas to higher alcohols using alkali promoted copper-cobalt-chromium oxide catalysts. The goals of this work have been to elucidate the structure of the active catalyst and to correlate the chemical nature of the catalyst with the yield of higher alcohols. An initial understanding of the component synergism operating in this complex, multicomponent oxide catalyst has been gained.

The remainder of this section is designed to provide the reader with a fundamental understanding of the work completed for this dissertation.

Table 1. Production, uses, and cost of C_3 to C_8 linear alcohols

Compound	Commercial method of production
1-propanol	o Coproduct of propane and butane oxidation o Byproduct of high pressure methanol synthesis
1-butanol	o Weizmann (fermentation) process o Acetaldehyde via aldol condensation o Byproduct propane and butane oxidation
1-pentanol	o Fractionation of the product from treatment of chlorinated pentanes with NaOH
1-hexanol	o Byproduct in synthesis of n-butyraldehyde from acetaldehyde
1-heptanol	o Not produced commercially in any quantity
1-octanol	o Byproduct in the hydrogenation of coconut oil fatty acids in production of 1-dodecanol

[a]In 1987 dollars.

[b]Mixed isomers.

[c]Not available.

Uses	Bulk basis cost ($/lb)[a]
o Various uses as solvent o Chemical intermediate for n-propyl acetate, propanol and n-propylated ureas o Various uses in perfume, food, and plastic industries	.45
o Nitrocellulose lacquers o Extractant in production of organic chemicals o Chemical intermediate	.35
o Amylacetate production o Pharmaceuticals o Solvent for gums and dyes	.48[b]
o Pharmaceuticals, perfumes o Solvent gums and dyes	.50
o Perfumes, cosmetics o Solvent for plasticizers o Chemical intermediates	--[c]
o Production of polyacrylic esters o Used in hydraulic systems to increase viscosity of mineral oils	.70

Subsequent divisions explore the reasons for selecting the alkali promoted copper-cobalt-chromium catalyst system, state the objectives of the thesis research, and summarize the work completed. Finally the general conclusions resulting from this work and suggestions for the direction of future research in this area are outlined.

Explanation of Dissertation Format

The four remaining sections found in this dissertation are written in a form suitable for publication in a technical journal. The research reported in the four sections represents original work conducted by the author.

LITERATURE REVIEW

Thermodynamics

Anderson has examined the thermodynamics of carbon monoxide hydrogenation in detail (6). At all temperatures, normal paraffins had lower free energies of formation than normal alcohols. Above 473 K, methane was the only organic compound thermodynamically preferred over free carbon produced through carbon monoxide disproportionation. It was concluded that the synthesis of normal alcohols by carbon monoxide hydrogenation required the use of highly selective catalysts.

Anderson also evaluated the equilibrium constants for reactions of synthesis gas to normal alcohols at typical Fischer-Tropsch reaction conditions (473-573 K, 1-3 MPa). All the normal alcohols, except methanol, had large equilibrium constants indicating that high conversions of synthesis gas to normal alcohols are thermodynamically possible.

In synthesis gas reactions, excess oxygen resulting from alkyl chain formation may be removed as either carbon dioxide, requiring carbon monoxide consumption, or as water, requiring hydrogen consumption. For a process using synthesis gas manufactured by steam reforming oxygen removal as water is economically favored because of the inherently large hydrogen to carbon monoxide ratio, while for coal gasifier produced synthesis gas oxygen removal as carbon dioxide is favored. As demonstrated with the following reactions, carbon dioxide is the thermodynamically preferred byproduct:

$$2CO + 4H_2 \rightarrow C_2H_5OH + H_2O \quad \Delta G^\circ_{523K} = -7.1 \text{ kcal/mol}$$

$$3CO + 3H_2 \rightarrow C_2H_5OH + CO_2 \quad \Delta G^\circ_{523K} = -11.8 \text{ kcal/mol}$$

This is a result of the negative free energy change associated with the water gas shift-reaction:

$$CO + H_2O \rightarrow CO_2 + H_2 \quad \Delta G^\circ_{523K} = -4.7 \text{ kcal/mol}$$

Higher Alcohol Catalysts

Alkali promoted methanol catalysts and catalysts based on iron, molybdenum, rhodium, and cobalt have all had varying degrees of success for the conversion of synthesis gas to higher alcohols. These are summarized in Table 2. In general higher alcohol catalysts contain two or more transition metals and an alkali promoter.

Historically two approaches toward higher alcohol catalyst development were taken. One approach was the modification of iron Fischer-Tropsch catalysts. In the early 1920s Fischer (7) developed the "Synthol" process in which an alkalinized iron oxide catalyst was exposed to synthesis gas at 673-723 K and 10-15 MPa. The product was a mixture of hydrocarbons, alcohols, aldehydes, ketones, and acids. The selectivity to oxygenates was poor (<10 wt %). Anderson (8, 9) and Shultz et al. (10) found that the selectivity of alkanized iron catalysts to higher alcohols could be improved if the catalysts were prenitrided through ammonia decomposition. Operating at 2 MPa and 503 K with catalysts composed of N/Fe molar ratios greater than 0.25, a product consisting of 20-25 wt % alcohols was formed. The higher alcohols were predominantly

Table 2. Literature survey of higher alcohol catalysts

Catalyst	Reference	T (K)	P (MPa)
Nitrided iron	10	503	2
$CuO/ZnO/K_2CO_3/Al_2O_3$	12	558	13
$Rh/Fe/SiO_2$	15	573	7
MoS_2/K_2CO_3	20	533	10
Mo/Ir or $Ru/Na_2O/Al_2O_3$	25, 28	528	9
$Ni/Cu/Na_2O/TiO_2$	29	573	6
$Co/Mo/K_2O/SiO_2$	34	523	5
Co/Cu/Cr/K	38	523	6

[a]Normalized with respect to total alcohols.

[b]Excluding H_2O and CO_2; remainder is hydrocarbons.

H_2/CO feed ratio	wt %[b] alcohols	Alcohol distribution[a] (wt %) C_1	C_2	C_3	C_4	C_{5+}	alcohol yield
1	24	1	36	16	12	35	0.02 g/g Fe/hr
0.5	100	64	4	6	15	11	0.6 g/g cat/hr
1	79	51	49	--	--	--	0.6 g/g cat/hr
1	90	52	32	12	3	1	0.1-0.3 g/g cat/hr
2	58	52	27	14	6	2	0.2 g/ml cat/hr
2	65	51	29	12	5	3	0.1 g/ml cat/hr
1	56	26	48	25	7	4	0.1 g/g cat/hr
3	97	24	39	22	14	--	0.1-0.3 g/g cat/hr

normal. It was determined that the 20-25 wt % alcohol selectivity levels could be attained only if ξ-Fe_2N was present after ammonia decomposition. Upon synthesis gas exposure a portion of the nitrogen in ξ-Fe_2N was replaced by carbon to form an iron carbonitride phase.

A second approach to higher alcohol catalyst development was the modification, primarily with alkali promoters, of methanol catalysts. Early work was concerned primarly with modification of zinc or zinc-chromium oxide catalysts, the original methanol catalysts which operated at high pressure (20-40 MPa) and high temperature (673-723 K). This work has been reviewed by Natta et al. (11), who concluded from these early investigations that:

1. The synthesis of higher alcohols was always related to the presence of strongly basic substances.
2. Among the higher alcohols produced, a relatively high proportion of isobutanol was formed.
3. Unlike modified Fischer-Tropsch catalysts, hydrocarbons were not observed in the product.

Only recently has alkali promotion of low pressure (5-15 MPa) and low temperature (548-598 K) copper-zinc oxide methanol catalysts been studied. Smith and Anderson (12) have obtained higher alcohol selectivities of up to 39 wt % using a commercial copper-zinc-aluminum oxide methanol catalyst promoted with 0.5 wt % potassium carbonate. Unlike modified Fischer-Tropsch catalysts the higher alochols formed are predominantly nonlinear with a high proportion of isobutanol. These researchers found that the selectivity to isobutanol was strongly dependent upon promoter

concentration, reaction temperature, and the H_2/CO ratio of the feed. Decreasing the H_2/CO feed ratio from 2 to 0.5 more than doubled the isobutanol selectivity. Increasing the reaction temperature from 533 K to 558 K increased the higher alcohol selectivity from 4 to 26 wt %. Above 573 K the catalyst steadily deactivated with time on stream. Investigating the differences in promotional effect of the Group IA elements, Vedage et al. (13) have found that the selectivity to higher alcohols increases in order Li < Na < K < Rb < Cs, which is the order of increasing basicity. Klier (14) has proposed that for alkali promoted methanol catalysts higher alcohols are formed by aldol condensation of aldehydic or enolic surface intermediates.

The most widely studied catalysts for synthesis gas conversion to oxygenated chemicals have been those based on rhodium. A typical formulation is rhodium and another metal on a support. The product consists almost exclusively of one and two carbon compounds. Bhasin et al. (15) have found that the addition of iron to rhodium resulted in ethanol as the primary C_2 product and methanol as the major product. However, the addition of manganese to rhodium resulted in the formation of acetaldehyde and acetic acid. In studies of rhodium on different metal oxide supports, Ichikawa (16, 17) noted the following differences in reactivity:

1. BeO, MgO and CaO promoted formation of methanol.
2. TiO_2, ZrO_2, La_2O_3, CeO_2, and ThO_2 promoted formation of ethanol.
3. Al_2O_3, SiO_2, SnO_4, V_2O_5, and WO_3 promoted formation of hydrocarbons.

Somorjai and Watson (18, 19) proposed that the ability of rhodium to

successfully synthesize C_2 oxygenated compounds was related to a synergistic effect between partially oxidized and fully reduced rhodium species. This synergistic effect was hypothesized to result from reduced metal sites dissociating carbon monoxide to form CH_x intermediates which migrated to oxidized rhodium sites where insertion of molecularly adsorbed carbon monoxide occurred, followed by hydrogenation to C_2 oxygenates.

Higher alcohol catalysts based on molybdenum have only recently appeared in the literature. Workers at Dow Chemical (20) have patented alkali promoted molybdenum sulfide catalysts. The selectivity to alcohols, primarily normal, was reported to be greater than 90 wt %. The product distribution obeyed Flory theory (see Appendix) with a chain propagation constant, α, of 0.3. One important advantage of the Dow catalyst over other higher alcohol catalysts is that it is not poisoned by hydrogen sulfide. Nonsulfided molybdenum catalysts have also been studied. Alkali promoted molybdenum oxide catalysts alone (21, 22) or with further promotion using nickel (23), iridium (24, 25), and ruthenium (26-28) have been reported to yield alcohol selectivities approaching 60 wt %. Despite the large number of molybdenum catalysts tested, very little characterization work has been reported.

Studies of the modification of cobalt, another Fischer-Tropsch metal for higher alcohol synthesis have also appeared in the literature. Without modification, synthesis gas conversion over cobalt catalysts results in normal hydrocarbons and no oxygenates (30-32). The product distribution obeys Flory theory with a chain growth probability factor of

0.7 to 0.8. At 473 K and 0.3 MPa with a synthesis gas of $H_2/CO = 1$, a typical cobalt Fischer-Tropsch catalyst has a production yield of .03 g product/g cat/hr (31). The earliest work with higher alcohol catalysts based on cobalt was performed by Taylor (33) using a Co/Cu/Mn catalyst prepared from CoS, CuO, and MnO. At 673 K and 20 MPa, an alcohol selectivity, primarily to normal alcohols, of 50 wt % was obtained. The alcohol distribution obeyed Flory theory with $\alpha = 0.27$. More recently Fujimoto and Oba (34) have examined silica supported cobalt catalysts promoted with molybdenum and potassium. At 523 K and 5 MPa synthesis gas was converted to a product consisting of 56 mol % normal alcohols and 44 mol % hydrocarbons at a rate of 0.1 g alcohol/g cat/hr. Both the alcohol and the hydrocarbon distribution obeyed Flory theory with chain growth probability factors of 0.36 and 0.46, respectively. Other modified cobalt catalysts investigated include cobalt promoted with iridium (35) and rhenium (36, 37). In both of these cases the oxygenate selectivity was less than 60 wt %. Interestingly, however, the oxygenate product was composed primarily of one and two carbon compounds, reminiscent of the rhodium catalysts previously discussed.

It is surprising that, considering the large number of higher alcohol catalysts reported, there have been few studies attempting to correlate the chemical nature of these catalysts with higher alcohol productivity. As a result the character of the active site(s) necessary for higher alcohol synthesis is little understood. However, further improvement of current higher alcohol catalysts may depend upon discerning active site(s) requirements.

The IFP Catalyst

The most promising of the higher alcohol catalysts yet to be reported in the literature is an alkali promoted cobalt-copper-chromium oxide catalyst patented by the Institut Francais du Petrole (IFP) (38). The catalyst is claimed to have a selectivity to higher alcohols, primarily normal, of greater than 97 wt %. The IFP higher alcohols process is designed for the production of higher alcohol mixtures for motor fuel enhancement (39-42). Of the higher alcohol synthesis catalysts reported, the IFP catalyst is the only catalyst which has been successfully tested in a demonstration (7000 bbl/yr) plant (43, 44).

The first IFP patent describes a catalyst comprised of at least four essential elements: copper, cobalt, a third metal, M, selected from Cr, Fe, V, and Mn, and an alkali, A. Zinc is an optional component. For a general formulation of $Cu_xCo_yM_zA_v$, the preferred atomic proportions are:

$$1.0 > x > 0.1$$

$$1.0 > y > 0.1$$

$$1.0 > z > 0.2$$

$$v = 0.001 \text{ to } 0.25 \text{ times the sum } (x+y+z)$$

The recommended method of catalyst manufacture involves the addition of an organic polyacid (citric, tartaric, etc.) to an aqueous solution of the metal salts. Upon evaporation of the water, the catalyst precursor powder obtained is calcined at 673 to 1273 K. The alkali element is incorporated by impregnation of the catalyst precursor powder by addition to the initial metal salt solution. Catalyst activation is not detailed.

From the data reported in the patent, the most selective catalyst is one with molar composition $CoCuCr_{.8}K_{.09}$ which has a selectivity to alcohols of 97 wt %. The catalyst precursor was prepared by evaporation of an aqueous solution containing $Cu(NO_3)_2 \cdot 3H_2O$, $2CoCO_3 \cdot 3Co(OH)_2 \cdot 4H_2O$, CrO_3, and citric acid. One quarter of a gram equivalents of citric acid per gram equivalent of metal ions were added to the solution. Potassium was incorporated by impregnation of the catalyst precursor with a potassium hydroxide solution. Details of catalyst calcination and activation were not provided. Using a feed gas of molar composition 66% H_2, 19% CO, and 13% CO_2, the production yield of alcohols, primarily normal, was found to be 0.3 g alcohols/g catalyst/hr at 523 K and 6 MPa. At comparable reaction conditions, a conventional methanol catalyst would yield 1.5 g methanol/g catalyst/hr (45), while a conventional supported cobalt Fischer-Tropsch catalyst would have a production yield of 0.9 g hydrocarbons/g catalyst/hr (32). If one examines the alcohol distribution reported for this catalyst, adherence to Flory theory with a chain growth probability factor, α, of 0.4 is found. Doubling the pressure increased α to 0.48 and doubled the alcohol yield.

The patent data also indicate that substitution of chromium by vanadium or manganese decreased the alcohol selectivity only slightly, but substitution by iron decreased the selectivity to 82 wt %. Inclusion of zinc at a molar ratio of 0.3 decreased alcohol selectivity to 84 wt %. Two later IFP patents (46, 47) allow for the incorporation of 0.5 to 40 wt % of a rare earth metal and smaller amounts of a Group VIII noble metal to the formulation already outlined. These metals increased the production yield by 25% while leaving the selectivity unchanged.

Workers at IFP have published the results of one study probing the chemical nature of their catalyst and further detailing catalyst preparation and activation procedures (48). Two catalyst preparation methods were presented. The first is the citrate complexation method outlined in the patent. In the article this method was modified slightly in that all metal nitrates and a vacuum evaporation were used. Glassy, amorphous intermediates which had a tendency for uncontrolled decomposition were reported to be produced after evaporation and drying. After calcination in air at temperatures above 623 K, catalysts with surface areas of 15-40 m^2/g were obtained. The second preparation method outlined was a metal carbonate coprecipitation from an aqueous solution of the metal nitrates using an alkali metal carbonate solution. The precipitate was washed, dried, calcined, and impregnated with alkali. No citric acid was added in this preparation.

A catalyst activation procedure consisting of exposing calcined catalysts to diluted hydrogen (P_{H_2} <.1 MPa) at 433-573 K was reported. According to the authors, a catalyst prepared and activated using the above methods will have a production yield of 0.08-0.2 g alcohols/g catalyst/hr at 523-583 K and 6 MPa with a H_2/CO molar feed ratio of 2. Without alkali promotion catalysts were found to induce uncontrollable methanation upon synthesis gas exposure. The authors speculated that the alkali cations suppress surface acidity thus preventing alcohol dehydration.

The article next elaborated the reactivity and chemical nature of a copper-cobalt-aluminum-zinc oxide catalyst prepared by carbonate precipitation and impregnation with sodium. This catalyst had a molar

selectivity to alcohols of 70% and a production yield of 0.15 g alcohol/g catalyst/hr at 563 K and 6 MPa using a synthesis gas with a H_2/CO molar ratio of 2. During the first few hours on stream, the alcohol selectivity was observed to increase from 55 to 70 mol %. The catalyst productivity increased from 0.03 to 0.10 g alcohol/g catalyst/hr over this period. Examination of the product composition reported for the catalyst reveals that the alcohol distribution is loosely described by the Flory equation with a 0.4 chain growth probability factor. The alcohol selectivity declined dramatically at reaction temperatures above 673 K and only methane was produced above 723 K.

X-ray diffraction (XRD) of the calcined catalyst revealed two phases, copper(II) oxide and a mixed metal oxide with a spinel structure. A spinel structure is a cubic close packed lattice of oxygen in which 1/8 of the tetrahedral holes are filled by a divalent cation and 1/2 of the octahedral holes are filled by a trivalent cation. Cation ordering produces alternating octants of AO_4 tetrahedra and B_4O_4 cubes. The resulting stoichiometry is AB_2O_4 where A is the divalent cation and B is the trivalent cation. Scanning transmission electron microscopy with X-ray emission microanalysis (STEM/XEM) indicated that the spinel phase was homogeneous. Using temperature programmed reduction (TPR) measurements, the authors deduced that during catalyst activation oxidized copper species were fully reduced to copper metal, while oxidized cobalt species were only partially reduced to metallic cobalt. STEM/XEM of steady-state catalysts revealed three items:

1. The spinel phase was depleted in cobalt and highly divided (1-3 nm) Co-Cu clusters were formed.
2. Carbon filaments containing Cu and Co were present.
3. Large crystallites (up to 0.5 μm) of Co_2C were found.

The authors also examined the influence of elemental composition on synthesis gas conversion for the $CuO/CoO/Cr_2O_3$ system. Their results are shown in Figure 1. Catalysts were prepared using the coprecipitation method. The degree of alkali promotion for these catalysts was not noted. Copper rich catalysts were found to produce primarily methanol with the activity going through a maximum for a Cu/Co molar ratio of 5 and a Cu/Cr molar ratio of 3. The methanol yield for the Cu/Co catalyst was 0.5 g methanol/g catalyst/hr. Chromium rich compositions were also reported to be selective to methanol but with low activity (<0.1 g/g cat/hr). Hydrocarbons were produced by cobalt rich catalysts, the predominate product being methane. The authors speculated that the component synergism responsible for higher alcohol formation in the Cu/Co/Cr system was a result of interaction between metallic cobalt, a Fischer-Tropsch catalyst, and copper(I) chromite, a methanol catalyst (49, 50). The mechanism of higher alcohol formation would involve the reaction of alkyl chains produced on metallic cobalt sites with undissociated carbon monoxide adsorbed on cuprous ion sites and subsequent higher alcohol desorption. This mechanism is similar to the mechanism proposed by Somorjai for C_2 oxygenate formation on rhodium catalysts. It is important to note that the conflict between TPR results which indicated complete reduction of oxidized copper species to copper metal and the

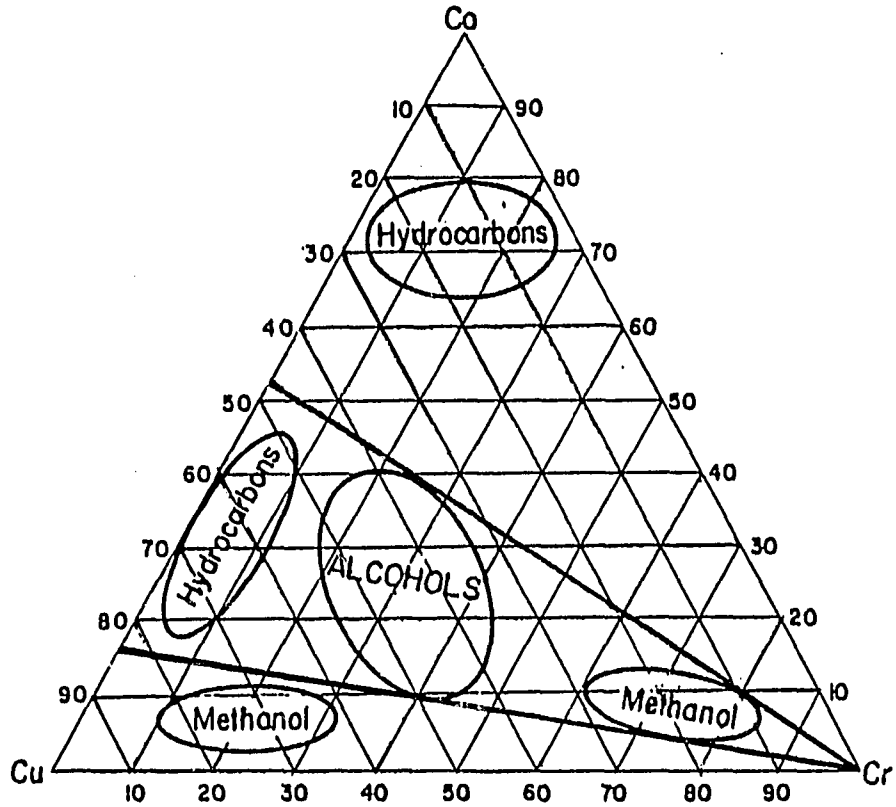

Figure 1. Selectivity as a function of composition in the ternary system CuO-CoO-Cr_2O_3 (from ref. 17).

speculated picture of component synergism involving copper(I) chromite was not addressed in the article.

Other Investigations of the IFP Catalyst

Chem Systems (51) was the first to report investigating the IFP catalyst formulation. A catalyst of molar composition $CuCoCr_{.8}K_{.09}$, prepared according to the IFP patent, resulted in a selectivity to alcohols of only 15 mol % with a production yield of 0.02 g alcohols/g catalyst/hr. The reaction conditions were identical to those used in the IFP patent, i.e., 6 MPa and 523 K with a feed gas of molar composition 66% H_2, 19% CO, and 13% CO_2. When the feed gas composition was changed to 65% H_2, 32% CO, and 3% CO_2, the alcohol selectivity increased to 29 mol % with no significant change in the alcohol yield. A chain growth probability factor of 0.42 was reported for the total product (hydrocarbons and alcohols combined). Incorporation of zinc into the catalyst formulation promoted the formation of aldehydes at the expense of alcohol production. A $CuCoCrZn_{.125}K_{.11}$ catalyst resulted in selectivities of 17 mol % to alcohols and 8 mol % to aldehydes with a total oxygenate yield of 0.014 g oxygenates/g catalyst/hr. Substituting other transition metals for chromium, Chem Systems found that the selectivity to oxygenates decreased in order:

$$Cr \geq Fe > V >> Mn$$

Of the numerous catalysts prepared and tested by Chem Systems, none achieved greater than 30 mol % selectivity to alcohols. In no case was the chemical nature of the catalysts investigated.

Hino et al. (52) have also examined a catalyst prepared according to the IFP patent. X-ray diffraction of calcined catalysts indicated two phases, CuO and a spinel mixed metal oxide. Using STEM/XEM the researchers found that the spinel phase was homogeneous and proposed a general formulation for the spinel of:

$$[Cu(II)_xCo(II)_{1-x}][Co(III)_{.5(x+1)}Cr(III)_{.5(3-x)}]O_4$$

where x varies between 0 and 0.9. TPR data were interpreted as indicating the reduction of Cu^{+2} to Cu^{o} and Co^{+3} to Co^{+2} with no change in Cr^{+3}. Reaction studies at 523 K and 0.1 MPa using an equimolar H_2/CO synthesis gas resulted in an alcohol selectivity of only 0.8 mol % for a $CuCoCr_{.8}K_{.09}$ catalyst. Increasing the pressure to 1 MPa increased the alcohol selectivity to 8.0 mol % with an alcohol yield of 0.002 g alcohol/g catalyst/hr. Hino et al. speculated, as did IFP workers, that component synergism in the Cu/Co/Cr system is a result of interaction between metallic cobalt sites and sites containing cuprous ions. Again, this speculation is in conflict with TPR results.

Experiments have been performed in which copper-zinc oxide methanol catalysts were impregnated with small amounts of iron (53) or cobalt (54, 55). These experiments were unsuccessful in that higher alcohols were not selectively produced. The maximum higher alcohol selectivity reported was 20 mol % for 1 wt % cobalt on copper-zinc-aluminum oxide catalyst. At this metal loading, the methanol activity was a factor of 50 less than the unpromoted methanol catalyst with a total production yield of 0.05 g product/g catalyst/hr at 543 K and 6.5 MPa. For the iron

catalyst, both the hydrocarbons and alcohols produced were reported to follow a Flory distribution with an α of .32 for the alcohols and 0.55 for the hydrocarbons. By observing the effects of isopropylamine addition to the synthesis gas, it was concluded that the alcohols were produced as a primary product and not through secondary reactions.

From the information reported in the above studies, three items are evident. First, other than IFP itself, no laboratory has been able to come close to the alcohol selectivity reported by IFP. Second, for the calcined catalyst, two phases appear to be present, CuO and a spinel structure of uncertain composition. Third, no correlations have been attempted between alcohol selectivity and the chemical nature of the catalyst. Many questions remain concerning the chemical nature of the activated catalyst. Is it primarily a reduced metal alloy, metal oxides, metal carbides, or some combination of the above? Is it a mixture of distinct, multifunctional phases or is it microscopically homogeneous?

RESEARCH OBJECTIVES

The general objective of the work completed for this dissertation was to identify the active phase(s) for the synthesis of normal alcohols by carbon monoxide hydrogenation in the copper-cobalt-chromium oxide catalyst system. There were three reasons for deciding to study the IFP higher alcohol catalyst in particular. First, the IFP catalyst has the greatest selectivity to higher normal alcohols of any catalyst yet reported. In addition, as evidenced by the demonstration plant studies, it is the only higher alcohol catalyst ready for commercial utilization. Second, the IFP catalyst behaves as a Fischer-Tropsch catalyst which is selective to alcohols. The alcohol production yield is comparable to hydrocarbon yields from cobalt Fischer-Tropsch catalysts. Also like cobalt Fischer-Tropsch catalysts, the products are exclusively normal and are distributed in accordance to Flory theory. This contrasts with alkali promoted copper-zinc oxide methanol catalysts where a non-Flory distribution of higher alcohols enriched in branched (especially isobutanol) alcohols is observed, and rhodium catalysts where only C_1 and C_2 compounds are produced. Third, the IFP catalyst affords the opportunity to examine a multicomponent catalyst with complex component synergism. The individual components are not selective for oxygenate formation. Cobalt oxide produces only hydrocarbons, while copper oxide and chromium oxide are inactive for carbon monoxide hydrogenation.

The specific objectives of the research completed for this dissertation were:

1. to identify the chemical nature of the copper-cobalt-chromium catalyst system both before and after activation.
2. to correlate the chemical nature of the catalyst with higher alcohol selectivity.
3. to understand the component interactions occurring in the catalyst and the component synergism responsible for higher alcohol synthesis.

To achieve these objectives, the following approach was implemented. First, the effect of catalyst preparation methods and reaction conditions on the catalytic behavior of the IFP catalyst were studied. The goal of this initial work was to identify a preparation or reaction condition parameter which resulted in a large variation in higher alcohol selectivity. This parameter was to provide the basis for a systematic study correlating the chemical nature of the catalyst with higher alcohol selectivity. A high pressure micro-reactor system with on-line analytical capability was designed and constructed for catalyst activity/selectivity evaluations. The reactor is detailed in Section IV. This initial work resulted in the highest alcohol selectivities for the copper-cobalt-chromium oxide catalyst yet to be found outside of IFP. Calcination temperature was identified as an important variable in determining the higher alcohol selectivity of the catalyst system. In the second phase of the project, the chemical nature of the copper-cobalt-chromium oxide catalyst was evaluated as a function of calcination temperature. X-ray diffraction and X-ray photoelectron spectroscopy were the primary analytical techniques employed. Because the activated catalysts were

sensitive to oxygen exposure, a controlled atmosphere X-ray diffraction cell was designed and constructed (see Section V). The result of the characterization work was that the higher alcohol selectivity of the IFP catalyst was correlated with the dispersion of copper metal in the catalyst. To further elucidate the nature of the component synergism operating in the IFP catalyst system, the mono- and bimetallic oxide catalysts were examined. One surprising result of this work was the observation that copper metal, which was inactive for carbon monoxide hydrogenation, was an active methanol catalyst when alkali promoted. Further characterization work was performed on the alkali promoted copper system to determine if the interaction of potassium with copper played a role in the copper-cobalt-chromium catalyst.

REVIEW OF PAPERS WRITTEN

The work completed for this dissertation has resulted in the preparation of four papers for publication. Sections II to V contain these papers. The remainder of this section outlines the contents of the papers.

In Section II, the effects of a variety of preparation parameters on the catalytic activity and selectivity for synthesis gas conversion to higher alcohols of potassium promoted copper-cobalt-chromium oxide catalysts have been investigated. Specifically, the effects of 1) metal salts used as precursors, 2) amount of citric acid used as a "complexant", 3) amount of potassium promoter, and 4) variation in catalyst calcination temperature were studied. Alcohol selectivities as great as 70 wt % with a production yield of 0.12 g/g cat/hr were obtained. C_2^+ alcohols accounted for 50 to 60 wt % of the alcohols produced. It was found that special attention must be paid to calcination temperature and, to a lesser extent, the other parameters mentioned.

In Section III, the chemical nature of alkali promoted copper-cobalt-chromium higher alcohol catalysts was evaluated as a function of calcination temperature using X-ray diffraction and X-ray photoelectron spectroscopy. The activated catalyst was comprised of copper metal and a cobalt-chromium spinel. Oxygenate production correlated with the dispersion of copper metal in the catalyst. Poorer copper dispersion and a decrease in oxygenate formation were observed with increasing calcination temperature. There was no evidence of cuprous ions or cobalt metal in the activated catalyst and it is therefore unlikely that the component

synergism responsible for higher alcohol formation is a result of alkyl chain growth on cobalt metal sites coupled with alcohol termination by CO molecularly adsorbed on cuprous ion sites.

In Section IV, it was determined that while copper metal is inactive for carbon monoxide hydrogenation, the selective synthesis (>93 wt %) of methanol with high activity occurs when unsupported copper catalysts are alkali promoted. Using X-ray photoelectron spectroscopy, it was found that under reaction conditions copper exists as a mixture of Cu^+ and Cu^o species. The initiation of catalytic activity correlated with the stabilization of the Cu^+ species. The chemical state of potassium under reaction conditions was elucidated to be potassium carbonate, the thermodynamically preferred phase. It was observed that the potassium must be well dispersed on the surface in order for the promotional effect to be imparted. The role of potassium was concluded to be the stabilization of Cu^+ species, active centers for methanol synthesis.

In Section V, the differences in promotional effect of the Group IA elements on unsupported copper catalysts for carbon monoxide hydrogenation were examined. Methanol was selectively produced on all catalysts at 523 K, 5 MPa, and with feed gas of molar composition $H_2/CO = 2$. The methanol synthesis rate increased by an order of magnitude from Li to Cs with the majority of the increase occurring from Na to K. On the basis of results from apparent activation energy measurements, X-ray photoelectron spectroscopy, and scanning electron microscopy, activity differences were attributed to differences in the concentration of Cu^+ species at the surface and not electronic effects. The alkali-cuprate

LiCuO was found not to be the active phase responsible for Cu^+ stabilization. Under conditions more favorable for higher alcohol synthesis, 573 K and $H_2/CO = 1$, little change in product selectivity was observed for the Na, K, Rb, and Cs promoted catalysts. However, the lithium promoted catalyst produced an equimolar mixture of normal alcohols and hydrocarbons. Both product distributions were found to give linear Flory plots with $\alpha = .3$ for alcohols and $\alpha = .5$ for hydrocarbons.

GENERAL CONCLUSIONS

The general conclusions resulting from the work completed for this dissertation are as follows:

1. Potassium promoted copper-cobalt-chromium oxide catalysts are selective for higher alcohol formation. Alcohol selectivities as great as 70 wt % with an alcohol yield of 0.12 g/g cat/hr were obtained.
2. The choice of metal salts used for catalyst preparation can have a marked influence on catalytic behavior. Salts with poor water solubility produce inhomogeneous catalyst precursors. Metal nitrates produced unstable catalyst precursors. The best combination of metal salts studied was $Co(ac)_2$, $Cu(NO_3)_2$, CrO_3, and KOH.
3. Citric acid and potassium addition steps in catalyst preparation are both beneficial in that they suppress methanation during start-up.
4. Increasing the calcination temperature used for catalyst preparation decreases both catalytic activity and selectivity to oxygenates. However, the hydrocarbon yield remains relatively constant.
5. The calcined catalyst is comprised of CuO and a spinel of composition $Co_{1.64}Cr_{1.36}O_4$.
6. Upon catalyst activation, CuO is reduced completely to Cu metal and the spinel is partially reduced to $Co_{1.34}Cr_{1.66}O_4$.

7. The oxygenate synthesis rate correlates well with the dispersion of copper metal in the catalyst. Poorer copper dispersion and decreased oxygenate yields are observed with increasing catalyst calcination temperature.
8. The chemical nature of the active catalyst is copper metal supported on a cobalt-chromium spinel. Impregnation of a $Co_{1.5}Cr_{1.5}O_4$ spinel with a copper salt resulted in higher alcohol production although the cobalt-chromium spinel alone produced only hydrocarbons. In addition, the catalytic activity increased indicating that copper plays an active role in oxygenate synthesis.
9. Alkali promoted unsupported copper metal (APUCM) catalysts are selective (>93 wt %) and active (8.3×10^{-5} $kg/m^2/hr$) methanol catalysts.
10. The rate of methanol synthesis on APUCM catalysts increases by an order of magnitude from Li to Cs with the majority of the increase occurring from Na to K.
11. The role of alkalis in APUCM catalysts is to stabilize the formation of Cu^+ species, known to be the active state of copper for methanol synthesis.
12. The chemical state of alkali in APUCM catalysis is in carbonate form, which is the thermodynamically preferred phase.
13. The alkali-cuprates, e.g., LiCuO, are not the active phase for methanol synthesis. These compounds decompose upon synthesis gas exposure to copper metal and alkali carbonate.

14. Unsupported copper may be further modified by alkali promotion to produce higher normal alcohols, as was found to be the case for lithium. Interestingly under reaction conditions normally employed for higher alcohol synthesis, none of the APUCM catalysts caused the formation of isobutanol.

RECOMMENDATIONS FOR FUTURE WORK

There appear to many avenues open for continued research in more fully understanding the copper-cobalt-chromium higher alcohol synthesis catalyst. In addition, the alkali promoted unsupported copper catalysts underscores the fact that there is still much to be learned concerning the role of alkalis in catalysis. I recommend the following experiments as the starting point for continued studies:

1. The preparation and characterization of $CoCr_2O_4$ spinel. This compound should not reduce and therefore will remove any ambiguity concerning the state of cobalt introduced by the partial reduction of $Co_{1.5}Cr_{1.5}O_4$ spinel. Impregnation of $CoCr_2O_4$ spinel with copper should again yield a higher alcohol synthesis catalyst.
2. The nature of the carbon monoxide adsorption sites should be probed by IR, NMR, or TPD to begin assessing the structure of the active sites.
3. It would be interesting to investigate if copper promotion of $NiCr_2O_4$, $FeCr_2O_4$, or $MnCr_2O_4$ also results in higher alcohol synthesis catalysts.
4. The interaction of alkalis and copper needs to be further investigated to determine the active phase for methanol synthesis. One technique which appears to be particularly suited for this work is solid state NMR. It may be enlightening to study copper impregnated alkali carbonates.

REFERENCES

1. Falbe, J. Phil. Trans. R. Soc. 2nd. A, 1981, 300, 205.

2. Greene, M. Chem. Eng. Prog. 1982, 78(8), 46.

3. Monick, J. Alcohols: Their Chemistry, Propèrties, and Manufacture; Reinhold: New York, 1978.

4. Weissermel, K.; Arpe, H. Industrial Organic Chemistry; Verlag Chemie: New York, 1978.

5. Chemical Marketing Reporter, 1987, 231(19), 40.

6. Anderson, R. B. In Catalysis; Emmett, P. H., Ed.; Reinhold: New York, 1956; Vol. 4, Chapter 1.

7. Fischer, F. Ind. Eng. Chem. 1925, 17, 574.

8. Anderson, R. Adv. Catal. 1953, 5, 355.

9. Anderson, R. Catal. Rev.-Sci. Eng. 1980, 21, 53.

10. Schultz, J.; Abelson, M.; Shaw, L.; Anderson, R. Ind. Eng. Chem. 1957, 49, 2055.

11. Natta, G.; Colombo, U.; Pasquon, I. In Catalysis; Emmett, P. H., Ed.; Reinhold: New York, 1957; Vol. 5, Chapter 3.

12. Smith, K.; Anderson, R. Can. J. Chem. Eng. 1983, 61, 40.

13. Vedage, F.; Himelfarb, P.; Simmons, G.; Klier, K. In Solid State Chemistry in Catalysis; Kaliagvine, S.; Mahay, A., Eds.; Elsevier: Amsterdam, 1984; pp 439-455.

14. Klier, K. Appl. Surf. Sci. 1984, 19, 267.

15. Bhasin, M.; Bartley, W.; Ellgen, P.; Wilson, T. J. Catal. 1978, 54, 120.

16. Ichikawa, M. Bull. Chem. Soc. Japan 1978, 51, 2268.

17. Ichikawa, M. Bull. Chem. Soc. Japan 1978, 51, 2273.

18. Somorjai, G.; Watson, P. J. Catal. 1981, 72, 347.

19. Somorjai, G.; Watson, P. J. Catal. 1982, 74, 282.

20. Quaderer, G.; Cochran, G. European Patent Application 0 119 609, 1984.

21. Tatsumi, T.; Muramatsu, A.; Tominaga, H. Chem. Lett. 1984, 685.

22. Tatsumi, T.; Muramatsu, A.; Tominaga, H. J. Catal. 1986, 101, 553.

23. Tatsumi, T.; Muramatsu, A.; Fununaga, T.; Tominaga, H. Chem. Lett. 1986, 919.

24. Kuwahara, Y.; Hamada, H.; Kintaichi, Y.; Ito, T.; Wakabayashi, K. Chem. Lett. 1985, 205.

25. Inoue, M.; Kurusu, A.; Wakamatsu, H.; Nakajima, K.; Inui, T. Appl. Catal. 1987, 29, 361.

26. Inoue, M.; Miyake, T.; Inui, T.; Takegami, Y. J. Chem. Soc., Chem. Commun. 1983, 70.

27. Inoue, M.; Miyake, T.; Takegami, Y.; Inui, T. Appl. Catal. 1984, 11, 103.

28. Inoue, M.; Miyake, T.; Takegami, Y.; Inui, T. Appl. Catal. 1987, 29, 285.

29. Uchiyama, S.; Obayashi, Y.; Shibata, M.; Uchiyama, T.; Kawata, N.; Konishi, T. J. Chem. Soc., Chem. Commun.1985, 1071.

30. Anderson, R. In Catalysis; Emmett, P. H., Ed.; Reinhold: New York, 1956; Vol. 4, Chapter 2.

31. Egiebor, N. C_1 Molec. Chem. 1985, 1, 253.

32. Bartholomew, C.; Revel, R. J. Catal. 1985, 24, 56.

33. Taylor, R. J. Chem. Soc. 1934, 1429.

34. Fujimoto, K.; Oba, T. Appl. Catal. 1985, 13, 289.

35. Kintaichi, Y.; Huwahara, Y.; Hamada, H.; Ito, T.; Wakabayashi, K. Chem. Lett. 1985, 1305.

36. Sugi, Y.; Takeuchi, K.; Matsuzaki, T.; Arakawa, H. Chem. Lett. 1985, 1315.

37. Takeuchi, K.; Matsuzaki, T.; Arakawa, H.; Sugi, Y. Appl. Catal. 1985, 18, 325.

38. Sugier, A.; Freund, E. U.S. Patent 4 122 110, 1978.

39. Sugier, A.; Freund, E.; LePage, J. U.K. Patent Application 2 047 249, 1980.

40. Freund, A.; Mikitenko, P.; Quang, D. Production of C_1-C_6 Alcohols from Synthesis Gas; Presented at the 2nd World Congress of Chemical Engineering, Montreal, PQ, October 1981.

41. Sugier, A.; Arlie, J.; Freund, E. The I.F.P. Way to Produce C_1-C_5 Alcohols for Use as a Gasoline Blending Component; Presented at the 4th International Symposium on Alcohol Fuels Technology, 1980.

42. Courty, P.; Arlie, J.; Convers, A.; Mikitenko, P.; Sugier, A. Hydro. Proc. 1984, 63(11), 105.

43. Ohno, T.; Yoshimoto, M.; Asselineau, L.; Courty, P.; Travers, P. Presented at the 1986 AIChE Spring National Meeting, New Orleans, LA, Apr. 1986.

44. Courty, P.; Forestiere, A.; Kawata, N.; Ohno, T.; Raimbault, C.; Yoshimoto, M. In Industrial Chemicals via C_1 Processes; Fahey, D., Ed.; ACS Monograph 328; American Chemical Society: Washington, DC, 1987, pp 42-68.

45. Klier, K. Adv. Catal. 1982, 31, 243.

46. Sugier, A.; Freund, E. U.S. Patent 4 291 126, 1981.

47. Sugier, A.; Freund, E. U.K. Patent Application 2 037 179, 1980.

48. Courty, P.; Durand, C.; Freund, E.; Sugier, A. J. Mol. Catal. 1982, 17, 241.

49. Apai, G.; Monnier, J.; Hanrahan, M. J. Chem. Soc., Chem. Commun. 1984, 212.

50. Monnier, J.; Hanrahan, M.; Apai, G. J. Catal. 1985, 92, 119.

51. Chem Systems Inc. Development of Alcohol-Based Synthetic Transportation Fuels from Coal-Derived Synthesis Gases; U.S. Department of Energy; DOE/ET/14858-T1 to T3, U.S. Government Printing Office: Washington, DC, 1980.

52. Hino, T.; Nomura, T.; Koyano, T. Sekiyu Gakkaishi 1984, 27, 257.

53. Sibilia, J.; Dominguez, J.; Herman, R.; Klier, K. Preprints of Papers, Division of Fuel Chemistry, American Chemical Society, 1984, 29, 226.

54. Lin, F.; Pennella, F. In Catalytic Conversions of Synthesis Gas and Alcohols to Chemicals; Herman, R., Ed.; Plenum: New York, 1984; pp 53-63.

55. Elliott, D.; Pennella, F. J. Catal. 1986, 102, 464.

ACKNOWLEDGEMENTS

I would like to express my sincere appreciation to Dr. Terry King for his guidance during my maturation into a competent, productive scientist. I am thankful that I could always count on his support and friendship. I would also like to thank Dr. Robert Wismer for serving as both my mentor and an example of professionalism during my undergraduate studies. Finally, I would like to thank my father, Preston Sheffer, my mother, Helen Cromer Sheffer, and the rest of my family for their love and support.

APPENDIX

Flory Product Distributions

Using a statistical approach, Flory (1) derived a mathematical expression for the molecular weight distribution resulting from a linear condensation polymerization. This expression has been shown to apply to any polymerization, regardless of the mechanism, where the primary step is the addition of carbon units one at a time onto the terminus of a growing linear chain with one polymer molecule being produced from each chain (2). It is assumed that in each stage of the polymerization process an equal opportunity for reaction is available to each growing chain, irrespective of the size of the chain. The method of chain termination is irrelevant except that termination by chain coupling is considered negligible. The mole fraction, m_n, of molecules in the polymer mixture which contain "n" structural units is found to be:

$$m_n = (1 - \alpha)\alpha^{(n-1)} \tag{1}$$

where α is the chain growth probability factor defined as:

$$\alpha \equiv r_p/(r_p + r_t) \tag{2}$$

The rates of chain propagation and termination are given by r_p and r_t, respectively.

If the added weight of each carbon unit in the compounds produced is the same, then the weight fraction distribution, w_n, is:

$$w_n = (1 - \alpha)^2 \, n\alpha^{(n-1)} \tag{3}$$

During the same time period that Flory was deriving equations 1 and 3, Schulz (3) independently derived a weight fraction distribution for the radical polymerization of vinyl monomers:

$$w_n = (\ln^2\alpha)n\alpha^n \tag{4}$$

At $\alpha > 0.5$, equations 4 and 5 are equivalent and referred to as the Schulz-Flory equation.

Equations 1 and 3 may be rearranged to:

$$\ln(m_n) = n\ln(\alpha) + \ln((1 - \alpha)/\alpha) \tag{5}$$

$$\ln(w_n/n) = n\ln(\alpha) + \ln((1 - \alpha)^2/\alpha) \tag{6}$$

Hence $\ln(m_n)$ or $\ln(w_n/n)$ may be plotted versus "n" to obtain theoretically a straight line whose slope is $\ln(\alpha)$. Note that the greater the value of α is the greater the mean molecular weight of the product.

For carbon monoxide hydrogenation, one can envision the growth of chains by single carbon units. In this respect the Schulz-Flory equation has been used to accurately represent the product distribution for many Fischer-Tropsch catalysts (4, 5). One problem with weight fraction distributions, however, is that the greater weight per carbon number for oxygenated end groups cannot be neglected, especially at small "n". Therefore equation 3 is generally applied only to hydrocarbons. To examine other functionalities or cases where more than one functionality is produced, equation 1 must be used. The ability of equation 1 to correctly model product distributions resulting from catalysts producing both hydrocarbons and oxygenates has been demonstrated

by Satterfield and Huff (6) for an alkalized iron catalyst. The α values reported in this dissertation have all been calculated from equation 1, the Flory equation. Carbon number distributions of hydrocarbons, alcohols, and aldehydes, both separately and as total product, were examined. In all cases linear Flory plots were obtained.

REFERENCES

1. Flory, P. J. Amer. Chem. Soc. 1936, 58, 1877.

2. Odian, G. Principles of Polymerization; McGraw-Hill: New York, 1970; pp. 260-263.

3. Schulz, G. Z. Phys. Chem., Abt. B. 1935, 30, 379.

4. Henrici-Olive, G.; Olive, S. Angew. Chem. Int. Ed. Engl. 1976, 15, 136.

5. Kellner, C.; Bell, A. J. Catal. 1981, 70, 418.

6. Satterfield, C.; Huff, G. J. Catal. 1982, 73, 187.

SECTION II: PARAMETRIC STUDY OF THE PREPARATION OF POTASSIUM PROMOTED COPPER-COBALT-CHROMIUM CATALYSTS FOR THE PRODUCTION OF HIGHER ALCOHOLS

ABSTRACT

The effects of a variety of preparation parameters on the catalytic activity and selectivity for synthesis gas conversion to higher alcohols of potassium promoted copper-cobalt-chromium oxides catalysts have been investigated. Specifically, the effects of 1) the metal salts used as precursors, 2) the amount of citric acid used as a "complexant", 3) the amount of potassium promoter, and 4) catalyst calcination temperature have been studied. Alcohol selectivities as great as 70 wt % with a production yield of 0.12 g/g cat/hr were obtained. C_2^+ alcohols accounted for 50 to 60 wt % of the alcohols produced. It was found that special attention must be paid to calcination temperature and, to a lesser extent, the other parameters mentioned.

INTRODUCTION

The conversion of synthesis gas to higher alcohols for gasoline blending or petrochemical uses remains an economically attractive objective (1). To this end a number of catalysts and processes have been proposed. Prominent among these proposed catalysts is the alkali promoted copper-cobalt-chromium mixed metal oxide catalysts patented by the Institut Francais du Pétrole (IFP) (2-6). This catalyst is claimed to produce normal alcohols with greater than 95 wt % selectivity. Higher alcohols (C_2^+) account for 25-75 wt % of the product. Unlike alkali promoted copper-zinc oxide catalysts which produce a mixture of branched alcohols enriched in isobutanol (7, 8), the IFP catalyst produces a Flory distribution of molecular weights. The catalyst is much like a cobalt Fischer-Tropsch synthesis catalyst (9) except that normal alcohols rather than normal hydrocarbons are produced.

Besides the investigations reported by IFP, very few studies of the copper-cobalt-chromium catalyst have been published. Chem Systems (10) have reported little success in duplicating the IFP patent claims of high oxygenate selectivity. Of the numerous catalysts prepared and tested by Chem Systems, the greatest oxygenate selectivity obtained was 30 wt %. Hino et al. (11) also found low oxygenate selectivity (9 mol %) but at a much lower operating pressure (1 MPa) than recommended. From these two previous investigations it is apparent that catalyst preparation may be a critical factor. Indeed, IFP researchers have indicated that "preparation of a good and reproducible catalyst ... is a difficult problem and all the preparation steps have to be controlled" (4).

However, to date no parametric investigations of catalyst preparation have been reported.

In this paper we report the results of our investigation into the effects of a variety of preparation parameters on the catalytic activity and selectivity of the IFP catalyst. Specifically, we have studied the effects of 1) the metal salts used as precursors, 2) the amount of citric acid used as a "complexant", 3) the amount of potassium promoter, and 4) catalyst calcination temperature. In addition, the effect of feed gas composition was studied. The goal of this work was to determine parametric variation associated with preparation procedures rather than to determine the optimum preparative approach. It was found that in order to achieve oxygenate selectivities approaching the IFP claim, special attention must be paid to calcination temperature and, to a lesser extent, the other parameters mentioned.

EXPERIMENTAL

Catalysts were prepared from homogeneous citrate complexes using methods outlined by Courty et al. (5). First, an aqueous solution of reagent grade $Co(acetate)_2 \cdot 4H_2O$, $Cu(NO_3)_2 \cdot 2\ 1/2\ H_2O$, CrO_3, and KOH of molar composition $CuCoCr_{.8}K_{.09}$ was prepared. Citric acid was then added to this solution to yield 1.0 gram equivalent of citric acid per gram equivalent of metals. The mixture was vacuum evaporated at room temperature to yield a thick slurry. This slurry was then dried for 12 to 24 hours at 350 K. The resulting powder was calcined in air at 623 K for 3 hours. Because the initial stages of calcination were very exothermic, the powder was brought up to calcination temperature using air diluted with helium. The partial pressure of oxygen was gradually increased from 5% to 20% over a one to two hour period during which the temperature of the bed was continually monitored to insure that hot spots did not develop. The molar composition of the calcined catalysts was confirmed using atomic absorption and flame emission spectroscopies. BET surface areas, determined from nitrogen adsorption isotherms, were collected at 77 K using a Micromeretics 2100E Accusorb instrument.

Catalytic activity and selectivity were determined in a single pass, fixed bed, flow reactor described elsewhere (12). All catalysts were treated with a 10% H_2 in Ar gas mixture at 548 K and atmospheric pressure for 5 hours before synthesis gas exposure. A small hot spot (5 to 10 K) passed quickly through the reactor upon hydrogen introduction indicating that reduction was occurring. A feed gas consisting of 58% H_2, 28% CO, and 14% Ar was then passed over the catalyst at a gas hourly

space velocity of 4000 hr^{-1}. Reaction pressure was raised to 5 MPa and reaction temperature was maintained at 548 K.

The reaction product gas was analyzed by on-line gas chromatography every 4 hours. The first sample was taken within ten minutes, the time to establish reactor pressure. Argon was used as an internal standard for activity calculations. Carbon monoxide conversions were less than 10 mol % minimizing heat and mass transfer limitations. Steady state was generally achieved after 12 hours on stream. The product in all cases consisted of n-alkanes, 1-n-olefins, n-alcohols, and n-aldehydes. Selectivities were evaluated in two manners. First, the fraction of product that consisted of hydrocarbons, alcohols, and aldehydes was found. Second, the chain growth probability factor, α, was determined for each fraction and for the overall product distribution. The chain growth probability factor was found by fitting the gas chromatographic data to the Flory equation:

$$\ln(m_n) = n \ln(\alpha) + \ln((1-\alpha)/\alpha)$$

where m_n is the mole fraction of product with n carbon atoms. A representative Flory plot for the alcohol product is shown in Figure 1.

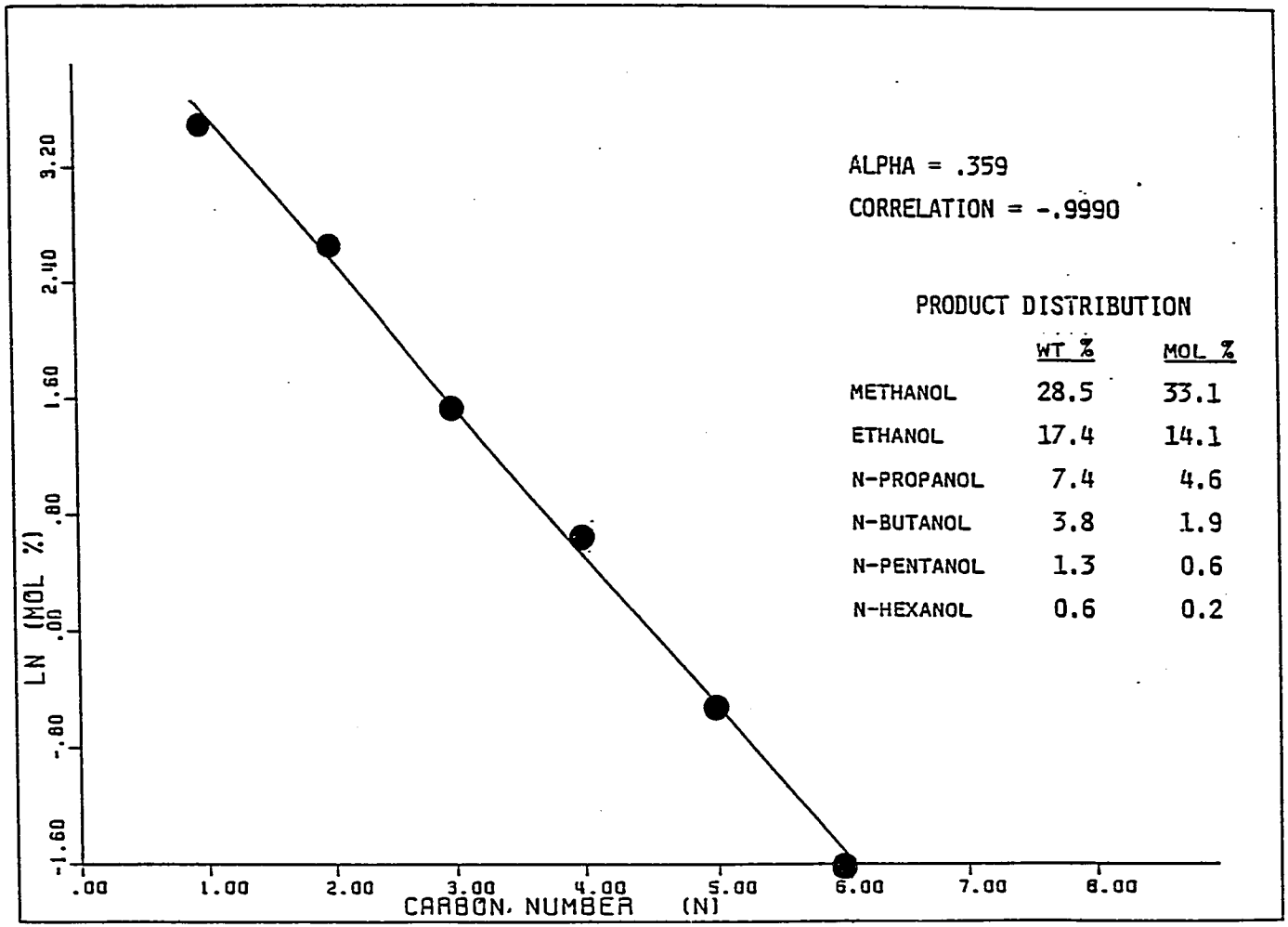

Figure 1. Example Flory plot for alcohols

RESULTS AND DISCUSSION

Effect of Choice of Metal Salts

A summary of the metal salt combinations prepared as catalysts and the resultant steady state activities and selectivities is given in Table 1. The first catalyst studied was prepared with $CoCO_3$ (46.5% Co by weight), $Cu(NO_3)_2$, CrO_3, and KOH, the same salts specified in the IFP patent for their most successful preparation. It was observed during the preparation that not all of the $CoCO_3$ was dissolving. When the catalyst was brought on stream only hydrocarbons, primarily methane, were produced initially. The carbon monoxide conversion was nearly 100% causing the temperature of the catalyst bed to rise sharply to 623 K. As the catalyst deactivated the bed temperature declined to 548 K after approximately 6 hours. Excessive methane formation during start-up has been noted by IFP (5). The alcohol selectivity gradually increased until steady state was established after approximately 20 hours. At steady state the selectivity to alcohols was 70 wt % which was much greater than that reported by previous researchers (10, 11) but still below the >95% claimed by IFP. The alcohol production yield, 0.12 g/g cat/hr, was lower than the 0.3 g/g cat/hr value reported in the patent, but comparable to the 0.08 to 0.20 g/g cat/hr value IFP reported in a later article (5). The distribution of alcohols, $\alpha = 0.37$, was also comparable to the $\alpha = 0.42$ value calculated from the patent data. At $\alpha = 0.37$, the fraction of C_2^+ alcohols in the alcohol product was 60 wt %. Surface areas were within the range expected for this preparation method (5). For a fairer comparison of catalytic activity, the activity expressed in

Table 1. Variation in catalytic behavior with choice of metal salts[a]

	Metal salts[b]	Surface area (m^2/g)	Selectivity (wt %)[c,d] HYD	ALC	ALD
1.	$CoCO_3$, KOH, $Cu(NO_3)_2$, CrO_3	50.0	30	70	0
2.	same as #1 except filtered[e]	8.2	26	30	44
3.	$Co(NO_3)_2$, KNO_3 $Cu(NO_3)_2$, $Cr(NO_3)_3$	20.5	51	49	0
4.	same as #3 except ignited during drying	12.2	80	20	0
5.	$Co(ac)_2$, KOH $Cu(ac)_2$, CrO_3	18.7	70	30	0
6.	$Co(ac)_2$, KOH $Cu(NO_3)_2$, CrO_3	28.9	33	58	9

[a]Steady state, T = 548 K, P = 5 MPa, $H_2/CO = 2$.

[b]Molar composition: $CuCoCr_{.8}K_{.09}$.

[c]Excluding CO_2 and H_2O.

[d]HYD = hydrocarbons, ALC = alcohols, ALD = aldehydes, ALL = all functionalities combined.

[e]Molar composition: $CuCo_{.7}Cr_{.7}K_{.07}$.

Product distribution (α)				Production rate of oxygenates (g/g cat/hr)	Activity $\frac{\text{mol CO}}{\text{m}^2 \text{ min}}$
HYD	ALC	ALD	ALL		
.44	.37	---	.40	0.12	3.0
.54	.44	.50	.50	0.050	5.4
.44	.41	---	.42	0.045	4.7
.55	.20	---	.50	0.010	3.7
.45	.37	---	.43	0.025	4.8
.46	.43	---	.43	0.12	5.8

terms of moles of carbon monoxide converted with respect to surface area is also included in Table 1.

Because of the large induction period observed for the first catalyst, a second preparation using the same metal salts, but this time filtering out the undissolved cobalt carbonate, was tested. A significant fraction of the cobalt was lost and the resulting catalyst molar composition was $CuCo_{0.7}Cr_{.7}K_{.07}$. When exposed to synthesis gas, this catalyst exhibited very little break-in indicating that the undissolved cobalt in the previous catalyst was responsible for the high rate of methane formation observed during start-up. The oxygenate selectivity is the same as the first catalyst, but aldehydes accounted for 60% of the oxygenate product.

In an effort to incorporate the recommended amount of cobalt into the catalyst in a homogeneous manner, metal nitrates were tried because of their excellent water solubility. The catalyst precursors formed with these salts were found to be very unstable. In fact, in the first attempt with this preparation, the precursor spontaneously ignited during drying at 350 K. The instability of the precursor is most likely related to nitration of citric acid. A second attempt with this preparation was successfully completed even though no change in the preparation procedure was made. The catalytic behavior of the successfully completed preparation (#3) and the precursor which ignited (#4) was very different although the metal composition of the two was similar. This result pointed to the possible importance of controlling temperature during

calcination. Excessive methane formation was not observed during start-up for either catalyst.

To avoid using metal nitrates, a preparation using cobaltous acetate ($Co(ac)_2$) and cupric acetate ($Cu(ac)_2$) was examined. Because cupric acetate has limited water solubility, chromium(VI) oxide (CrO_3), a strong acid, was used instead of chromium acetate to assist in dissolving the cupric acetate. Even with the use of chromic acid not all the cupric acetate dissolved. Precursors formed using these salts were very stable, but had to be monitored closely during calcination to avoid the development of hot spots. This catalyst (#5) had poor selectivity to oxygenates, perhaps a result of copper inhomogeneity caused by the limited solubility of cupric acetate. Again no methanation was observed during start-up.

The final choice of metal salts investigated consisted of cobaltous acetate, which was found to have good water solubility, cupric nitrate, and chromium trioxide, the latter to keep the solution acidic and avoid cupric acetate precipitation. The resulting opaque solution was filtered and a negligible amount of a blue precipitate was collected. The precipitate was later analyzed by atomic absorption and found to consist mainly of copper. The catalyst precursor formed was found to undergo rapid decomposition during calcination at approximately 473 K with the evolution of heat and gas. The catalyst (#6) had activity and selectivity to oxygenates comparable to the cobalt carbonate catalyst (#1). No induction period was observed.

The absence of methanation during start-up, the good yield of oxygenates, and the relative stability of catalyst precursors prompted the metal salt combination of $Co(ac)_2$, $Cu(NO_3)_2$, CrO_3, and KOH to be the combination of choice for the remainder of the catalysts to be reported in this paper.

Effect of Feed Gas Composition

It is known that alkali promoted copper-zinc oxide (7) and sulfided molybdenum (13) catalysts require H_2/CO ratios of unity or lower to achieve the maximum selectivity to alcohols. IFP has reported that reducing the H_2/CO ratio when using the copper-cobalt-chromium catalyst increases the C_2^+ fraction of the alcohols produced without increasing the formation of by-products (1). Below a H_2/CO of unity, the overall conversion decreases (6).

The results of decreasing the H_2/CO ratio of the feed for catalyst #6 are presented in Table 2. The average molecular weight of all functionalities, as reflected by the chain growth probability factor, was observed to increase. The overall selectivity to oxygenates was relatively constant with the fraction of aldehydes increasing and alcohols decreasing. The activity decreased by a factor of 3 when the H_2/CO ratio is reduced from 1.0 to 0.5.

The addition of carbon dioxide to the synthesis gas is known to increase the activity of copper-zinc oxide methanol catalysts (14), but not copper-chromium oxide methanol catalysts (15). For the copper-cobalt-chromium oxide system, the presence of CO_2 is reported not to affect the alcohol yield (6). Two different concentrations of carbon dioxide in the

Table 2. Effect of feed composition on catalytic activity and selectivity[a]

Feed composition $H_2/CO/CO_2$ (vol %)	Selectivity (wt %)[b,c] HYD	ALC	ALD	Product distribution (α) HYD	ALC	ALD	ALL	Production rate of oxygenates (g/g cat/hr)	Activity $\frac{\mu mol\ CO}{m^2\ min}$
2/1/0	33	58	9	.46	.43	---	.43	0.12	5.8
1/1/0	37	46	17	.54	.50	.36	.50	0.12	6.9
1/2/0	31	28	41	.57	.50	.42	.51	0.045	2.3
3.4/1/0.6	48	48	4	.55	.50	---	.52	0.090	5.0
2/1/0.6	39	54	7	.57	.50	---	.54	0.085	4.0

[a] Steady state, T = 548 K, P = 5 MPA, Catalyst #6 (surface area = 28.9 m^2/g).

[b] Excluding CO_2 and H_2O.

[c] HYD = hydrocarbons, ALC = alcohols, ALD = aldehydes, ALL = all functionalities combined.

feed were examined in this study. The first CO_2 containing feed gas studied had a H_2/CO molar ratio of 3.4 with a CO/CO_2 molar ratio of 0.6 and was the feed gas composition IFP used for their patent results. As indicated in Table 2, the production yield of alcohols was slightly lower. Part of the decrease in yield was the result of a decrease in alcohol selectivity. As the results for a feed gas with a H_2/CO ratio of 2 and the same CO/CO_2 ratio indicate, a portion of the loss in selectivity was attributable to the higher H_2/CO ratio. It is interesting that the addition of CO_2 to the feed caused an increase in the average molecular weight of the product comparable to simply decreasing the H_2/CO ratios.

Effect of Amount of Citric Acid Added

The addition of citric acid to the initial solution of metal salts is reported to be necessary for the formation of catalyst precursors with homogeneous composition (16). The citric acid is assumed to act as a complexing agent. Because of the instability of catalyst precursors formed by combining citric acid with metal nitrates, it was decided to investigate whether citric acid is vital to catalyst preparation. The results obtained are summarized in Table 3.

The catalyst prepared without citric acid was very active upon start-up resulting in 100% conversion of carbon monoxide to mostly methane. Steady state was established after 16 hours on stream. It is suspected that the induction period is a result of poor cobalt homogeniety similar to the $CoCO_3$ prepared catalyst. The steady state oxygenate production yield for this catalyst was quite low, although the selectivity

Table 3. Variation in catalytic behavior with citric acid addition[a]

g. eq. acid / g. eq. metals	Surface area (m^2/g)	Selectivity (wt %)[b,c] HYD	ALC	ALD	Product distribution (α) HYD	ALC	ALD	ALL	Production rate of oxygenates (g/g cat/hr)	Activity $\frac{\mu mol\ CO}{m^2\ min}$
0	11.3	55	35	10	.52	.47	.41	.48	0.020	2.0
0.2	38.3	45	52	3	.53	.42	---	.49	0.055	2.4
1	29.0	33	58	9	.46	.43	---	.43	0.12	5.8
2.2	22.9	40	60	0	.37	.30	---	.34	0.090	7.9

[a] Steady state, T = 548 K, P = 5 MPa, $H_2/CO = 2$, catalyst composition: $CuCoCr_{.8}K_{.09}$.

[b] Excluding CO_2 and H_2O.

[c] HYD = hydrocarbons, ALC = alcohols, ALD = aldehydes, ALL = all functionalities combined.

to oxygenates was modest. The incorporation of a small amount of citric acid to the metal salt solution resulted in a catalyst which did not produce excessive methane upon introduction of synthesis gas, indicating that citric acid does improve metal homogeniety. In addition, the oxygenate production yield increased by a factor of four, but primarily through an increase in surface area.

As the amount of citric acid was further increased, catalytic activity increased and the average molecular weight of the product decreased. Perhaps the increased carbon introduced by citric acid was not completely removed during catalyst calcination or reduction. The remaining carbon may then have modified the surface in a manner similar to effects noted on iron Fischer-Tropsch catalysts. Espinoza and Snel (17) have reported that when iron Fischer-Tropsch catalysts are treated with benzene the value of the chain growth parameter (α) decreases from .5 to .3. The activity of the catalyst was not affected. The authors suggest that a modification of active sites and not site poisoning was responsible.

Effect of Potassium Loading

Using arguments centered on the donation of electron density by basic potassium compounds, it is expected that the promotion of cobalt catalysts with potassium would increase oxygenate selectivity, increase the average molecular weight of the product, and decrease catalytic activity (18). The later two of these have been observed on potassium impregnated Co/Al_2O_3 catalysts (19). An increase in oxygenate selectivity has been reported for a potassium promoted $Co/Mo/SiO_2$ catalyst (20).

For the copper-cobalt-chromium oxide catalyst, IFP has reported that without alkali promotion uncontrolled methanation occurs below 563 K (5). It was thought that the role of potassium was to suppress alcohol dehydration by decreasing surface acidity.

In our study, a catalyst prepared without potassium produced only methane during start-up, but after 4 hours on stream the catalyst reached the steady state activity and selectivity values given in Table 4. Although the selectivity to alcohols was modest, there was nevertheless a good alcohol production yield. When potassium was added to the formulation, methanation during start-up was suppressed and the selectivity to oxygenates was increased. Since citric acid was added to the initial metal salt solution it is assumed that the catalyst had a homogeneous distribution of the metal components. If segregated cobalt metal resulting from hydrogen reduction is responsible for the methanation activity upon feed gas exposure, then potassium must either prevent this segregation or interact directly with cobalt metal to suppress its activity.

As the molar amount of potassium was increased, the activity decreased. This is consistent with what is predicted for an electronic effect resulting from electron donation to cobalt by potassium (18). However, no increase in the average molecular weight of the product was observed, indicating that the potassium may simply dilute the surface. The selectivity to oxygenates was relatively unaltered, but the fraction of aldehydes comprising the oxygenate product increased. The

Table 4. Change in catalytic behavior with potassium addition[a]

Potassium[b] amount	Surface area (m^2/g)	Selectivity (wt %)[c,d] HYD	ALC	ALD	Product distribution (α) HYD	ALC	ALD	ALL	Production rate of oxygenates (g/g cat/hr)	Activity $\frac{\mu mol\ CO}{m^2\ min}$
0	24.0	61	39	0	.42	.41	---	.42	0.075	8.7
.045	23.7	49	40	11	.52	.40	---	.46	0.080	6.0
.09	29.0	33	58	9	.46	.43	---	.43	0.12	5.8
.14	15.0	42	24	34	.47	.45	.32	.45	0.050	4.9
.30	18.6	43	21	36	.51	.35	.37	.45	0.0215	2.0

[a] T = 548 K, P = 5 MPa, $H_2/CO = 2$, steady state.

[b] Molar composition of catalyst: $CuCoCr_{.8}K_x$.

[c] Excluding CO_2 and H_2O.

[d] HYD = hydrocarbons, ALC = alcohols, ALD = aldehydes, ALL = all functionalities combined.

area of the catalysts decreased at the higher potassium concentrations. A similar phenomenon has been observed for potassium promoted copper-zinc-aluminum oxide catalysts (7).

Effect of Calcination Temperature

The poor catalytic behavior of the metal nitrate prepared catalyst which ignited during drying (catalyst #4 of Table 1) suggested that calcination temperature may be an important parameter in preparing catalysts active and selective for alcohol formation. No information regarding the effect calcination temperature or the selectivity and activity of the copper-cobalt-chromium oxide system has been previously reported.

The calcination temperature of the catalyst precursor was found to have a pronounced influence on both the selectivity and yield of oxygenates (see Table 5). The carbon number distribution of the products was unaffected as exhibited by the constant chain growth probability factors. A plot of the hydrocarbon and oxygenate yields as a function of calcination temperature is shown in Figure 2. A four-fold decrease in oxygenate production was observed with little change in the hydrocarbon yield. This suggests that as the calcination temperature was raised, active sites for alcohol synthesis were lost, but they were not necessarily converted to hydrocarbon producing sites. Hydrocarbon formation may occur on cobalt which segregated during catalyst preparation. Since the same catalyst precursor was used in all cases, the cobalt segregation must be related to inhomogenieties in the initial metal salt solution. The lack of methanation during start-up and the low yield of hydrocarbons

Table 5. Effect of calcination temperature on catalytic activity[a]

Calcination temperature (K)	Surface area (m^2/g)	Selectivity (wt %)[b,c] HYD	ALC	ALD	Product distribution (α) HYD	ALC	ALD	ALL	Production rate of oxygenates (g/g cat/hr)	Activity $\frac{\mu mol\ CO}{m^2\ min}$
623	29.0	33	58	9	.46	.43	---	.43	0.12	5.8
798	18.8	47	20	33	.49	.48	.49	.47	0.07	4.6
973	10.6	56	18	26	.44	.40	.45	.42	0.025	4.1
1148	7.2	67	15	18	.47	.45	.45	.42	0.015	3.4

[a] T = 548 K, P = 5 MPa, $H_2/CO = 2$, Catalyst #6.

[b] Excluding CO_2 and H_2O.

[c] HYD = hydrocarbons, ALC = alcohols, ALD = aldehydes, ALL = all functionalities combined.

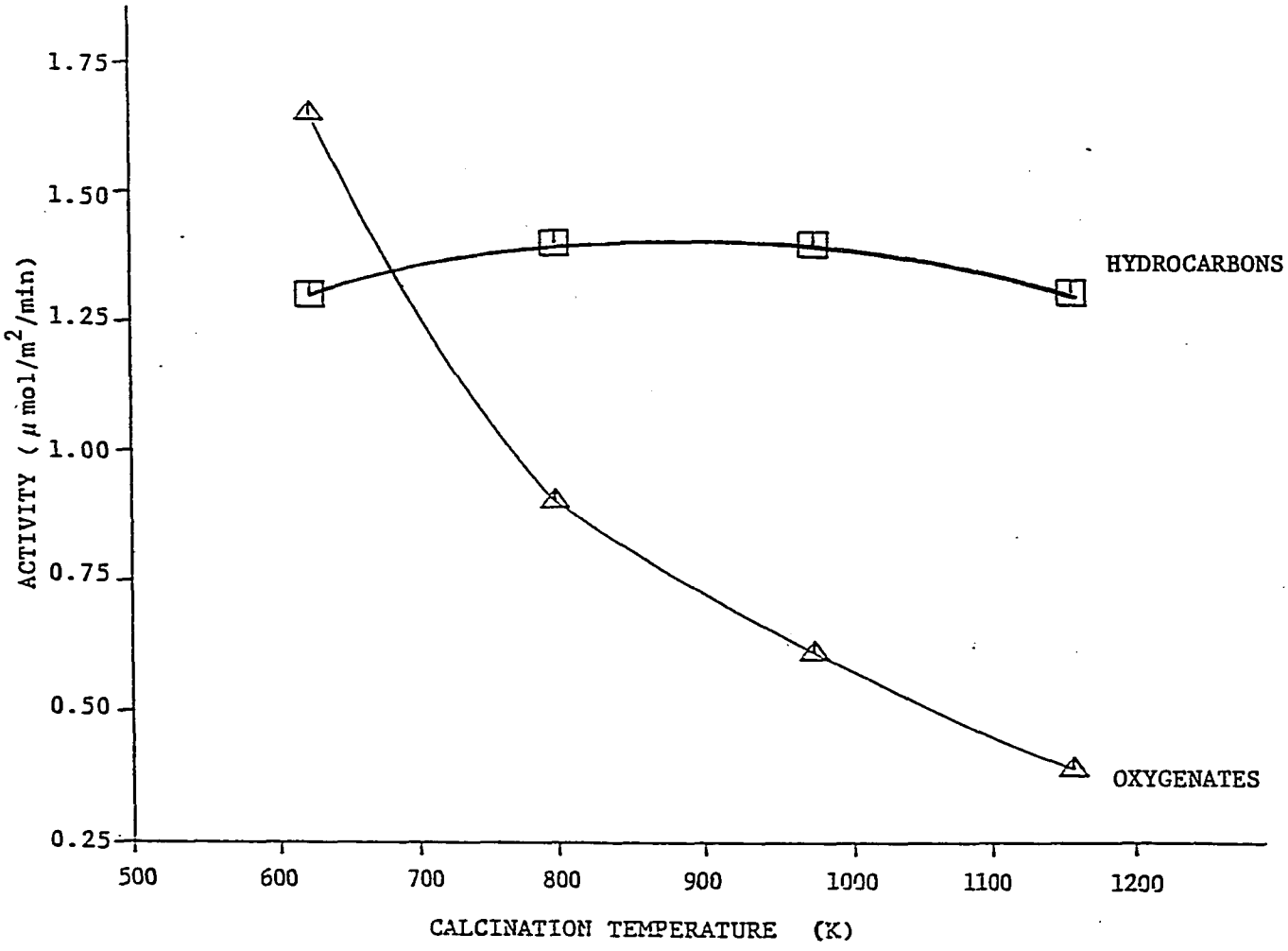

Figure 2. Synthesis rate of hydrocarbons and oxygenates as a function of calcination temperature

indicates that the amount of segregated cobalt was quite small as cobalt is known to be very active for hydrocarbon synthesis (21). In addition, the decrease in the chain growth probability factor from approximately 0.65 for typical cobalt Fischer-Tropsch catalysts (22) to 0.45 for the catalysts examined here may be indicative of the interaction between cobalt and copper metals. For supported ruthenium catalysts, a decrease in the fraction of higher hydrocarbons has been reported upon copper addition (23, 24).

SUMMARY

Synthesis gas conversion studies using potassium promoted copper-cobalt-chromium oxide catalysts prepared by citrate complexation methods resulted in alcohol selectivities as great as 70 wt % with an alcohol yield of 0.12 g/g cat/hr. The alcohols produced were exclusively normal and the alcohol distribution was consistent with Flory theory. C_2^+ alcohols accounted for approximately 50 to 60 wt % of the alcohols produced.

The choice of metal salts used in the preparation was found to have a marked influence on catalytic behavior. Salts with poor water solubility produced inhomogeneous catalyst precursors as evidenced by excessive methanation activity during start-up or poor oxygenate selectivity. Metal nitrates produced very unstable catalyst precursors. The best combination of metal salts studied was $Co(ac)_2$, $Cu(NO_3)_2$, CrO_3, and KOH.

Lower H_2/CO feed gas ratios increased the average molecular weight of the product, and decreased activity. The addition of CO_2 to the feed had little effect on activity, but, similar to the effect of H_2/CO ratios, increased the fraction of C_2^+ products.

Citric acid and potassium addition were both beneficial in that they suppressed methanation during start-up. Citric acid increased component homogeniety, while potassium either suppressed cobalt segregation during reduction or interacted directly with the cobalt metal formed by segregation. Increasing the amount of citric acid added to the initial metal salt solution resulted in a decrease in the average molecular weight of

the product and enhanced activity. Increasing the amount of potassium promotion decreased activity and had little effect on the average molecular weight of the product.

Calcination temperature was found to have the greatest influence on the yield of oxygenates. Both catalytic activity and selectivity to oxygenates were decreased with increasing calcination temperature. However, the hydrocarbon yield and the molecular weight distribution of each fraction remained relatively constant.

In conclusion, the potassium promoted copper-cobalt-chromium oxide system was found to be a viable catalytic system for the conversion of synthesis gas to higher oxygenates. Work is needed to understand the chemical nature of the catalyst in order to gain insight into how to optimize preparation procedures. The best preparation parameter to base an investigation directed toward correlating higher alcohol synthesis with the chemical nature of the catalyst would be calcination temperature, since increasing the calcination temperature from 623 to 1148 K monotonically decreased the oxygenate yield by a factor of four.

REFERENCES

1. Courty, P.; Forestiere, A.; Kawata, N.; Ohno, T.; Raimbault, C.; Yoshimoto, M. In Industrial Chemicals via C_1 Processes; Fahey, D. R., Ed.; ACS Symposium Series 328; American Chemical Society: Washington, D.C., 1987; pp. 42-68.

2. Sugier, A.; Freund, E. U.S. Patent 4 122 110, 1978.

3. Sugier, A.; Freund, E. U.S. Patent 4 291 126, 1981.

4. Sugier, A.; Mikitenko, P.; Quang, D. Production of C_1-C_6 Alcohols from Synthesis Gas; 2nd World Congress of Chemical Engineering, Montreal, October 4-9, 1981.

5. Courty, P.; Durand, D.; Freund, R.; Sugier, A. J. Mol. Cat. 1982, 17, 241.

6. Courty, P.; Arlie, J.; Convers, A.; Mikitenko, P.; Sugier, A. Hydroc. Proc. 1984, 63(11), 105.

7. Smith, K.; Anderson, R. Can. J. Chem. Eng. 1983, 61, 40.

8. Calverley, E.; Anderson, R. J. Catal. 1987, 104, 434.

9. Anderson, R. In Catalysis; Emmett, P., Ed.; Reinhold: New York, 1956; Vol. 4, Chapter 2.

10. Chem Systems Research and Development Group Development of Alcohol-Based Synthetic Transportation Fuels from Coal-Derived Synthesis Gases; U.S. Department of Energy. U.S. Government Printing Office: Washington, D.C., 1980; DOE/ET/14858-TI to T3.

11. Hino, T.; Noura, T.; Koyano, T. Sekiyu Gakkaishi 1984, 27, 257.

12. Sheffer, G.; King, T. S. Submitted for publication in J. Catal.

13. Quarderer, G.; Cochran, G. European Patent Appl. 0 119 609, 1984.

14. Klier, K.; Chatikavanij, R.; Herman, R.; Simmans, G. J. Catal. 1982, 74, 343.

15. Monnier, J.; Apai, G.; Hanrahan, M. J. Catal. 1984, 88, 523.

16. Courty, P.; Marcilly, C. In Preparation of Catalysts III; Poncelet, G.; Grange, P.; Jacobs, P., Eds.; Elsevier: Amsterdam, 1983; pp. 485-519.

17. Espinoza, P.; Snel, R. J. Chem. Soc., Chem. Commun. 1986, 1796.

18. Snel, R. C_1 Mol. Chem. 1986, 1, 427.

19. Castner, D.; Santilli, D. In Catalytic Materials; Whyte, T.; Dalla Betta, R.; Derovane, E.; Baker, R., Eds.; ACS Symposium Series 248; American Chemical Society: Washington, D.C., 1984; pp. 42-56.

20. Fujimoto, K.; Oba, T. Appl. Catal. 1985, 13, 289.

21. Vannice, M. J. Catal. 1977, 50, 228.

22. Egiebor, N. C_1 Mol. Chem. 1985, 1, 253.

23. Bond, G.; Turnham, B. J. Catal. 1976, 45, 128.

24. Lai, S.; Vickerman, J. J. Catal. 1984, 90, 337.

ACKNOWLEDGEMENTS

The authors gratefully acknowledge the receipt of start-up funds from the Shell Faculty Development Fund. One of the authors (GRS) wishes to thank the Amoco Foundation for fellowship support.

SECTION III: INVESTIGATION OF THE CHEMICAL NATURE OF ALKALI PROMOTED COPPER-COBALT-CHROMIUM OXIDE HIGHER ALCOHOL CATALYSTS AS A FUNCTION OF CALCINATION TEMPERATURE

ABSTRACT

The chemical nature of alkali promoted copper-cobalt-chromium higher alcohol catalysts has been evaluated as a function of calcination temperature using X-ray diffraction and X-ray photoelectron spectroscopy. The activated catalyst was determined to be comprised of copper metal and a cobalt-chromium spinel. Oxygenate production correlated with the dispersion of copper metal in the catalyst. Poorer copper dispersion and a decrease in oxygenate formation were observed with increasing catalyst calcination temperature. There was no evidence of cuprous ions or cobalt metal in the activated catalyst and it is therefore unlikely that component synergism is a result of alkyl chain growth on cobalt metal sites coupled with alcohol termination by CO molecularly adsorbed on copper(I) chromite.

INTRODUCTION

Alkali promoted copper-cobalt-chromium oxide catalysts are known to convert synthesis gas in high yields to normal alcohols (1-3). The oxygenate selectivity has been reported to exceed 95 wt % of which 25-60 wt % consists of higher alcohols. The product distribution follows a Flory distribution indicating the catalysts resemble Fischer-Tropsch synthesis catalysts rather than alkali promoted methanol synthesis catalysts (4, 5).

Because of the unique catalytic behavior and composition of these catalysts, they offer an opportunity to investigate catalyst component synergism. It is known that cobalt oxide is very active for the Fischer-Tropsch synthesis (6, 7). Copper oxide (8) and chromium oxide are inactive for carbon monoxide hydrogenation. Copper-chromium oxide, however, is a selective methanol catalyst (9). In addition, a potassium promoted copper-chromium oxide catalyst of molar composition Cu:Cr:K = 1:4:2 has been reported to produce up to 35% isobutanol at 763 K and 180 bar (10, 11). However, this behavior is more comparable to that of alkali copper-zinc oxide catalysts (4, 5) than to the system of interest here.

From the above information one might speculate that component synergism in the copper-cobalt-chromium oxide system is a result of interaction between cobalt and copper-chromium oxide. Cobalt would provide alkyl chain growth, while copper-chromium oxide would be responsible for chain termination as alcohols. However, catalysts prepared by impregnating copper-chromium (12) on copper-zinc oxide

(13, 14) methanol catalysts with cobalt or iron have not been successful in synthesizing higher alcohols.

Very little information regarding the chemical nature of the copper-cobalt-chromium oxide catalyst has been published and, consequently, little is known about the nature of the component synergism responsible for higher alcohol synthesis. Courty and co-workers (2, 15) have reported that calcinced copper-cobalt-chromium or aluminum oxide catalysts are comprised of cupric oxide and a spinel mixed metal oxide. Hino et al. (16) have reported similar results. Both research groups concluded from scanning transmission electron microscopy with X-ray emission micro-analysis (STEM-XEM) observations that the spinel was homogeneous and not a mixture of different spinel phases. As a result, Hino et al. proposed that the spinel was of composition:

$$[Cu(II)_a Co(II)_{1-a}][Co(III)_{(a+1)/2} Cr(III)_{(3-a)/2}]O_4$$

where $0 \leq a \leq 0.9$. Using temperature programmed reduction both groups also observed that all the copper in the calcined catalyst was completely reduced to copper metal and that cobalt was only partially reduced. Steady state catalysts were also examined by Courty and co-workers using STEM-XEM. They found that the spinel phase was strongly depleted in cobalt and observed the formation of highly divided (1-3 nm) Cu-Co clusters. Although their TPR results indicate otherwise, both Courty and co-workers and Hino et al. speculated that copper(I) species were stabilized in the spinel or as copper chromite. These species were proposed to be responsible for the molecular adsorption of CO under

reaction conditions. Metallic cobalt, also thought to be present in the catalyst, would be responsible for the dissociative adsorption of CO and the formation of C-C bonds. Higher alcohol synthesis was hypothesized to occur in a manner previously discussed. There is, however, little evidence to support this view of component synergism in the copper-cobalt-chromium system.

Our previous work with this catalyst has shown that calcination temperature is an important parameter in determining the oxygenate yield (3). Increasing the calcination temperature from 623 K to 1148 K decreased the oxygenate synthesis rate from 1.6 to 0.4 $\mu mol/m^2/min$. The rate of hydrocarbon synthesis was approximately constant. These results suggested that by increasing the calcination temperature active sites for alcohol synthesis were lost, but not necessarily converted to hydrocarbon producing sites. Elucidation of the chemical nature of the copper-cobalt-chromium system as a function of calcination temperature should therefore provide valuable insight into the nature of the component synergism.

In this paper, we report the results of our study of the chemical nature of the alkali promoted copper-cobalt-chromium catalyst as a function of calcination temperature using X-ray diffraction and X-ray photoelectron spectroscopy. The goal of this study was to correlate oxygenate selectivity and activity with the phase(s) found by catalyst characterization. In addition, we investigated the alkali promoted mono- and bimetallic oxide systems. The nature of the component synergism operable in the copper-cobalt-chromium oxide system is discussed on the basis of the detailed characterization outlined above.

EXPERIMENTAL

Catalysts were prepared via homogeneous citrate complexes using methods outlined previously (3). The calcined copper-cobalt-chromium catalyst samples were all prepared from the same catalyst precursor thus eliminating any chemical differences resulting from precursor preparation. For the mono- and bimetallic oxide preparations, the molar ratio of potassium ions to transition metal ions was maintained at 0.032, the same as the ternary metal catalyst system. For the bimetallic oxide preparations, the molar ratio of the metals was unity. Cobaltous acetate ($Co(ac)_2$), cupric nitrate ($Cu(NO_3)_2$), chromium trioxide (CrO_3), and potassium nitrate (KNO_3) were used as metal salts. Molar compositions of the calcined catalysts were confirmed using atomic absorption and flame emission spectroscopies.

Surface areas were calculated from multipoint BET adsorption isotherms using nitrogen or krypton at 77 K. Adsorption isotherms were obtained using a Micromeretics 2100E Accusorb surface area analyzer. Nitrogen was used as the adsorbate when surface areas were greater than 5 m^2/g. The molecular areas of nitrogen and krypton used for calculation were 16.2 and 21.0 $Å^2$ respectively.

The catalytic behavior of all catalysts was determined in a single pass, fixed bed, flow microreactor system described elsewhere (17). Before synthesis gas exposure, all catalysts were exposed to a 10% H_2 in argon gas mixture at 548 K for 5 hours. A feed gas consisting of 58% H_2, 28% CO, and 14% Ar was used at a gas hourly space velocity of 4000 hr^{-1}. All studies were performed at 5 MPa and 548 K. By diluting the more active

catalysts with α-SiO_2, the conversion of carbon monoxide was maintained at less than 10 mol % in all runs, thus minimizing heat and mass transfer limitations. Mixtures of hydrocarbons, alcohols, and aldehydes, exclusively normal, were produced. In cases where C_2^+ compounds were formed, product distributions were found to be consistent with the Flory equation:

$$\ln(m_n) = n \ln(\alpha) + \ln((1-\alpha)/2)$$

where m_n is the mole fraction of product with n carbon atoms and α is the chain growth probability factor.

Powder X-ray diffraction patterns were obtained with a Picker theta-theta diffractometer using MoKα radiation. α-SiO_2 was mixed with all samples at a concentration of 5 wt % as an internal standard. The d-spacing of the (101) reflection was referenced to 3.342 Å. The step-size was 0.04 degrees per step with a three second per step counting time. Synthesis gas exposed catalyst diffraction patterns were collected under argon using a specially designed cell previously described (17). The following procedure was used. First, the catalyst was exposed to argon while the temperature of the cell was increased to 548 K. A gas mixture of 10% hydrogen in argon was then passed over the sample for 4 hours at atmospheric pressure. This gas was replaced by synthesis gas of molar composition $H_2/CO = 2$ and the pressure was increased to 1.0 MPa, the upper limit of the cell. The catalyst was treated with synthesis gas for 4 hours, after which the cell was purged with argon and transported to the diffractometer. Because of attenuation of the signal by the beryllium

window on the cell, the counting time was increased to six seconds per step.

X-ray photoelectron spectra were obtained with an AEI 200B spectrometer using AlKα radiation. Samples were prepared by loading the catalyst into soda-lime glass tubing, performing the appropriate treatment, and then evacuating and sealing the tubes. Reduced samples were treated with a 10% H_2 in Ar mixture for 4 hours at atmospheric pressure. Synthesis gas treated samples were first reduced as just described and then exposed to a synthesis gas of molar composition $H_2/CO = 2$ for 4 hours at atmospheric pressure. The tubes were transported to and opened in a helium dry box attached directly to the spectrometer. Samples were mounted by spreading the catalyst powder on plastic adhesive tape. The carbon 1s peak was referenced to 285.0 eV for binding energy calculations.

RESULTS

X-ray Diffraction

The copper-cobalt-chromium catalyst precursor was found to be amorphous. The powder X-ray diffraction patterns of the calcined catalyst series are shown in Figure 1. Cupric oxide and a spinel structure (a_0 = 8.251 Å) were the only phases identified at all calcination temperatures. A spinel structure is a cubic close packed lattice of oxygen in which 1/8 of the tetrahedral holes are filled by a divalent cation and 1/2 of the octahedral holes are filled by a trivalent cation. Cation ordering produces alternating octants of AO_4 tetrahedra and B_4O_4 cubes. The resulting stoichiometry is AB_2O_4 where A is the divalent cation and B is the trivalent cation.

Qualitatively the data presented in Figure 1 indicate two items for increasing calcination temperature. First, there is no change in the position of the spinel or cupric oxide reflections. Second, the amount of cupric oxide relative to the spinel phase appears to be increasing. The d-spacings of the spinel and cupric oxide reflections are given in Table 1. Only those reflections which occur with minimum overlap of the two phases are listed. There is no change in the unit cell size, as reflected by the d-spacings, of either phase. The d-spacings for cupric oxide agree well with those in the literature (18). A variety of copper, cobalt, and/or chromium spinels have been reported in the literature. These spinels and their respective lattice parameters are listed in Table 2. No spinels comprised of all three metals, e.g., CuCoCrO, have been reported. It is not possible to identify the composition of the

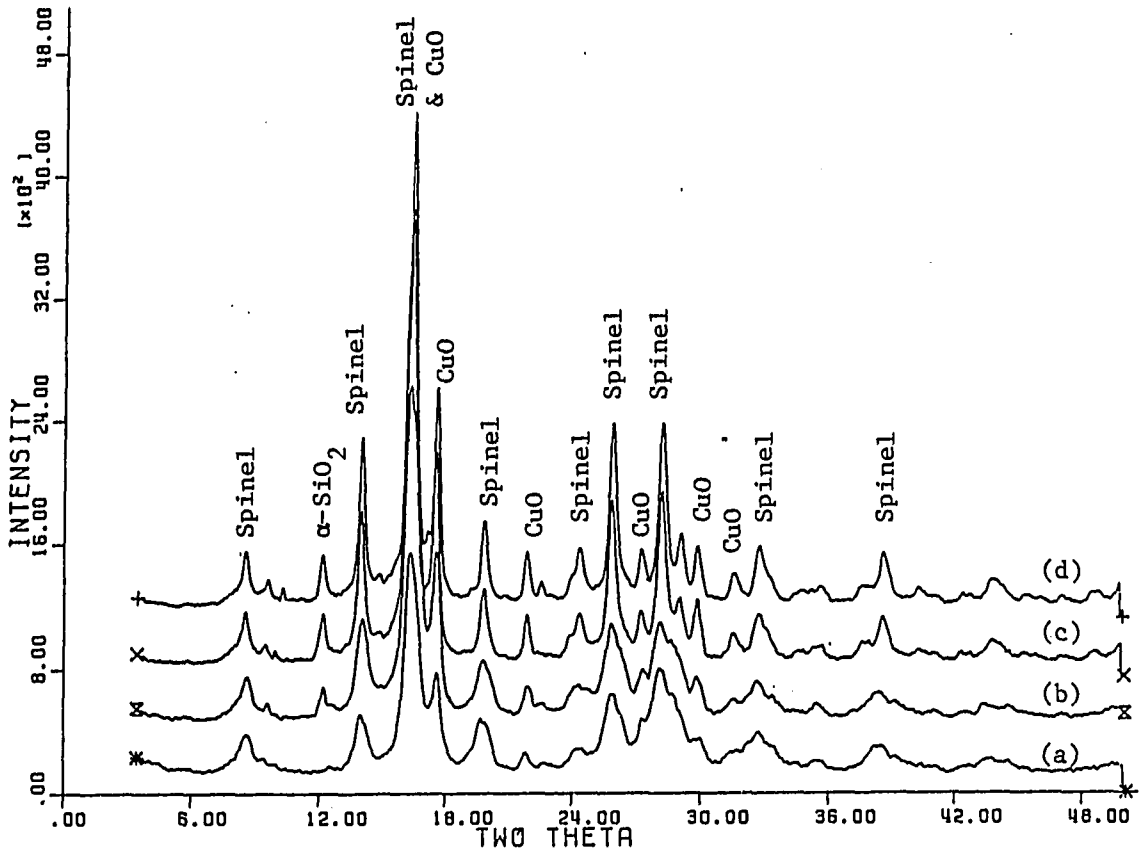

Figure 1. Powder X-ray diffraction pattern of $CuCoCr_{.8}K_{.09}$ catalyst as a function of calcination temperature:

(a) 623 K

(b) 798 K

(c) 973 K

(d) 1148 K

Table 1. d-Spacings of spinel and cupric oxide reflections as a function of catalyst calcination temperature

Calcination temperature (K)	Spinel d-spacings (Å) (400)	(440)	(533)	(731)	CuO d-spacings (Å) (111)	(202)	(113)
623	2.064	1.460	1.258	1.077	2.330	1.876	1.504
798	2.063	1.460	1.261	1.079	2.325	1.869	1.502
973	2.060	1.458	1.259	1.073	2.330	1.867	1.509
1148	2.061	1.457	1.258	1.075	2.326	1.869	1.507

Table 2. Lattice parameters of copper-cobalt-chromium spinels

Spinel	Lattice parameter a_o (Å)	Reference
$Cu(II)Cr(III)_2O_4$	8.344	--[a]
$Co(II)Cr(III)_2O_4$	8.333	19
$Co(II)Co(III)Cr(III)O_4$	8.209	19
$Cu(II)Co(III)_2O_4$	8.084	20
$Co(II)Co(III)_2O_4$	8.084	19

[a]Joint Committee on Powder Diffraction Standards #26-508.

spinel found in this study by simple comparison of unit cell sizes since, as will be discussed later, there is a large number of spinels with variable composition which can have identical cell sizes.

To quantitate the relative amounts of each phase present, the integrated area of the (202) cupric oxide peak was normalized with respect

to the (400), (220), and (111) peaks of the spinel. These peaks were chosen because there is no overlap with any other peak at any calcination temperature. The ratio of the cupric oxide area to the spinel area as a function of calcination temperature is shown in Figure 2. A factor of 2.5 increase in the amount of cupric oxide visible in the diffraction pattern relative to the amount of spinel is observed.

X-ray diffraction of synthesis gas exposed catalysts indicated that the cupric oxide reduced completely to copper metal. The spinel phase was slightly affected as evidenced by the small shift of the reflections to lower d-spacings (see Table 3). No additional phases were detected. Comparison of the copper metal peak areas to the spinel peak areas as was done for the calcined catalysts revealed little variation among the samples. However, the copper metal peak width decreased monotonically from the catalyst which had been calcined at 623 K to the catalyst which had been calcined at 1148 K. Mean copper metal particle sizes were calculated from the peak width of the Cu(111) reflection using the Scherrer equation (21):

$$\bar{d} = 0.89\ \lambda_{Mo}/\cos\ \theta/(w_s - w_i)^{\frac{1}{2}}$$

where $\bar{d}$ is the mean crystallite particle diameter, λ_{Mo} the wavelength for molybdenum radiation, θ the Bragg angle, w_s the peak width at half height of the Cu(111) reflection, and w_i the instrumental peak width correction factor. The values obtained are given in Table 4.

When reduced catalysts were exposed to air, heat generation occurred indicating sample reoxidation. The powder diffraction patterns of the

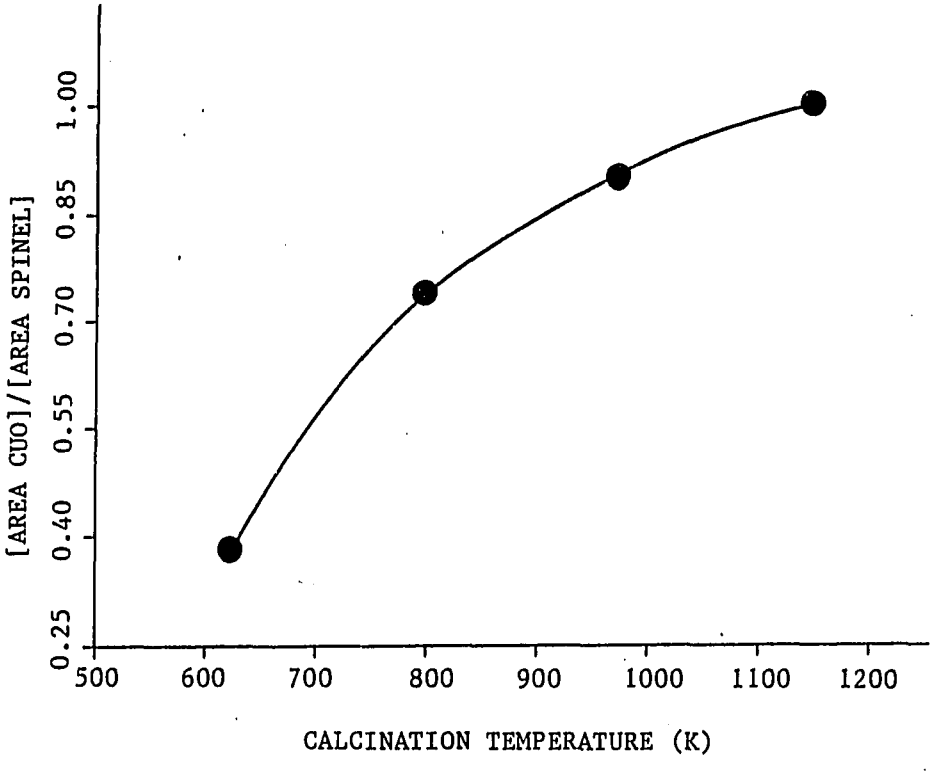

Figure 2. Change in the relative amount of CuO visible in the powder X-ray diffraction pattern as a function of calcination temperature

Table 3. d-Spacings of spinel and copper metal reflections in synthesis gas exposed catalysts

Calcination temperature (K)	Spinel d-spacings (Å) (400)	(440)	(533)	(731)	Copper metal d-spacings (Å) (111)	(200)
623	--	1.466	1.264	1.080	2.085	1.809
798	--	1.464	1.263	1.079	2.089	1.812
973	--	1.466	1.268	1.082	2.089	1.811
1148	--	1.466	1.268	1.082	2.089	1.811

Table 4. Mean copper metal particle diameter of synthesis gas exposed catalysts as a function of calcination temperature

Calcination temperature (K)	Mean copper particle diameter (nm)
623	9.5
798	12.4
973	17.6
1148	22.9

reoxidized catalysts indicated that a portion of the copper metal was oxidized to cupric and cuprous oxide. As qualitatively observed in Figure 3, the amount of copper reoxidized decreased with increasing calcination temperature of the catalyst. The d-spacings of the spinel were the same as those observed for the synthesis gas treated catalysts (see Table 3).

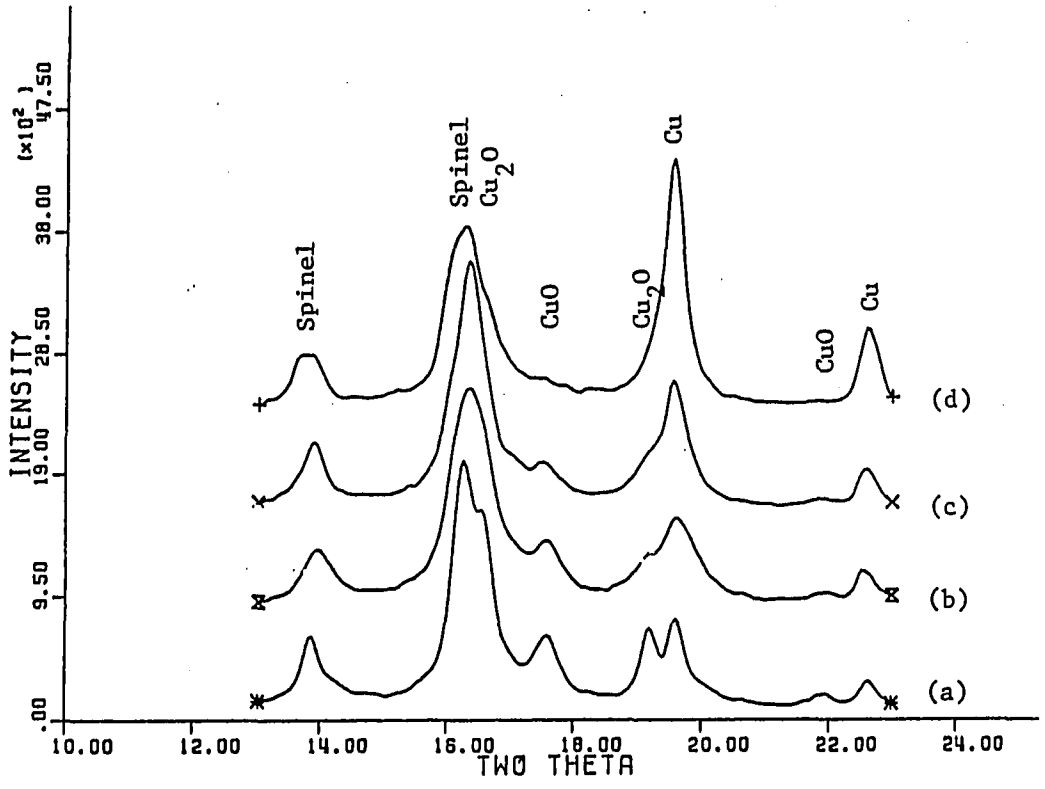

Figure 3. Powder X-ray diffraction patterns of calcined catalysts after reduction and exposure to air:

(a) calcined at 623 K

(b) calcined at 798 K

(c) calcined at 973 K

(d) calcined at 1148 K

X-ray Photoelectron Spectroscopy

X-ray photoelectron spectroscopy results for the samples prepared at the lowest and highest calcination temperatures are summarized in Table 5. Results are reported for catalysts after calcination, reduction, and synthesis gas exposure. Catalysts prepared at intermediate calcination temperatures had similar results.

Potassium exhibits very little chemical shift so that no information concerning its chemical state can be deduced. The intensity of the potassium signal was observed to be very strong. Since only a minor amount of potassium was incorporated into the catalysts, the strength of the signal indicates that the catalyst surfaces are enriched in potassium. The citrate complexation method is known to cause the formation of potassium carbonate (17). However, inspection of the C-1s spectra revealed no carbonate formation in the copper-cobalt-chromium catalyst system. In addition, inspection of the C-1s spectra of calcined or synthesis gas exposed catalysts provided no evidence of any metal carbide formation.

The chromium binding energies given in Table 5 are typical of Cr^{+3} species (22). Chromium trioxide, the metal salt used to form the catalyst precursor, is a strong oxidizer and the reduction of Cr^{+6} to Cr^{+3} was not unexpected. Although chromium(III) oxides are reducible (23), no change in the chromium $2p_{3/2}$ position or peak shape was observed upon hydrogen or synthesis gas exposure which would suggest further chromium reduction at these conditions.

Table 5. X-ray photoelectron spectroscopy results

Calcination temperature (K)	Treatment	Binding energies (eV) K(2p3/2)	Cr(2p3/2)	Co(2p3/2)	Cu(2p3/2)	Cu(α+ hν)
673	calcined	293.0	576.1	780.1	933.8	1851.4
	reduced	293.0	575.9	779.9	932.0	1851.3
	syn-gas	293.1	576.2	780.3	932.0	1851.1
1148	calcined	293.0	576.0	779.9	933.7	1851.4
	reduced	293.0	576.0	780.0	931.9	1851.3
	syn-gas	293.2	576.4	780.0	932.2	1851.1

The cobalt binding energies shown in Table 3 are typical of Co^{+2} or Co^{+3} species (22). The difference in binding energies of Co^{+2}/Co^{+3} species in mixed cobalt oxide compounds, such as spinels, is not great enough to allow differentiation of the two species. No change in peak position was observed for the hydrogen and synthesis gas exposed samples, nor was any shoulder or peak at lower binding energies which could be assigned to fully reduced cobalt species observed. However, the intensity of the Co-$2p_{1/2}$ and Co-$2p_{3/2}$ satellite peaks was found to be much greater for the hydrogen and synthesis gas exposed samples. Frost et al. (24) have observed similar intense satellite peaks for high spin Co^{+2} ions, while diamagnetic Co^{+3} and low spin Co^{+2} ions had much less intense satellites.

In order to evaluate the three oxidation states of copper (0, +1, +2), one must examine both the core emitted photoelectrons and the X-ray induced Auger transitions. Cu^{+2} and Cu^{o}/Cu^{+1} together are distinguished by two peaks in the Cu-$2p_{3/2}$ spectrum. Cu^{+2} species have a binding energy of approximately 933.5 eV and Cu^{o}/Cu^{+} species together have a binding energy of approximately 932.2 eV (22, 25). In addition the Cu-$2p_{3/2}$ spectrum of Cu^{+2} species contains satellite peaks due to shake-up processes. To distinguish the Cu^{o} and Cu^{+} oxidation states, the X-ray induced Auger transitions were examined. Specifically the Auger parameter, α, was calculated. α is defined by:

$$\alpha = KE_{2p_{3/2}} - KE_{LMM}$$

where $KE_{2p_{3/2}}$ is the kinetic energy of the Cu-$2p_{3/2}$ photoelectron line and KE_{LMM} is the kinetic energy of the Cu-$L_3,M_{4,5}M_{4,5}$ Auger transition.

One advantage of the Auger parameter is that sample charging effects subtract out. In general Auger parameters are tabulated as $\alpha+h\nu$, where $h\nu$ is the energy of the excitation source. The value is then independent of the excitation source. Cu^{+} species have $\alpha+h\nu$ values of 1849.4 ± 0.4 eV, while Cu^{o} species have values of 1851.2 ± 0.4 eV.

For the catalysts in this study, the data in Table 3 show that the copper in the calcined catalysts was present as Cu^{+2}. A strong satellite structure was also observed in the calcined catalyst spectra. Upon hydrogen and synthesis gas exposure, the copper was fully reduced to copper metal. There was no indication in the Auger transition of any Cu^{+} species.

Mono- and Bimetallic Catalysts

Reactor studies

The molar composition and the surface areas of the mono- and bimetallic catalysts both after calcination and after synthesis gas reaction are presented in Table 6. As is commonly observed (4, 17), the addition of potassium increased the amount of sintering upon reduction. Chromium containing catalysts had larger surface areas than copper and cobalt alone or mixed. The catalytic behavior of these catalysts is summarized and compared to that for the copper-cobalt-chromium system in Table 7.

As mentioned earlier, unpromoted cobalt is a very active Fischer-Tropsch catalyst. Our results indicated that the activity or selectivity of cobalt was not altered by using the citrate complexation method of preparation. When potassium was introduced, three changes in catalytic

Table 6. Composition and surface areas of mono- and bimetallic catalysts

Molar composition	Surface areas (m^2/g) calcined	used
Co	--[a]	2.36
$CoK_{.032}$	2.18	0.56
Cu	--[a]	2.27
$CuK_{.032}$	1.85	0.76
$CrK_{.032}$	28.3	29.1
$CoCuK_{.064}$	1.30	0.78
$CoCrK_{.064}$	59.4	65.9
$CuCrK_{.064}$	16.0	14.8

[a]Not measured.

behavior were noted. First, the activity decreased by a factor of 5. Second, oxygenates are produced with modest (∿40 wt %) selectivity. Third, the average molecular weight of the product decreased, as reflected by the 37% decrease in α with potassium promotion of cobalt. A comparable decrease in activity has been observed by Fujimoto and Oba (26) for a potassium promoted silica supported cobalt catalyst under similar reaction conditions. However, their data indicate only a small increase, from 10 wt % to 20 wt %, in oxygenate selectivity. The 37% decrease in α observed in our study was surprising. Other studies of the influence of potassium on Fischer-Tropsch cobalt/kieselguhr catalysts found that potassium had little influence on the product selectivity, unlike iron catalysts where α increased with potassium promotion (6). It is possible

Table 7. Catalytic behavior of mono- and bimetallic catalysts[a]

Catalyst	Selectivity (wt %)[b,c]			Product distribution (α)				Activity
	HYD	ALC	ALD	HYD	ALC	ALD	ALL	$\frac{\mu mol\ CO}{m^2\ min}$
Co	100	--	--	.67	--	--	.67	900
$CoK_{.032}$	60	11	29	.46	.39	.36	.42	184
Cu	75	25	--	0	0	--	0	<0.4
$CuK_{.032}$	5	95	--	0	0	--	0	36
$CrK_{.032}$	100	--	--	0	--	--	0	0.03
$CoCuK_{.064}$	54	28	18	.34	.11	.32	.33	23
$CoCrK_{.064}$	100	0	0	.60	0	0	.60	0.7
$CuCrK_{.064}$	1	99	0	0	0	--	0	7.0
$CuCoCr_{.8}K_{.092}$	33	58	9	.46	.43	--	.43	5.8

[a]Steady state, T = 548 K, P = 5 MPA, $H_2/CO = 2$.

[b]Excluding H_2O and CO_2.

[c]HYD = hydrocarbons, ALC = alcohols, ALD = aldehydes, ALL = all functionalities combined.

that potassium simply blocks cobalt sites at the surface which would decrease activity and increase the dispersion of cobalt sites. Bartholomew and Reuel (27) have reported both a decrease in activity and a decrease in the average chain length of the hydrocarbon product with increasing dispersion for unpromoted, supported cobalt catalysts. Only a small increase in oxygenate selectivity was noted. However, their study was conducted at atmospheric pressure and in general the formation of oxygenates from synthesis gas requires 3-10 MPa pressure.

Our study found unpromoted, unsupported, copper catalysts to be inactive for carbon monoxide hydrogenation in agreement with other researchers (8, 28, 29). Surprisingly, the incorporation of potassium resulted in a very active and selective methanol catalyst. Details concerning the promotional effect of potassium on copper may be found elsewhere (17). Briefly, potassium was found to stabilize the formation of Cu^{+} species which have been implicated as active sites for methanol synthesis in other catalytic systems under reaction conditions.

The preparation of a catalyst containing both copper and cobalt yielded a catalyst with characteristics of the individual components, i.e., methanol and a hydrocarbon/aldehyde mixture were produced. The decrease in activity compared to alkali promoted cobalt or copper alone indicated that some interaction between copper and cobalt must be occurring. A 26% decrease in the hydrocarbon chain growth parameter was also observed. Similar decreases in activity and the average molecular weight of the product have been reported for copper introduction onto supported ruthenium Fischer-Tropsch catalysts (30, 31).

A potassium promoted copper-chromium catalyst resulted in an active and selective methanol catalyst. No higher alcohols were observed. However, the level of potassium promotion, temperature, and pressure used in our study are all much less than that used in the work of Tahara, presented earlier. The methanol synthesis rate of the potassium promoted copper-chromium catalyst is a factor of 5 greater than that reported for an unpromoted catalyst with a copper to chromium molar ratio of unity (32). Since our study has found that copper alone is promoted by potassium to produce methanol, the increase in rate may be attributable to this interaction.

Cobalt-chromium oxide catalyst exhibited very low activity and was selective to hydrocarbons. When the reaction temperature was raised above 573 K uncontrollable methanation occurred, probably a result of cobalt metal formation. The similarity of the product distribution of cobalt metal with the cobalt-chromium catalyst suggests that a small amount of segregated cobalt metal is responsible for catalytic activity in the cobalt-chromium system.

X-ray diffraction

The powder X-ray diffraction results for calcined and reduced potassium promoted catalyst samples are summarized in Table 8. No potassium phases were observed in any of the diffraction patterns. This is to be expected considering the low concentrations of potassium used.

For the monometallic catalysts, both cobalt oxide and copper oxide fully reduced to the metals. Cobalt metal forms a mixture of the face centered cubic form and the hexagonal form (α-Co) as has been observed by

Table 8. X-ray diffraction results for potassium promoted mono- and bimetallic catalyst systems

Catalyst	Calcined phase(s)		Reduced phase(s)	
	Major	Minor	Major	Minor
$CoK_{.032}$	Co_3O_4	CoO	Co, α-Cα	--
$CuK_{.032}$	CuO	--	Cu	--
$CrK_{.032}$	Cr_2O_3	--	Cr_2O_3	--
$CoCuK_{.064}$	CoO, CuO	Co_3O_4	Co, Cu	α-Co
$CoCrK_{.064}$	$Co_{1.5}Cr_{1.5}O_4$	--	$Co_{1.5}Cr_{1.5}O_4$	--
$CuCrK_{.064}$	CuO, $CuCr_2O_4$	Cr_2O_3, $CuCrO_2$	$CuCrO_2$, Cu	Cr_2O_3, $CuCr_2O_4$

Hofer and Peebles (33). As was observed in the copper-cobalt-chromium system, chromium(III) oxide did not reduce at the reduction temperatures used in this study.

The cobalt-copper oxide catalyst precursor formed a mixture of the cobalt and copper oxides upon calcination. Cobalt oxide is known to dissolve up to 25 mol % CuO with no change in the cell parameters (34), therefore, mixing of the two phases in the calcined catalyst may have occurred. There was no evidence for the formation of cobalt-copper spinels. These spinels are very sensitive to preparation procedures (20) and apparently do not form using the citrate complexation method of preparation. Upon reduction total phase segregation into Co and Cu metal was observed. Cobalt and copper metal have an extremely limited miscibility region (35) and hence alloy formation is not expected.

The copper-chromium catalyst contained a variety of phases. The reduced catalyst was primarily Cu metal and $CuCrO_2$. The presence of $CuCrO_2$ agrees with previous work (32) where $CuCrO_2$ was shown to be the active phase for methanol synthesis.

The cobalt-chromium catalyst was observed to form a spinel with an equimolar ratio of the two metals. The stability of both the +2 and +3 oxidation states for cobalt allows for the formation of a variety of cobalt-chromium spinels ranging in composition from $CoCr_2O_4$ to Co_2CrO_4. In these spinels octahedral Co^{+3} ions are reported to be in a low spin (diamagnetic) state while tetrahedral Co^{+2} ions are in a high spin state. In Table 9 the d-spacings of the reflection planes for the spinel formed in this study are compared to other cobalt-chromium spinel compositions.

Table 9. d-Spacings for cobalt-chromium spinels

Spinel composition	d-Spacing (Å) (311)	(400)	(511)	(440)	(533)	(731)	Reference
$CoCr_2O_4$	2.512	2.083	1.604	1.473	1.271	1.085	19
$Co_{1.5}Cr_{1.5}O_4$	2.493	2.067	1.592	1.462	1.261	1.077	average[a]
Co_2CrO_4	2.475	2.052	1.580	1.451	1.252	1.069	19
calcined catalyst[b]	2.488	2.064	1.589	1.458	1.259	1.074	this work
reduced catalyst[b]	2.489	2.065	1.592	1.461	1.260	1.077	this work

[a]Based on linearity of unit cell sizes (19).

[b]Composition: $Co_{1.5}Cr_{1.5}K_{.064}$.

The d-spacings for $Co_{1.5}Cr_{1.5}O_4$ were calculated by averaging the values of the d-spacings for $CoCr_2O_4$ and Co_2CrO_4. The use of a linear relationship to calculate the change in d-spacings with increasing cobalt content has been shown to be valid by Bracconi et al. (19). The agreement between the calculated and experimentally determined d-spacings for the equimolar cobalt-chromium spinel is excellent indicating that the citrate complexation preparation method yields a very homogeneous spinel. The spinel was stable under a reducing atmosphere as evidenced by no change in the d-spacings and no observation of additional phases in the diffraction pattern.

DISCUSSION

The powder X-ray diffraction patterns of the calcined copper-cobalt-chromium catalysts indicated the presence of a spinel compound and cupric oxide. This is consistent with the results of Courty and co-workers (2, 15) and of Hino et al. (16) presented earlier. The composition of the spinel is difficult to determine from X-ray diffraction results alone, since as evident from the data in Table 2, the replacement of Co^{+2} ions by Cu^{+2} ions on tetrahedral sites in the spinel has little or no effect on the lattice parameter. Consequently the diffraction pattern of $CuCoCrO_4$, for example, would be identical to that for Co_2CrO_4. However, the composition of the octahedral positions (Cr^{+3} or Co^{+3}) does influence the unit cell size as shown in Table 9. Comparing the d-spacings of the spinel found in the calcined catalysts (see Table 1) with the d-spacings of cobalt-chromium spinels (see Table 9), it is possible to assign a variable composition to the catalyst spinel of:

$$[Cu(II)_xCo(II)_{1-x}][Co(III)_{0.64}Cr(III)_{1.36}]O_4$$

where $0 \leq x \leq 1$. One notes that if $x = 0$ the spinel composition is $Co_{1.64}Cr_{1.36}O_4$. The Co/Cr ratio would be 1.21, which is very close to 1.25, the Co/Cr ratio formulated into the catalyst. For $0 < x \leq 1$, a mass balance dictates that a portion of the cobalt must exist outside of the spinel. However, at all of the calcination temperatures studied, the spinel and cupric oxide were the only phases observed. The possibility of obtaining a poorly crystallized Co oxide phase at a calcination temperature of 1148 K is unlikely. Additionally, cobalt oxide has a very

low solubility in cupric oxide (20), eliminating the possibility of cobalt being incorporated into cupric oxide and not being detected. Hence it is deduced that the spinel found in the calcined catalysts has composition $Co_{1.64}Cr_{1.36}O_4$ with no copper incorporation. The increase in the amount of cupric oxide relative to the spinel (see Figure 2) is interpreted as a decrease in the cupric oxide dispersion, i.e., the cupric oxide becomes more visible as it forms larger particles at the expense of smaller particles.

When the catalyst is reduced and exposed to synthesis gas, two changes in the catalyst occur. First, all of the Cu^{+2} species in the calcined catalyst are reduced to copper metal. There is no evidence from either XPS or XRD of any Cu^{+2} or Cu^{+} species. Since the smallest mean copper particle diameter in the synthesis gas exposed catalysts is 9.5 nm (see Table 4), much larger than the approximately 2.0 nm limit necessary for a particle to be visible by X-ray diffraction, all of the copper in the sample will be observable by XRD. Hence, the XRD copper metal peak area to spinel peak area would be expected to be invariant, as was experimentally observed. The increase in the copper metal particle diameter in the synthesis gas exposed catalysts with increasing calcination temperature reflects a decrease in the dispersion of copper metal similar to that observed for cupric oxide in the calcined catalysts. The decrease in copper metal dispersion with increasing calcination temperature is also indicated by the decrease in reoxidation of copper metal upon exposure of the reduced catalysts to air. Second, cobalt undergoes a partial reduction as indicated by the slightly larger d-spacings for the

spinel in the synthesis gas exposed catalysts (see Table 3) as compared to the d-spacings for the calcined catalysts (see Table 1). Comparison of the diffraction lines of the synthesis gas exposed catalysts to those of the calcined catalyst suggests that the spinel in the calcined catalyst is reduced to $Co_{1.34}Cr_{1.66}O_4$. A mass balance indicates that approximately one-third of the cobalt in the sample is not incorporated into the spinel structure. The increase in the intensity of the cobalt satellite peaks in the X-ray photoelectron spectra is evidence of the reduction of some of the Co^{+3} ions to Co^{+2}. The absence of a clearly defined shoulder or peak in the X-ray photoelectron spectra which could be assigned to cobalt metal indicates that either the cobalt present outside of the spinel is Co^{+2} or, if reduced fully, the cobalt metal formed is not in an appreciable concentration at the catalyst surface. A point of interest is that the cobalt-chromium spinel is partially reduced only upon the addition of copper to the system. A similar phenomenon is observed for Fischer-Tropsch iron catalysts where the addition of small amounts of iron to the catalyst increases the reduction rate of iron oxide (36). As a result, lower reduction temperatures may be utilized. The overall extent of reduction of the cobalt-chromium spinel is not affected by the copper dispersion as evidenced by the invariance of the d-spacings for the reduced catalysts (see Table 3).

The picture of the catalyst which evolves from the above discussion is that in the activated catalyst copper metal is supported on a cobalt-chromium spinel. As an initial evaluation of this hypothesis, a portion of the equimolar cobalt-chromium spinel previously prepared was impregnated with cupric nitrate. The amount of cupric nitrate used was calculated to

yield two monolayers of copper metal. The overall molar composition of the resulting catalyst was $CoCrCu_{.6}K_{.05}$. After impregnation by incipient wetness and drying at 543 K, the catalyst was reduced in diluted hydrogen. No intermediate calcination step was used. The catalytic behavior of the catalyst is compared to that of the spinel and previous results (3) for a $CuCoCr_{.8}K_{.09}$ catalyst prepared via citrate complexation methods in Table 10. While the cobalt-chromium spinel alone did not produce oxygenates, impregnation of the spinel with copper yielded a selectivity to oxygenates of 60 wt %. Furthermore, an increase in catalytic activity is observed indicating that copper plays an active role in the synthesis of oxygenates. This role is further emphasized if the activity data previously reported for the copper-cobalt-chromium catalyst is plotted as a function of the mean copper metal particle diameter of the synthesis gas exposed catalysts as found by XRD (see Figure 4). Oxygenate synthesis is directly related to copper metal dispersion.

The questions to be explored is what is the nature of the component synergism responsible for oxygenate formation. Although their TPR studies indicate otherwise, both Courty et al. (2) and Hino et al. (16) speculated that copper is only partially reduced to copper metal and that a portion of the copper is stabilized as Cu^+ through formation of a copper(I)-aluminum or copper(I)-chromium oxide. The Cu^+ phases, which are known to be active for methanol synthesis (32) and have been shown to form in the copper-zinc oxide (37), copper-chromium oxide (32), and copper-potassium methanol catalyst (17) systems, would then be responsible for termination to alcohols of alkyl chains growing on cobalt metal clusters. Our results

Table 10. Comparison of catalytic behavior of copper impregnated cobalt-chromium spinel[a]

Catalyst	Preparation	Selectivity (wt %)[b,c] HYD	ALC	ALD	Product distribution (α) HYD	ALC	ALD	ALL	Activity $\frac{\mu mol\ CO}{m^2\ min}$
$Cu_{.6}CoCrK_{.05}$	copper nitrate impregnation of $CoCrK_{.064}$	40	58	2	.47	.36	--	.42	1.0
$CuCoCr_{.8}K_{.09}$	citrate complexation	33	58	9	.46	.43	--	.43	5.8
$CoCrK_{.064}$	citrate complexation	100	--	--	.60	--	--	.60	0.4

[a]Steady state, T = 548 K, P = 5 MPa, $H_2/CO = 2$.

[b]Excluding H_2O and CO_2.

[c]HYD = hydrocarbon, ALC = alcohols, ALD = aldehydes, ALL = all functionalities combined.

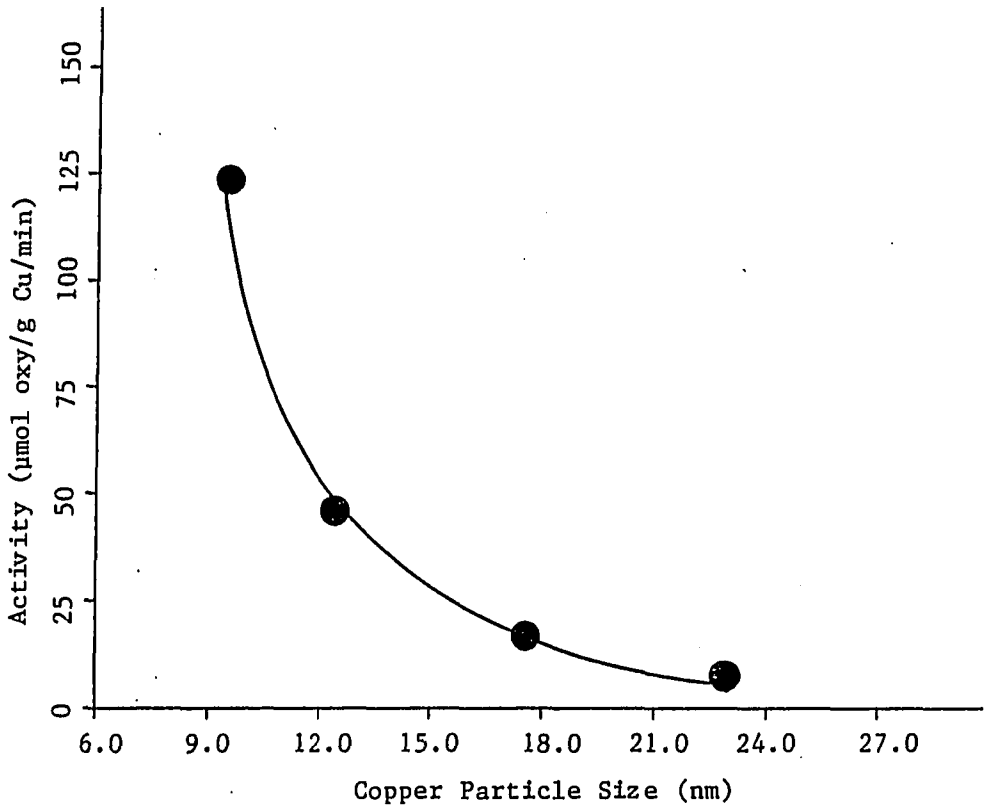

Figure 4. Oxygenate synthesis rate as function of copper metal particle diameter in synthesis gas exposed catalysts

indicate that there is no evidence for the formation of Cu^+ or cobalt metal species at the catalyst surface. Therefore, the previously proposed view of component synergism is improbable.

Small copper-cobalt metal clusters of 1-3 nm diameter, such as those observed on copper-cobalt-aluminum catalysts (2), would most likely be inactive for carbon monoxide hydrogenation as the activity of supported cobalt (27) and ruthenium (38) catalysts is reported to decrease with increasing dispersion. The data of Bartholomew and Reuel (27) indicate that cobalt or alumina is inactive at a dispersion of 17% which corresponds to a mean particle diameter of approximately 4 nm. Similarly, Lin and Pennella (12) have found that cobalt impregnation of copper-zinc-alumina oxide methanol catalysts simply deactivated the active sites for methanol synthesis for cobalt loadings up to approximately 1 wt %. Only when the cobalt loading was increased to greater than 1 wt % did the synthesis of hydrocarbons occur. The selectivity to higher oxygenates never exceeded 20 wt % for any of the various cobalt loadings they studied. The addition of copper to small cobalt metal clusters would depress the cobalt activity even further, as is observed for supported ruthenium-copper catalysts (30, 31). The alkali promoted cobalt-copper catalyst examined in this study indicated no enhancement of higher oxygenate productivity although interaction between copper and cobalt must have been occurring as evidenced by a greater decrease in activity than that due to averaging of the individual components. The formation of a cobalt-chromium spinel, therefore, appears necessary to obtain high oxygenate selectivity.

The modification of copper(I)-chromium oxide methanol sites by potassium is discounted by the results of this study as well since no higher alcohol formation was observed for the alkali promoted copper-chromium catalyst. At the same time the absence of higher oxygenate formation for the potassium promoted copper-chromium oxide catalyst underscores the fact that cobalt appears to be a necessary component for higher oxygenate formation in the copper-cobalt-chromium oxide system.

Copper metal is known to be susceptible to electronic interactions with some supports. Chen et al. (28) found that when copper metal was supported on Cr_2O_3 or ZrO_2, which are p-type semiconductors, the turnover rate for carbon monoxide hydrogenation increased by an order of magnitude over that of bulk copper. The authors proposed that a very localized interaction between copper and the support occurs at the point where the two materials are in contact. It was suspected that the active sites involved the combination of Cu^o and a copper species with electronic structure between Cu^o and Cu^+, induced by the electronic effect of the support. We have observed previously that unsupported copper-lithium catalysts can produce a Flory distribution of hydrocarbons and alcohols (17). The activity of the catalyst was 10 μmol $CO/m^2/min$ comparable to that for the copper-cobalt-chromium system. Unlike other copper-alkali catalysts examined, the copper-lithium catalyst contained copper metal species which appeared by XPS to be electron-rich. In addition, the concentration of Cu^+ species in the copper-lithium catalyst was significantly lower than the other copper-alkali catalysts.

A distinct possibility exists that copper is electronically modified on a potassium promoted cobalt-chromium spinel. A decrease in copper dispersion, i.e., larger particles, as was observed with increasing catalyst calcination temperature, would result in a decrease in the amount of copper/spinel interaction and thus a decrease in catalytic activity. However, no direct evidence was obtained in our study that the electronic state of copper had indeed been altered. The role of oxidized cobalt species in the catalyst system may be to provide further electronic modification of the chromia or else stabilize molecularly adsorbed carbon monoxide at the copper interface (39).

A question which becomes apparent is why does potassium promotion of the cobalt catalyst cause an increase in oxygenate production and would not this interaction be important in the Cu-Co-Cr system? The answer may involve the presence of oxidized cobalt species. These species are speculated to be responsible for the formation of C_2 oxygenates on SiO_2 supported cobalt catalysts modified with Ru and Sr (40). The answer could also involve the role of potassium in a manner similar to that operable in copper-lithium catalysts. In any case, since the alkali promoted copper-cobalt catalyst examined in this study exhibited no increase in selectivity to higher oxygenates above that associated with potassium promoted cobalt, it would appear that the behavior of cobalt-copper-chromium system is not related to the interaction of potassium promoted cobalt species with copper.

SUMMARY

Using powder X-ray diffraction, it has been determined that calcined potassium promoted copper-cobalt-chromium higher alcohol synthesis catalysts of molar composition $CuCoCrK_{.09}$ are comprised of cupric oxide and a spinel of composition $Co_{1.64}Cr_{1.36}O_4$. Upon hydrogen reduction and synthesis gas exposure, cupric oxide is fully reduced to copper metal and the cobalt-chromium spinel is partially reduced to $Co_{1.34}Cr_{1.66}O_4$. X-ray photoelectron spectroscopy results confirmed that copper was fully reduced and cuprous species were present. XPS of the reduced catalysts also indicated an increase in the concentration of high-spin Co^{+2} species and an absence of cobalt metal species at the surface. The absence of both cuprous ions and cobalt metal species excludes the possibility that component synergism is a result of alkyl chains grown on cobalt metal sites interacting with molecularly adsorbed carbon monoxide or cuprous ion sites.

The oxygenate synthesis rate was found to correlate well with the dispersion of copper metal in the catalyst. Poorer copper dispersion and decreased yields of oxygenates were observed with increasing calcination temperature of the catalyst. The picture of the chemical nature of the active catalyst which evolved from the characterization studies is that copper metal is supported on a cobalt-chromium spinel. This view was supported by evaluating the catalytic behavior of a cupric nitrate impregnated cobalt-chromium. Although the cobalt-chromium spinel alone formed only hydrocarbons, the copper impregnated spinel produced 60 wt %

oxygenates. In addition, catalytic activity increased indicating that copper plays an active role in oxygenate synthesis.

Evaluation of the potassium promoted mono- and bimetallic catalysts produced a variety of catalytic behavior. Copper metal, which is inactive for carbon monoxide hydrogenation, was promoted by potassium to render a very active and selective methanol catalyst. Cobalt metal, a traditional Fischer-Tropsch catalyst, produced 40 wt % oxygenates when promoted with potassium. However, a copper-cobalt bimetallic catalyst did not result in an increase in the selectivity to higher oxygenates indicating that formation of a cobalt-chromium spinel is necessary for selective higher alcohol catalysts.

More work is needed to discern the nature of the active site in more detail and understand what the role of copper metal and the cobalt-chromium spinel is in the mechanism for higher alcohol synthesis.

REFERENCES

1. Sugier, A.; Freund, E. U.S. Patent 4 122 110, 1978.

2. Courty, P.; Durnad, D.; Freund, E.; Sugier, A. J. Mol. Catal. 1982, 17, 241.

3. Sheffer, G.; King, T. Submitted for publication in Appl. Catal.

4. Smith, K.; Anderson, R. Can. J. Chem. Eng. 1983, 61, 40.

5. Smith, K.; Anderson, R. J. Catal. 1984, 85, 428.

6. Anderson, R. In Catalysis; Emmett, P., Ed.; Reinhold: New York, 1956; Vol. 4, Chapter 2.

7. Vannice, M. J. Catal. 1977, 50, 228.

8. Klier, K. Adv. Catal. 1982, 31, 243.

9. Apai, G.; Monnier, J.; Hanrahan, M. J. Chem. Soc. Chem. Commun. 1984, 212.

10. Tahara, H.; Tatuki, Y.; Simizu, J. J. Soc. Chem. Ind. (Japan) 1940, 43, 8213.

11. Tahara, H.; Komiyauma, D.; Kodama, S.; Ishibashi, T. J. Soc. Chem. Ind. (Japan) 1942, 45 (supplement), 89.

12. Lin, F.; Pennella, F. In Catalytic Conversions of Synthesis Gas and Alcohols to Chemicals; Herman, R., Ed.; Plenum: New York, 1984; pp. 53-63.

13. Elliott, D.; Pennella, F. J. Catal. 1986, 102, 464.

14. Sibilia, J.; Dominguez, J.; Herman, R.; Klier, K. Preprints of Papers, Division of Fuel Chemistry; American Chemical Society: Washington, DC; 1984, 29, 226.

15. Courty, P.; Marcilly, C. In Preparation of Catalysts III; Poncelet, G.; Grange, P.; Jacobs, P., Eds.; Elsevier: Amsterdam, 1983; pp. 485-519.

16. Hino, T.; Nomura, T.; Kayano, T. Sekiyu Gakkaishi 1984, 27, 257.

17. Sheffer, G.; King, T. Submitted for publication in J. Catal.

18. Joint Committee on Powder Diffraction Standards, file #4-836.

19. Bracconi, P.; Bertnod, L.; Dufour, L. Ann. Chem. (Paris) 1979, 4, 331.

20. Rasines, I. J. Appl. Cryst. 1972, 5, 11.

21. Anderson, J. Structure of Metallic Catalysts; Academic Press: New York, 1975; pp. 365-368.

22. Handbook of X-ray Photoelectron Spectroscopy; Muilenberg, G. E., Ed.; Physical Electronics: Eden Prairie, Minnesota, 1976.

23. Tauster, S.; Fund, S.; Baker, R.; Horsley, J. Science 1981, 221 1121.

24. Frost, D.; McDowell, C.; Woolsey, I. Mol. Phys. 1974, 27, 1473.

25. McIntyre, N.; Rummery, T.; Cook, M.; Owen, D. J. Electrochem. Soc. 1976, 123, 1123.

26. Fujimoto, K.; Oba, T. Appl. Catal. 1985, 13, 289.

27. Bartholomew, C.; Reuel, R. Ind. Eng. Chem. Prod. Res. Dev. 1985, 24, 56.

28. Chen, H-W.; White, J.; Ekerdt, J. J. Catal. 1977, 50, 228.

29. Vannice, M. J. Catal. 1977, 50, 228.

30. Bond, G.; Turnham, B. J. Catal. 1976, 45, 128.

31. Lai, S.; Vickerman, J. J. Catal. 1984, 90, 337.

32. Monnier, J.; Hanrahan, M.; Apai, G. J. Catal. 1985, 92, 119.

33. Hofer, L.; Peebles, W. J. Amer. Chem. Soc. 1947, 69, 897.

34. Delorme, C. Bull. Soc. Franc. Miner. Crist. 1958, 81, 19.

35. Hultgren, R.; Desai, P.; Hawkins, D.; Gleiser, M.; Kelley, K. Selected Values of the Thermodynamic Properties of Binary Alloys; American Society for Metals: Metals Park, Ohio, 1973; pp. 652-655.

36. Roper, M. In Catalysis in C_1 Chemistry; Keim, W., Ed.; Reidel: New York, 1983; pp. 41-88.

37. Herman, R.; Klier, K.; Simmons, G.; Finn, B.; Bulko, J.; Kobylinski, T. J. Catal. 1979, 56, 407.

38. Kellner, C.; Bell, A. J. Catal. 1982, 75, 251.

39. Fierro, J.; Garcia de la Banda, J. Catal. Rev. - Sci. Eng. 1986, 28, 265.

40. Sugi, Y.; Takeuchi, K.; Matsuzaki, T.; Arakawa, H. Chem. Lett. 1985, 1315.

ACKNOWLEDGEMENTS

The authors gratefully acknowledge the receipt of start-up funds from the Shell Faculty Development Fund. In addition, this work was aided, in part, by a Grant-in-Aid of Research from Sigma Xi, the Scientific Research Society. One of the authors (GRS) wishes to thank the Amoco Foundation for fellowship support. Appreciation is also extended to Dr. Robert Jacobson of Ames Laboratory, for use of X-ray diffraction equipment, and to James Anderegg for assistance in collection of X-ray photoelectron spectra.

SECTION IV: INVESTIGATION OF THE PROMOTIONAL EFFECT OF POTASSIUM ON UNSUPPORTED COPPER CATALYSTS FOR METHANOL SYNTHESIS

ABSTRACT

Unsupported copper metal was inactive for the hydrogenation of carbon monoxide. However, when promoted with potassium, the selective synthesis (>93 wt %) of methanol with high activity was found to occur. Using X-ray photoelectron spectroscopy (XPS), it was determined that under reaction conditions copper exists as a mixture of Cu^{+} and Cu^{o} species. The initiation of catalytic activity correlated with the stabilization of the Cu^{+} species. The chemical state of potassium was determined to be potassium carbonate, the thermodynamically preferred phase under reaction conditions. It was observed that the potassium must be well dispersed on the surface in order for the promotional effect to be imparted. The role of potassium was concluded to be the stabilization of Cu^{+} species, active centers for methanol synthesis.

INTRODUCTION

Audibert and Raineau (1) suspected as early as 1928 that traces of Group IA elements may promote the formation of methanol over copper metal. This suspicion resulted from their observation that copper catalysts prepared by precipitation using alkali hydroxide resulted in the synthesis of methanol, while those precipitated by ammonium hydroxide were inactive. However, when the addition of alkali to ammonium hydroxide precipitated catalysts proved ineffective, the researchers concluded that there was no connection between activity and alkali content. Instead they suggested reduced cupric or cuprous oxide alone renders an active methanol catalyst.

Later Eguchi (2) reported that the addition of trace amounts of alkali to cupric oxide did produce a very active and selective methanol synthesis catalyst. Eguchi found that pure copper oxide that had been reduced was unable to produce methanol under any conditions. The inertness of unsupported copper metal toward carbon monoxide hydrogenation has been recently supported by the work of Klier (3).

Vedage et al. (4) have reported that the incorporation of alkali hydroxides into copper-zinc oxide methanol catalysts improved the synthesis rate. Cesium was found to be the best Group IA promoter with a two-fold increase in rate over the unpromoted catalyst being observed. It was suggested that the role of cesium was to increase the concentration of surface hydroxy groups which react with carbon monoxide to produce intermediate formate species. The formate species were then

reduced by hydrogen to form methanol and regenerate surface hydroxyls (5-7).

In our laboratory we have recently investigated the promotional effect of potassium on unsupported copper catalysts for the hydrogenation of carbon monoxide. We have found that potassium promoted copper catalysts are active and selective methanol synthesis catalysts. In this paper we report the results of the detailed characterization of various potassium promoted catalysts by powder X-ray diffraction (XRD), X-ray photoelectron spectroscopy (XPS), and scanning electron microscopy (SEM) with energy dispersive spectroscopy (EDS). Microreactor studies of the variation in catalytic behavior with potassium promotion are also reported. The purpose of this study was to determine the interaction between potassium and copper responsible for the formation of a methanol catalyst. Specifically, the chemical state of both copper and potassium and the manner by which promotion occurs have been examined.

EXPERIMENTAL

Catalysts were prepared by methods similar to those outlined by Courty et al. (8). Briefly, citric acid was added to aqueous solutions of cupric nitrate and potassium nitrate to yield one gram equivalent of acid per gram equivalent of copper and potassium. The resulting solution was evaporated under vacuum at room temperature to form a thick slurry. The slurry was dried overnight at 353 K. The solid obtained was then calcined at 623 K in air for 4 hours. It was observed that at approximately 473 K the catalyst precursor rapidly decomposed with the evolution of large amounts of heat and gas. The potassium to copper molar ratio of the calcined catalysts was verified by flame emission and atomic absorption spectroscopies.

For purposes of comparison two alternate preparation procedures were used. The first used the same technique as outlined above except that cupric acetate was substituted for cupric nitrate. The second procedure was a direct impregnation of reagent grade cupric oxide with an aqueous solution of potassium carbonate.

All catalysts were tested in a single-pass, fixed bed, flow micro-reactor system outlined in Figure 1. The unit was designed for operation up to 623 K and 15 MPa. Feed gases were H_2 (>99.995%), Ar (>99.995%) and CO (>99.3%) which were further purified with molecular sieve 4A. Gases were metered using Brooks mass flow controllers.

The reaction vessel consisted of a 0.25 m long, type 304 stainless steel tube of 0.0092 m internal diameter. The amount of reaction occurring on the reactor and tubing walls in the system was found to be

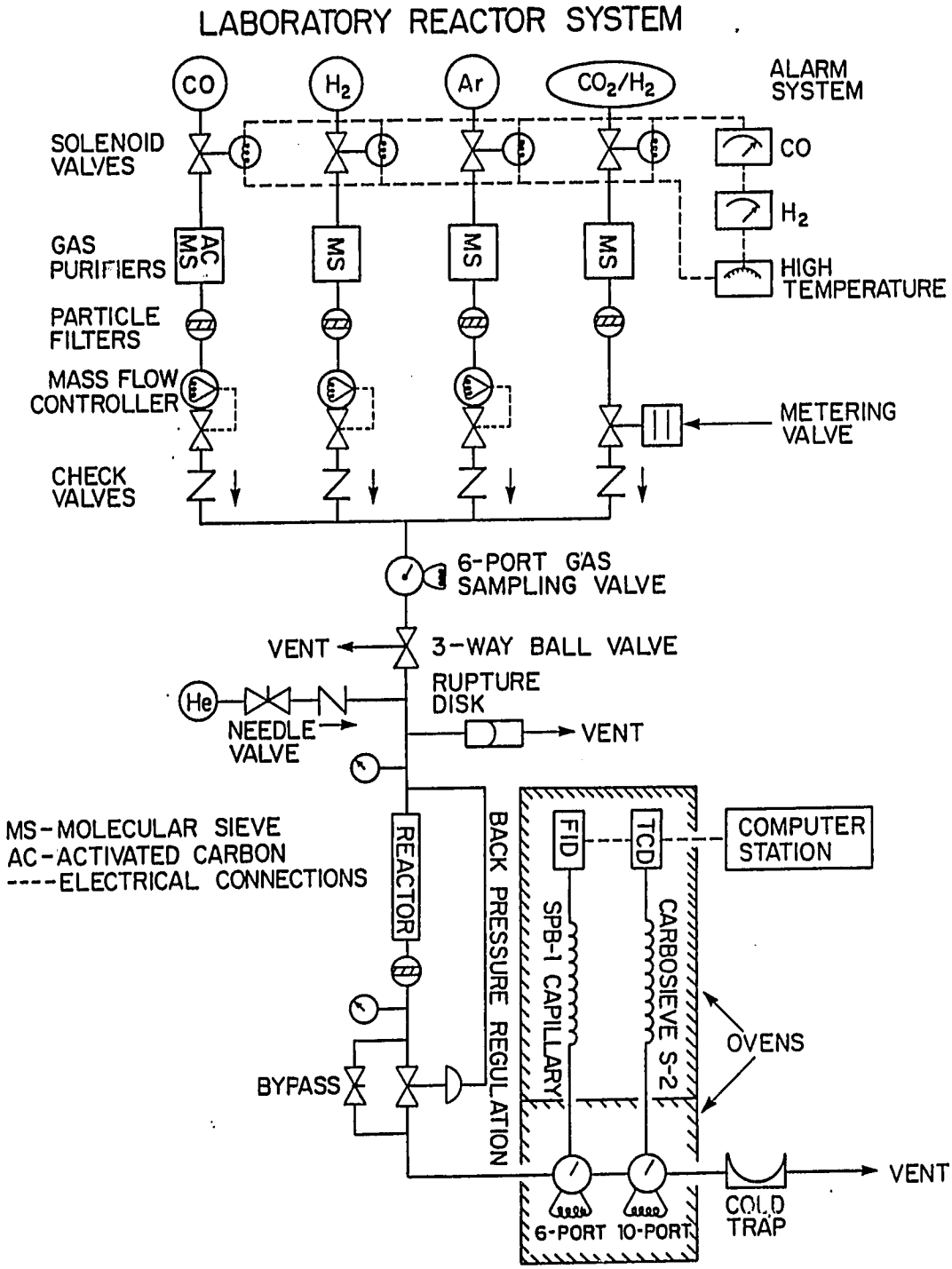

Figure 1. Diagram of high pressure micro-reactor system

negligible by blank runs where the reactor was filled with powdered quartz. An air fluidized aluminum oxide bath regulated by a time proportional controller was used to maintain reactor temperature. The internal reactor temperature was measured by a subminiature thermocouple moved within a stainless steel protection sheath positioned axially in the reactor.

To maintain elevated reactor pressure, an air actuated pressure control valve was placed downstream from the reactor. The controller for the valve sensed the inlet reactor pressure because of condensable products. To minimize reactor pressure drop and avoid internal heat and mass transport limitations, the reactor was loaded with catalyst particles of 0.00013 to 0.00025 m diameter (60/100 mesh).

On-line product analysis was performed by gas chromatography every one hour. Samples were collected at elevated temperature and atmospheric pressure using two gas sampling valves with 0.0005 L sample loops. All post-reactor lines and valves are heated to reaction temperature in order to avoid product condensation. Organic products were separated with a 0.00025 m ID, 30 m long Supelco SPB-1 capillary column operated with a split ratio of approximately 80:1. Ar, CO, and CO_2 were separated on a Supelco S-2 carbosieve column. H_2 and H_2O concentrations were not determined. Organic compounds were detected using a flame ionization detector, while the inorganic compounds were detected with a thermal conductivity cell. Compound sensitivity factors for each detector were established experimentally and were in good agreement with those reported by Dietz (9). Both columns were located in a single oven, which was

ramped from 263 K to 553 K at 10 K/min for maximum product separation. Data were acquired and analyzed with a Spectra-Physics 4000 lab station.

For safe operation the reactor was designed to automatically shut-down if hazardous levels of hydrogen or carbon monoxide were detected or if reactor over-temperature occurred. System over-pressure was protected against by placing a rupture disk assembly at the inlet of the reactor.

All reaction studies employed a $H_2/CO/Ar$ synthesis gas of molar composition 2/1/0.5 at a gas hourly space velocity of 4000 hr^{-1}. Argon served as an internal standard for calculation of activity. Temperature and total pressure were maintained at 548 K and 5 MPa, respectively. Before synthesis gas exposure the calcined catalysts were reduced in situ with a mixture of 10% H_2 in argon mixture at atmospheric pressure and 548 K. With this pretreatment procedure cupric oxide was found by thermal gravimetric analysis to reduce completely to copper metal within 15 minutes. A small temperature gradient (5-10 K) passed quickly through the reactor during pretreatment. No temperature gradient was noted during synthesis gas reaction. Carbon monoxide conversions never exceeded 5 mol % minimizing heat and mass transfer limitations. The equilibrium conversion of carbon monoxide to methanol was calculated to be 37 mol % at 548 K and 5 MPa.

Surface areas of the unsupported catalysts were calculated from multipoint BET adsorption isotherms using Kr at 77 K. Adsorption isotherms were obtained using a Micromeretics 2100E Accusorb surface area analyzer.

Powder X-ray diffraction patterns were obtained with an automated Picker theta-theta diffractometer using MoKα radiation. The step-size was 0.04 degrees per step with a three second per step counting time. Low quartz (α-SiO_2) was used as an internal standard and was mixed with all samples at a 5 wt % concentration. The d-spacing of the (101) reflection was referenced to 3.342 Å.

Scanning electron micrographs were collected using a Joel Model JSM-U3 scanning electron microscope. Energy dispersive X-ray spectra were obtained using a Tracor/Northern 2000 microanalyzer. Samples were mounted on graphite stubs. To insure adequate conductivity of the samples, 300 Å of gold was sputtered onto the samples.

X-ray photoelectron spectra were obtained with an AEI 200B spectrometer using Al Kα radiation ($h\nu$ = 1486.6 eV). Binding energies were assigned by referencing the carbon 1s peak of adventitious carbon to 285.0 eV. Samples were prepared by loading the catalyst into soda-lime glass tubing, performing the appropriate treatment and then evacuating and sealing the tubes. Both hydrogen and synthesis gas treatments were performed at atmospheric pressure. The tubes were transported to and opened in a helium dry box attached directly to the spectrometer. Samples were mounted by pressing the catalyst powder onto indium foil.

RESULTS

Reactor Studies

The surface areas after synthesis gas reaction of the various catalyst compositions tested are given in Table 1. The values are similar to that reported for an unsupported copper catalyst prepared via a copper hydroxy nitrate precursor (3). A decrease in surface area is observed with increasing amounts of potassium promotion. A similar effect has been reported for alkali promotion of copper-zinc oxide catalysts (5, 10). Apparently potassium facilitates catalyst sintering.

Catalytic activity and selectivity for carbon monoxide hydrogenation as a function of potassium content are plotted in Figure 2. The results reported are the values found after the catalyst had been on stream for 10 hours. Methanol was produced immediately upon synthesis gas exposure and the rate varies little over the first 10 hours. Activities were normalized with respect to the surface area of used catalysts. The selectivity to methanol was high (>93 wt %) with methane as the only by-product. As a comparison, cesium promoted copper-zinc oxide synthesis catalysts have selectivities of 99 mol % (7). Only minor amounts of carbon dioxide were observed.

Unpromoted copper was found to be inactive. Addition of only 1.2 mol % of potassium to copper caused the methanol synthesis rate to increase to 8.3×10^{-5} kg/m^2/hr. Interestingly increasing the mole fraction of potassium to 0.26, a 20 fold increase, resulted in an increase in catalytic activity of only a factor of 1.6.

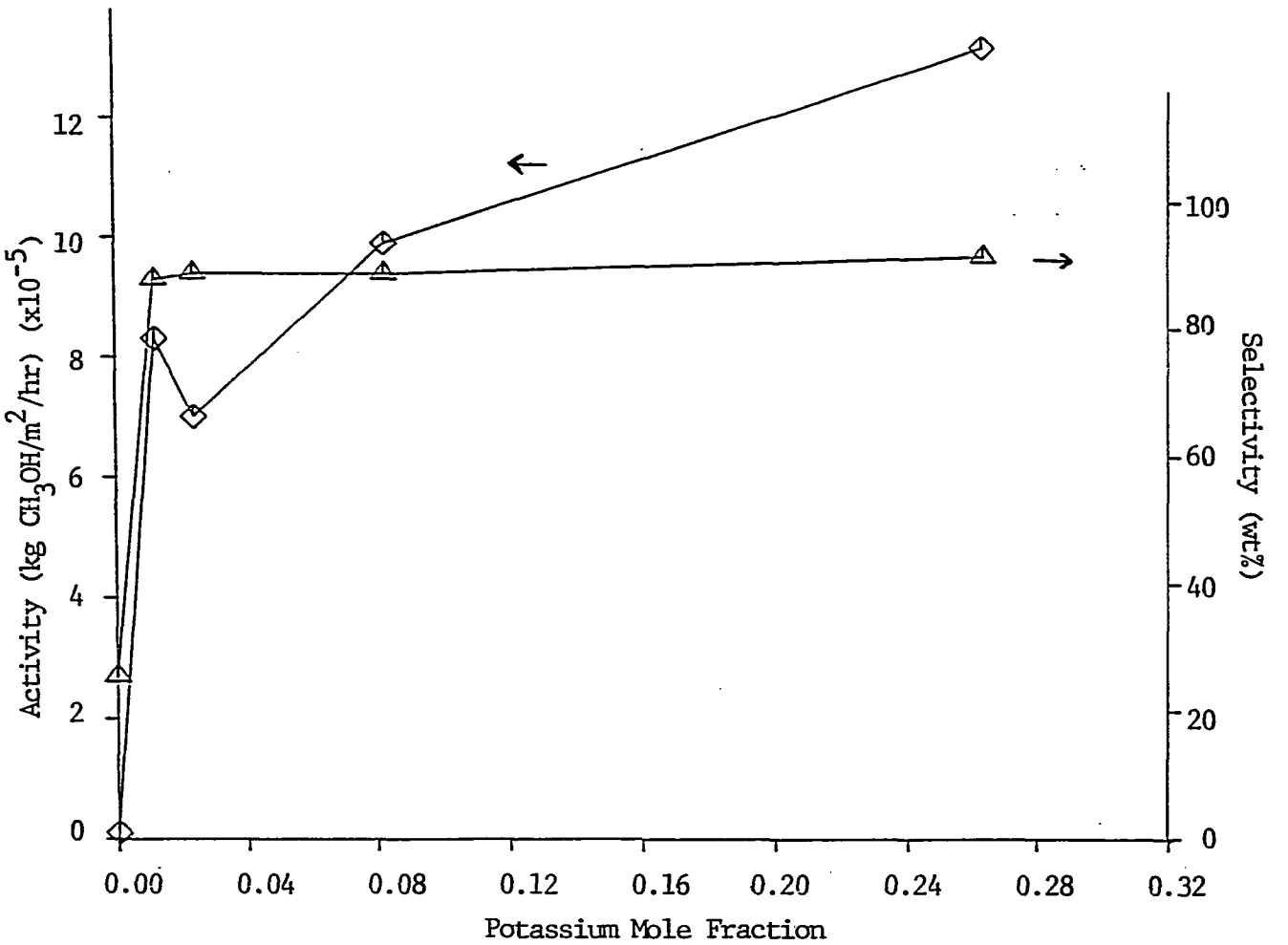

Figure 2. Methanol activity and selectivity of potassium promoted copper catalysts

Table 1. Composition and surface areas of Cu-K catalysts prepared via homogeneous citrate complexes

Molar composition	Mole fraction potassium[a]	Used catalyst surface area (m^2/g)
CuK_0	0	1.22
$CuK_{0.012}$	0.012	0.71
$CuK_{0.025}$	0.024	0.76
$CuK_{0.09}$	0.083	0.89
$CuK_{0.36}$	0.265	0.33

[a]Defined by mol K/(mol K + mol Cu).

In an effort to avoid the rapid decomposition associated with cupric nitrate catalyst precursors, an alternative preparation method substituting cupric acetate for cupric nitrate was studied. Also, to evaluate whether the citric acid complexation preparation method was necessary for the promotional effect of potassium on copper to be imparted, a potassium carbonate impregnated cupric oxide catalyst was examined. The activities of these alternatively prepared catalysts are compared to a cupric nitrate prepared catalyst of similar composition in Table 2.

The cupric acetate prepared catalyst was found to be a factor of 4 less active than the cupric nitrate prepared catalyst. It was noted during preparation of this catalyst that the complete dissolution of cupric acetate was not occurring. The potassium carbonate impregnated

Table 2. Activity of alternate preparations

Molar composition	Used catalyst surface area (m^2/g)	Methanol activity $kg/m^2/hr \times 10^5$
$CuK_{.025}$[a]	0.76	7.0
$CuK_{.032}$[b]	0.63	1.7
$CuK_{.032}$[c]	2.87	4.8

[a]Cupric nitrate preparation of homogeneous citrate complex.

[b]Cupric acetate preparation of homogeneous citrate complex.

[c]Potassium carbonate impregnation of cupric oxide.

cupric oxide catalyst, on the other hand, has activity comparable to that of the cupric nitrate derived catalyst. The cupric oxide used for this preparation was found to be inactive for carbon monoxide hydrogenation. Hence, the promoting effect of potassium may be imparted through simple impregnation as well as the more involved citrate complex preparation previously outlined.

X-ray Diffraction

The powder X-ray diffraction pattern for the used $CuK_{.36}$ catalyst is shown in Figure 3. For comparison, the pattern obtained for copper metal powder mixed with 5 wt % α-SiO_2 is also shown. Even with the large amount of potassium, copper metal was the only observed phase. No potassium phases were detected in the calcined, reduced, or used catalysts indicating the potassium is well dispersed. The d-spacings for the copper

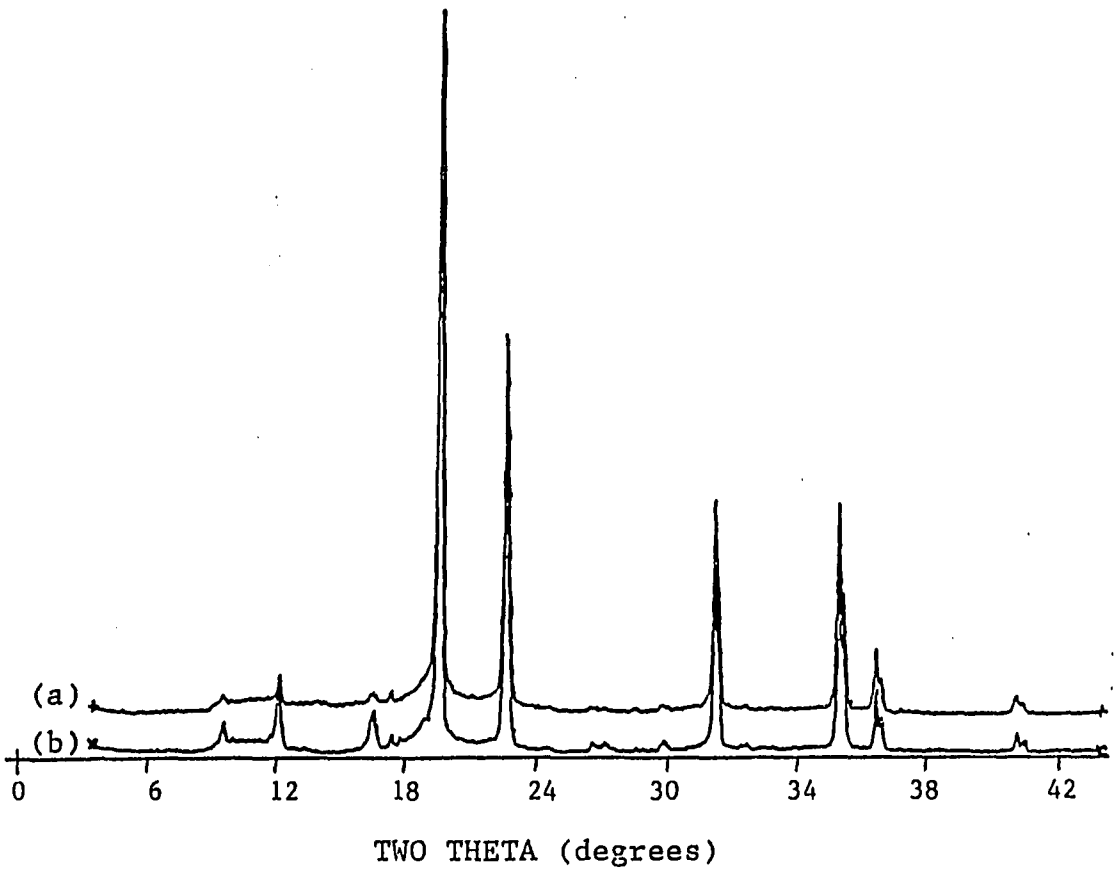

Figure 3. Powder X-ray diffraction patterns:

(a) Reduced $CuK_{.36}$ catalyst

(b) Copper metal powder

metal phase in the catalyst were in excellent agreement with those reported in the literature (11).

X-ray Photoelectron Spectroscopy

X-ray photoelectron spectra of the calcined, reduced, and synthesis gas exposed $CuK_{.36}$ catalyst were collected. The binding energies of the Cu $2p_{3/2}$ photoemitted electrons are given in Table 3. The 933.0 eV binding energy for the calcined catalyst was assigned to Cu^{+2} species (12). The Cu $2p_{3/2}$ photoelectron spectrum of the calcined catalyst was observed to have a satellite peak at 941.2 eV. The appearance of a satellite peak is indicative of Cu^{+2} species (13). The reduced and synthesis gas exposed catalysts were found to have Cu $2p_{3/2}$ binding energies of 931.5 and 931.7 eV, respectively. These peaks were assigned to either Cu^{+} or Cu^{o} species (12). Differentiation of Cu^{+} and Cu^{o} species in XPS is possible only through examination of the $L_3M_{4,5}M_{4,5}$ X-ray induced Auger transitions. Specifically, the difference in kinetic energy of the X-ray induced Auger transition and the $2p_{3/2}$ photoemitted electron is evaluated. This difference is referred to as the Auger parameter, α. Because the kinetic energy of the photoemitted electron is dependent upon the energy of the excitation source, $h\nu$, a modified Auger parameter defined by:

$$\alpha + h\nu = KE_{LMM} - KE_{2p_{3/2}} + h\nu$$

is generally used. KE_{LMM} and $KE_{2p_{3/2}}$ are the kinetic energies of the $L_3M_{4,5}M_{4,5}$ X-ray induced Auger emitted electrons and the $2p_{3/2}$ photoemitted electrons, respectively. The modified Auger parameter is

Table 3. Cu $2p_{3/2}$ binding energies of $CuK_{.36}$ catalyst

Treatment	Binding energy (eV)
calcined	933.0
hydrogen reduced	931.5
synthesis gas exposed	931.7

independent of the excitation energy since $h\nu - KE_{2p_{3/2}}$ is simply the binding energy of the $2p_{3/2}$ photoemitted electron. The advantage of the Auger parameter is that static charge effects subtract out. The X-ray induced Auger transitions for the calcined, reduced, and synthesis gas exposed $CuK_{.36}$ catalyst are shown in Figure 4. The calcined catalyst was found to have one peak at 1850.8 eV, while the reduced and synthesis gas exposed catalysts had two peaks at 1848.8 and 1850.6 eV, respectively. For comparison, the modified Auger parameters of copper(II) oxide, copper(I) oxide, and copper metal are reported to be 1850.9 eV, 1848.9 eV, and 1851.2 eV (14). Cu^{+2} and Cu^{o} are indistinguishable by the Auger parameter. Using the Cu $2p_{3/2}$ spectra, the calcined catalyst has already been interpreted to contain only Cu^{+2} species and the position of the Auger transition is in agreement with that evaluation. The reduced and synthesis gas exposed samples, which the Cu $2p_{3/2}$ spectra indicated to be comprised of either Cu^{o} or Cu^{+} species, had Auger transitions corresponding to both species. Hence, upon hydrogen exposure, the Cu^{+2} species in the calcined catalyst reduced only partially to copper metal with the remainder being stabilized in the Cu^{+} state.

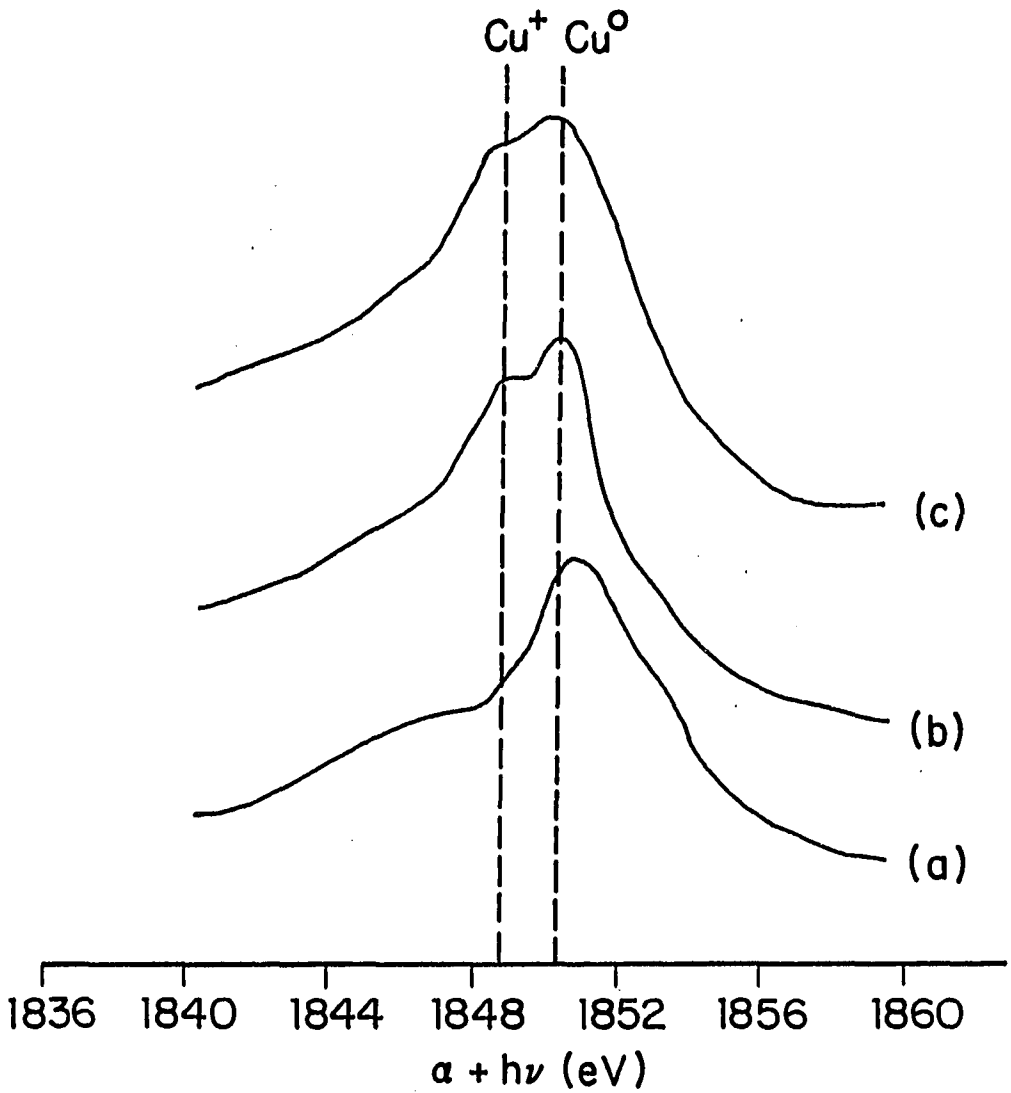

Figure 4. $L_3M_{4,5}M_{4,5}$ X-ray induced Auger transitions for $CuK_{.36}$ catalyst:

(a) calcined

(b) hydrogen reduced

(c) synthesis gas exposed

Synthesis gas exposure did not significantly alter the Auger transitions of the reduced catalyst.

The carbon and potassium X-ray photoelectron spectrum for the reduced $CuK_{.36}$ catalyst is shown in Figure 5. The peaks at 292.9 eV and 296.0 eV were assigned to potassium $2p_{3/2}$ and $2p_{1/2}$ photoemitted electrons, respectively. Unfortunately potassium compounds exhibit very little chemical shift so that information on the chemical state of potassium could not be obtained. The peak at 285.0 is the C-1s reference peak resulting from adventitious carbon. The small peak appearing at 289.2 eV has been assigned to C 1s in a carbonate structure. For comparison, the X-ray photoelectron spectrum of potassium carbonate is also plotted in Figure 5. The similarity of the potassium and carbonate peak intensities suggests that the majority of the potassium in the catalyst may be in the carbonate form. This possibility will be discussed in detail later.

Comparison of Alternate Preparations

The disparity in the methanol synthesis rates of the cupric nitrate and cupric acetate prepared catalysts prompted us to investigate these preparations in further detail. X-ray photoelectron spectroscopy in the Cu $2p_{3/2}$ region revealed only one peak at a binding energy of 931.8 eV for the reduced catalysts. As before, this was assigned to Cu^+ or Cu^o species. The Cu $L_3M_{4,5}M_{4,5}$ X-ray induced Auger transitions for the reduced catalysts are compared in Figure 6. Qualitatively the concentration of Cu^+ species relative to Cu^o was observed to be considerably less for the cupric acetate prepared catalyst. Scanning electron microscopy

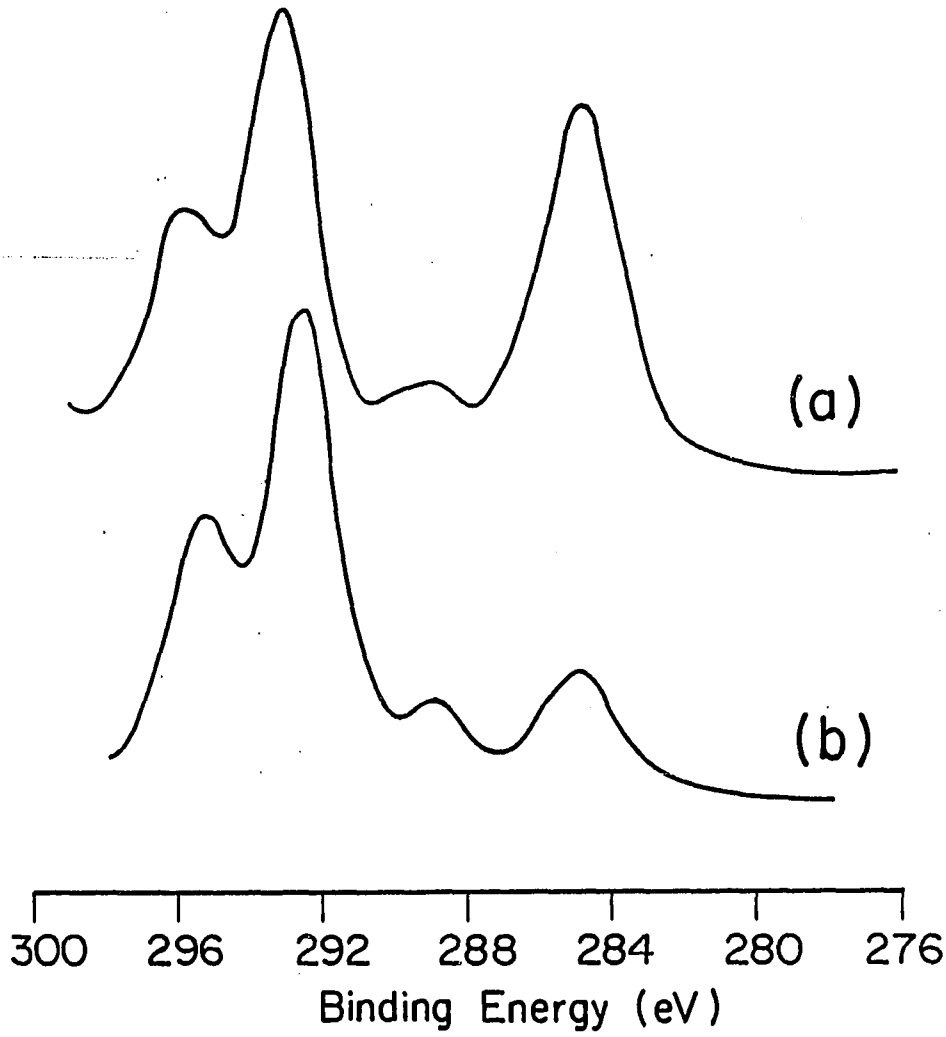

Figure 5.. Carbon and potassium X-ray photoelectron spectra:

(a) $CuK_{.36}$ catalyst

(b) potassium carbonate

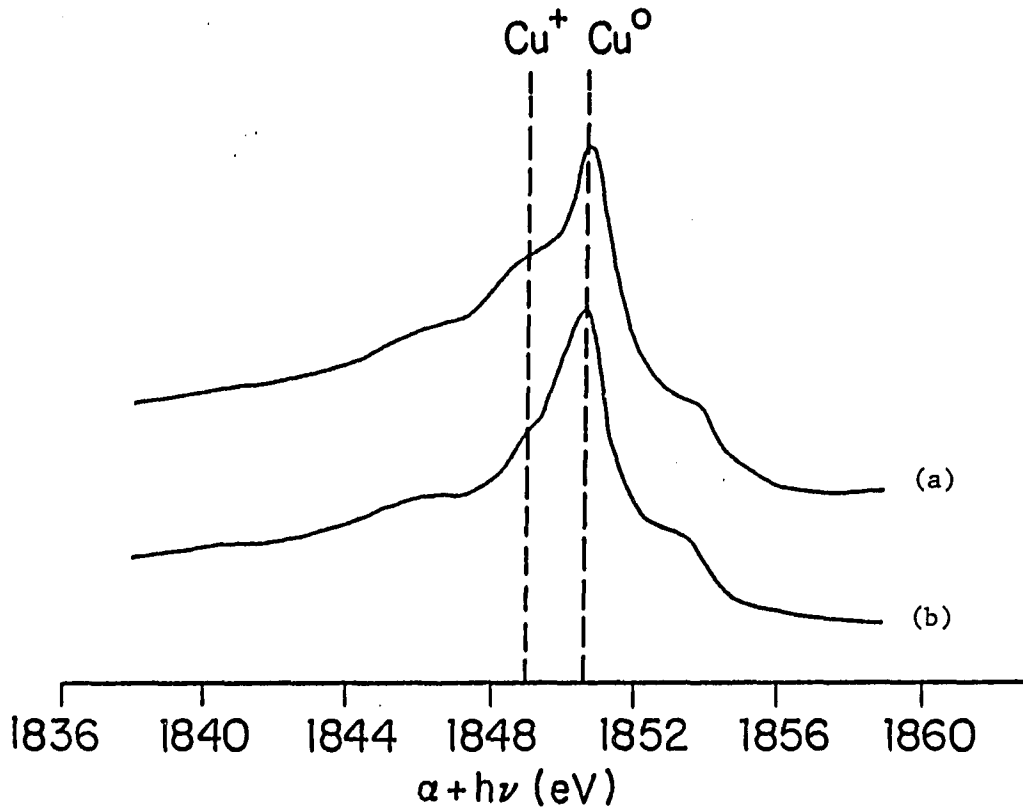

Figure 6. $L_3M_{4,5}M_{4,5}$ X-ray induced Auger transitions for citrate complex prepared catalysts in reduced state:

(a) cupric nitrate precursor

(b) cupric acetate precursor

and energy dispersive spectroscopy of the two preparations revealed distinct differences as shown in Figures 7 and 8. Copper particles in the catalyst prepared with cupric nitrate appear to have small crystallites (75-150 nm) or "warts" dispersed over them. The morphology and energy dispersive spectrum for the copper particle shown in Figure 7 was found to be representative of the entire sample. Although the resolution of energy dispersive spectroscopy does not permit chemical identification of these small crystallites, experiments on alkali promoted silver catalysts have revealed a similar morphology. Using Auger spectroscopy the "warts" on the promoted silver catalysts were determined to be composed of alkali (15). The catalyst prepared from cupric acetate is much different in that it contains patches of a needle structure. Other areas on this catalyst were similar in morphology to the cupric nitrate prepared catalyst. The energy dispersive spectra of the areas with and without the needle clusters indicate that the clusters are enriched in potassium while "needle free" areas have less potassium than for the cupric nitrate prepared catalyst.

Figure 7. Scanning electron microscopy and energy dispersive spectroscopy of reduced cupric nitrate prepared catalyst:

(a) scanning electron micrograph

(b) energy dispersive spectrum

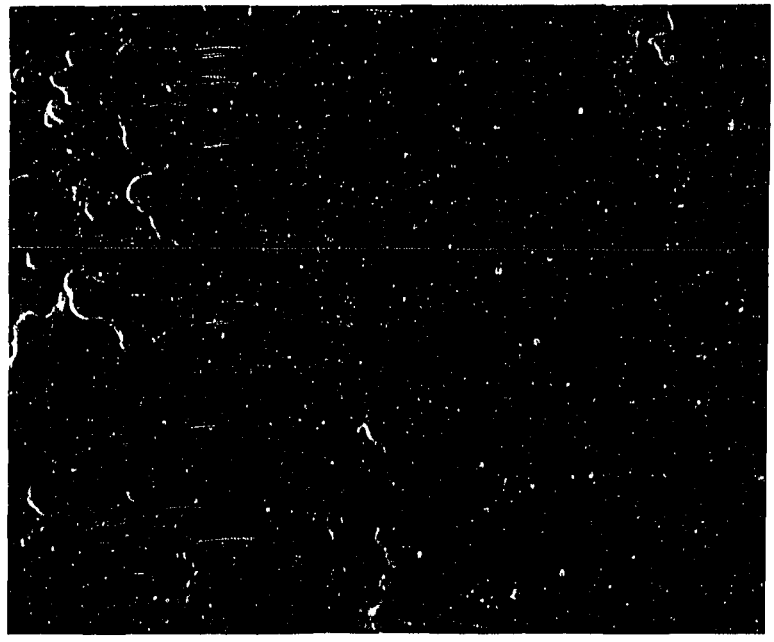

5 μ

(a)

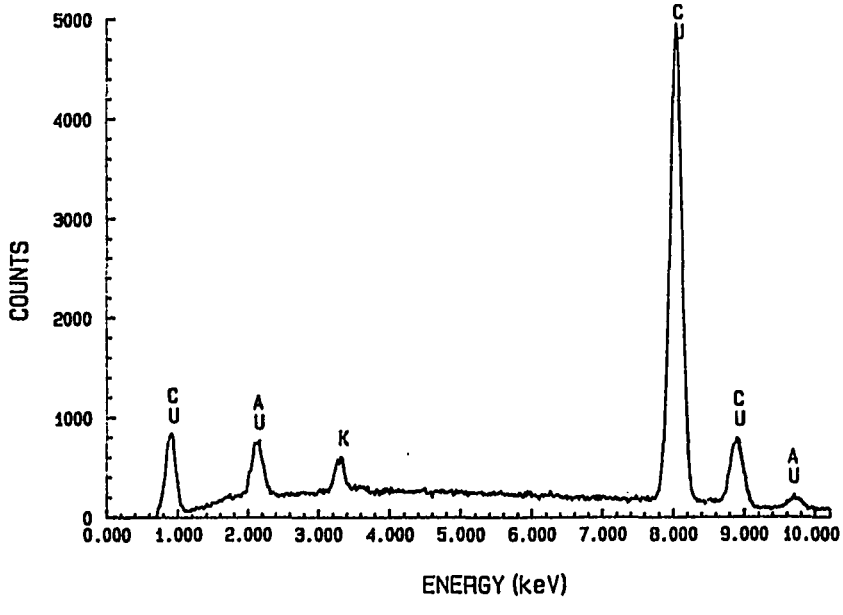
5000
4000
3000
2000
1000
0
COUNTS
CU
AU
K
CU
CU
AU
0.000
1.000
2.000
3.000
4.000
5.000
6.000
7.000
8.000
9.000
10.000
ENERGY (keV)

(b)

Figure 8. Scanning electron microscopy and energy dispersive spectroscopy of reduced cupric acetate prepared catalyst:

(a) scanning electron micrograph

(b) energy dispersive spectrum collected in area of needle clusters

(c) energy dispersive spectrum collected in area away from needle clusters

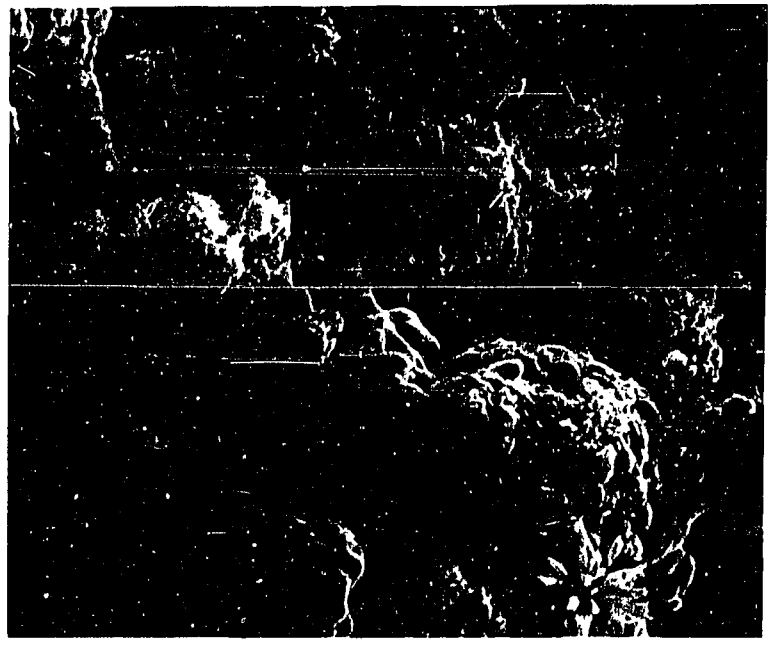

5 μ

(a)

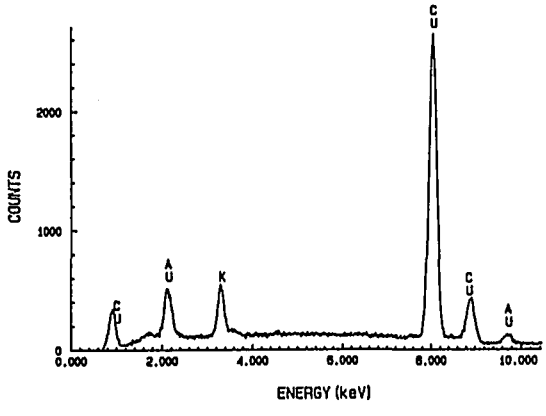
COUNTS
2000
1000
0
0.000
2.000
4.000
6.000
8.000
10.000
ENERGY (keV)
C U
A U
K

(b)

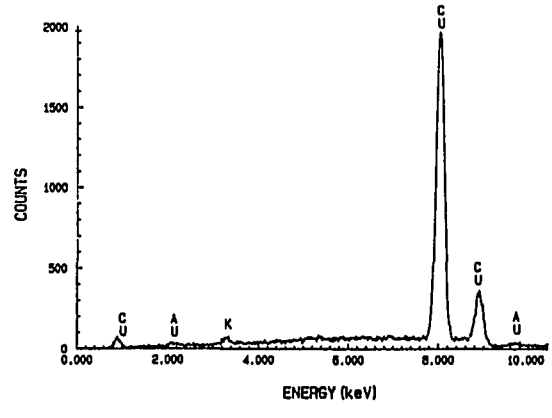
COUNTS
2000
1500
1000
500
0
0.000
2.000
4.000
6.000
8.000
10.000
ENERGY (keV)
C U
A U
K

(c)

DISCUSSION

As expected the unpromoted copper catalyst was inactive for carbon monoxide hydrogenation and no promotion attributable to the preparation technique itself was observed. We evaluated the catalytic behavior of reagent grade potassium carbonate as well and found it too is inactive. Hence, there is truly a synergistic effect involved in the synthesis of methanol on unsupported potassium-copper catalysts.

Nunan and co-workers (7) have reported a methanol synthesis rate of .56 kg/kg cat/hr at 523 K and 7.6 MPa with a synthesis gas ratio of 2.333 using a copper-zinc oxide catalyst impregnated with 0.8 mol % Cs. The methanol synthesis rate was observed to pass through a maximum at the 0.8 mol % promotion amount. Using an activation energy correction of 18.3 kcal/mol (7), a linear total pressure correction (16), and a surface area of 18.8 m^2/g (5), the methanol synthesis rate is 4.4×10^{-5} $kg/m^2/hr$ at the conditions used in our study. This is a factor of two lower than the 8.3×10^{-5} $kg/m^2/hr$ methanol synthesis rate found here for a 1.2 mol % potassium promoted unsupported copper catalyst. In addition we have found no decrease in catalytic activity even with 26 mol % potassium in the catalyst. It is probable that the preparation method used here increases the dispersion of potassium throughout the catalyst and as a result suppresses active site blocking which can occur with impregnation methods where the promoter is distributed only on the surface.

X-ray photoelectron spectroscopy results indicated that the calcined catalyst contains only Cu^{+2} species, which upon hydrogen exposure are reduced to a mixture of Cu^{+} and Cu^{o} species. Since unsupported copper metal was inactive for carbon monoxide hydrogenation, the Cu^{+} species must be responsible for the initiation of catalytic activity observed with the potassium promoted unsupported copper catalysts. Methanol synthesis activity has been correlated with the existance of cuprous ions in copper-chromium oxide catalysts (17) and in copper-zinc oxide catalysts (14, 18) as well. In both cases, the second component stabilizes Cu^{+} species by phase formation. In Cu-Cr oxide, this is achieved by formation of $CuCrO_2$ (19), while in copper-zinc oxide, the Cu^{+} species occupy substitutional and/or interstitial sites in the zinc oxide lattice (17). The mechanism by which potassium stabilizes cuprous ions on unsupported copper catalysts could not be elucidated with the characterization techniques used in this study. In particular, no cuprous or potassium phases were detected in the powder X-ray diffraction pattern even with 26 mol % potassium in the catalyst. If phase formation (between copper and potassium) was responsible for Cu^{+} stabilization, then a literature review suggests only one possibility, KCuO, which has been synthesized by Hestermann and Hoppe (20).

The importance of potassium dispersion in the unsupported copper system is clearly demonstrated by the alternative preparation using cupric acetate in place of cupric nitrate. As the SEM/EDS and XPS data indicate, the concentration of potassium into needle clusters on the surface resulted in a decrease of the amount of Cu^{+} species at the surface

and a subsequent decrease in catalytic activity. The poorer dispersion of potassium in this catalyst was probably a result of the poor water solubility of cupric acetate as noted earlier. The ability to promote methanol synthesis on cupric oxide by potassium carbonate impregnation may suggest that copper on a high surface area support would also be promoted by potassium impregnation. However, we did not evaluate this avenue.

The chemical state of potassium in the unsupported copper catalysts was suggested by XPS to be potassium carbonate. Experimentally we found that potassium citrate, the probable potassium phase precursor when using citric acid complexation preparation methods, decomposed to potassium carbonate when calcined. As noted in the introduction, it has been proposed for alkali promoted copper-zinc oxide catalysts that the rate of methanol synthesis is increased as a result of carbon monoxide reaction with alkali hydroxide to produce alkali formate species which are hydrogenated to methanol. Since the characterization techniques used in our study could neither confirm or discount the presence of potassium hydroxide, thermodynamic calculations were performed to provide further insight into the chemical nature of potassium under synthesis gas conditions. The reactions of interest are:

$$2KOH + CO \rightarrow K_2CO_3 + H_2 \qquad \Delta G^{o}_{573\ K} = -35 \text{ kcal/mol}$$

$$K_2O_2 + CO \rightarrow K_2CO_3 \qquad \Delta G^{o}_{573\ K} = -109 \text{ kcal/mol}$$

$$K_2O + 2CO + 2H_2 \rightarrow K_2CO_3 + CH_4 \qquad \Delta G^{o}_{573\ K} = -96 \text{ kcal/mol}$$

Since the reaction of all other potassium compounds with synthesis gas to form potassium carbonate results in a decrease in free energy, potassium carbonate is the thermodynamically stable phase under synthesis gas at reactor temperature. To confirm the above results, potassium hydroxide was exposed to synthesis gas for 12 hours at 573 K. The product was identified as potassium carbonate by X-ray diffraction and wet chemistry.

Since potassium hydroxide is not stable under synthesis gas conditions, its role in enhancing the methanol synthesis rate by promoting the formation of formate species is doubtful. The results of our work suggest that potassium interacts with copper to increase the concentration of Cu^{+} active sites.

SUMMARY

It has been found that potassium does promote unsupported copper catalysts for the selective synthesis (>93 wt %) of methanol from synthesis gas. The methanol synthesis rate, 8.3×10^{-5} kg/m^2/hr, was twice that of cesium promoted copper-zinc oxide catalysts.

The chemical state of both copper and potassium was investigated. X-ray photoelectron spectroscopy results indicated that the calcined catalysts contain only Cu^{+2} species, which upon hydrogen exposure are reduced to a mixture of Cu^{+} and Cu^{o} species. Since copper metal alone was inactive for carbon monoxide hydrogenation, the initiation of methanol synthesis activity on the promoted catalysts correlated with the stabilization of the Cu^{+} species. It was observed that the potassium must be well dispersed on the surface in order for the promotional effect to be imparted. The chemical state of potassium appeared to be potassium carbonate, which was shown to be the thermodynamically preferred phase under reaction conditions.

Since alkali hydroxides are unstable under reaction conditions, the synthesis of methanol by the hydrogenation of alkali formate intermediates formed through the reaction of carbon monoxide with alkali hydroxide is discounted as being the source of the promotional effect. Instead the promotional effect of potassium on copper is the result of the ability of potassium to stabilize Cu^{+} species upon catalyst reduction.

REFERENCES

1. Audibert, E.; Raineau, A. Ind. Eng. Chem. 1928, 11, 1105.

2. Eguchi, T. Fuel Economist 1936, 11, 417.

3. Klier, K. Adv. Catal. 1982, 31, 243.

4. Vedage, G.; Himelfarb, P.; Simmons, G.; Klier, K. In Solid State Chemistry in Catalysis; ACS Symposium Series 279, American Chemical Society: Washington, D.C., 1985; Chapter 18.

5. Klier, K. Appl. Surf. Sci. 1984, 19, 267.

6. Klier, K. In Catalysis or the Energy Scene; Kaliaguine, S.; Mahay, A., Eds.; Elsevier: Amsterdam, 1984; pp. 439-455.

7. Nunan, J.; Klier, K.; Young, C.-W.; Himelfarb, P. B.; Herman, R. G. J. Chem. Soc., Chem. Commun. 1986, 193.

8. Courty, P.; Durand, D.; Freund, E.; Sugier, A. J. Mol. Catal. 1982, 17, 241.

9. Dietz, W. A. J. Gas Chrom. 1967, 5(2), 68.

10. Smith, K.; Anderson, R. Can. J. Chem. Eng. 1983, 61, 40.

11. Joint Committee on Powder Diffraction Standards, file number 4-836.

12. Handbook of X-ray Photoelectron Spectroscopy; Muilenberg, G. C., Ed.; Physical Electronics: Eden Prairie, Minnesota, 1976.

13. Frost, D.; McDowell, C.; Ishitani, A. Mol. Phys. 1972, 24, 861.

14. Karwaci, E.; Anewalt, M.; Brown, D. M. Preprints of Papers; Division of Fuel Chemistry, American Chemical Society, 1984, 29, 210.

15. Mross, W. D. Catal. Rev.-Sci. Eng. 1983, 25, 591.

16. Agny, R.; Takoudis, C. Ind. Eng. Chem. Prod. Res. Dev. 1985, 24, 50.

17. Monnier, J. R.; Hanrahan, M.; Apai, G. J. Catal. 1985, 92, 119.

18. Herman, R.; Klier, K.; Simmons, G.; Finn, B.; Bulko, J.; Kobylinski, T. J. Catal. 1979, 56, 407.

19. Apai, G.; Monnier, J.; Hanrahan, M. J. Chem. Soc., Chem. Commun. 1984, 212.

20. Hestermann, K.; Hoppe, R. Z. Anorg. Allg. Chem. 1968, 360, 113.

ACKNOWLEDGEMENTS

We gratefully acknowledge the receipt of start-up funds from the Shell Faculty Development Fund. One of the authors (GRS) wishes to thank the Amoco Foundation for fellowship support. In addition we wish to thank Dr. Robert Jacobson (Ames Laboratory) for use of the X-ray diffractometer and Mr. James Anderegg for assistance in X-ray photoelectron spectra collection.

SECTION V: DIFFERENCES IN THE PROMOTIONAL EFFECT OF THE GROUP IA ELEMENTS ON UNSUPPORTED COPPER CATALYSTS FOR CARBON MONOXIDE HYDROGENATION

ABSTRACT

The differences in promotional effect of the Group IA elements on unsupported copper catalysts for carbon monoxide hydrogenation have been examined. Methanol was selectively produced on all catalysts at 523 K, 5 MPa, and with a feed gas of molar composition $H_2/CO = 2$. The methanol synthesis rate increased by an order of magnitude from Li to Cs with the majority of the increase occurring from Na to K. On the basis of apparent activation energy measurements, X-ray photoelectron spectroscopy, and scanning electron microscopy results, activity differences were attributed to differences in the concentration of Cu^+ species at the surface and not electronic effects. The alkali-cuprate LiCuO was determined not to be the active phase responsible for Cu^+ stabilization. Under conditions more favorable for higher alcohol synthesis, 573 K and $H_2/CO = 1$, little change in selectivity was observed for the Na, K, Rb, and Cs promoted catalysts. However, the lithium promoted catalyst produced an equimolar mixture of normal alcohols and hydrocarbons. Both product distributions were found to give linear Flory plots with $\alpha = .3$ for alcohols and $\alpha = .5$ for hydrocarbons.

INTRODUCTION

The ability of potassium to promote unsupported copper for the synthesis of methanol from carbon monoxide and hydrogen has been reported previously (1). The role of potassium was to stabilize cuprous ions under reduction and reaction conditions. The mechanism of the potassium-copper interaction responsible for the formation of cuprous ions was not elucidated. However, phase formation, for example KCuO, was suggested as one possible mechanism for cuprous ion stabilization.

Klier and co-workers have reported that the Group IA elements also promote the synthesis of methanol over copper-zinc oxide catalysts (2, 3). The promotional effect increased monotonically from Li to Cs. At high temperatures and low H_2/CO ratios, the selectivity to higher alcohols was enhanced and increased from 6 wt % for Li to 15 wt % for Cs. At similar promotion levels and reaction conditions, except higher pressure, Smith and Anderson have reported selectivities to higher alcohols as great as 34 wt % for copper-zinc-aluminum oxide catalysts impregnated with potassium carbonate (4). Unlike molybdenum sulfide (5, 6) and copper-cobalt-chromium (7, 8) higher alcohol catalysts where the alcohol distribution is consistent with the Flory equation, alkali promoted copper-zinc oxide catalysts have an alcohol distribution which is better modeled by a chain growth scheme allowing for one to two carbon addition to the growing alcohol at the hydroxylated carbon atom or the carbon atom directly next to it (4). This scheme accounts for the high isobutanol fraction (up to 36%) found in the higher alcohol product. The ability of the Group IA elements to promote the higher alcohol synthesis for

unsupported copper-alkali catalysts under conditions (high temperature, low H_2/CO ratio) favorable for higher alcohol formation has not been previously investigated.

In this study we have examined the difference in promotional effect of the Group IA elements on unsupported copper catalysts. Catalytic behavior was evaluated under both methanol synthesis conditions (523 K, $H_2/CO = 2$) and under conditions more favorable for higher alcohol synthesis (573 K, $H_2/CO = 1$). The chemical nature of the catalyst was probed using X-ray photoelectron spectroscopy, powder X-ray diffraction, scanning electron microscopy, and apparent activation energy measurements. The role of alkali-cuprate compounds, e.g., LiCuO, as active phases in the copper-alkali catalysts was also investigated.

EXPERIMENTAL

Details of catalyst preparation have been reported previously (1). Briefly, catalyst precursors were derived by vacuum evaporation of an aqueous solution of copper nitrate and the appropriate alkali nitrate with citric acid. Copper and alkali concentrations were verified by atomic absorption and flame emission spectroscopies of the calcined catalysts. Surface areas were determined from multipoint BET adsorption isotherms obtained with a Micromeretics 2100E Accusorb instrument using Kr at 77°K as the adsorbate.

Catalysts were evaluated in a single-pass, fixed bed micro-reactor system detailed elsewhere (1). All catalysts were reduced in situ before synthesis gas exposure using a 10% H_2 in argon gas mixture at 523 K and atmospheric pressure. A small temperature rise (10 to 15 K) was noted initially upon hydrogen exposure. Carbon monoxide conversions were less than 10 mol % minimizing heat and mass transfer limitations as well as avoiding methanol equilibrium conditions.

Powder X-ray diffraction patterns were obtained with an automated Picker theta-theta diffractometer using Mo Kα radiation. The step-size was 0.04 degrees per step with a six second per step counting time. Low quartz (α-SiO_2) was used as an internal standard and was mixed throughly with all samples at a concentration of 5 wt %. The d-spacing of the α-SiO_2 (101) reflection was referenced to 3.342 Å. To avoid sample exposure to air after reduction or synthesis gas exposure, a sample chamber utilizing a beryllium window was constructed. The design of the cell is shown in Figure 1. Heating tape was used to heat the samples

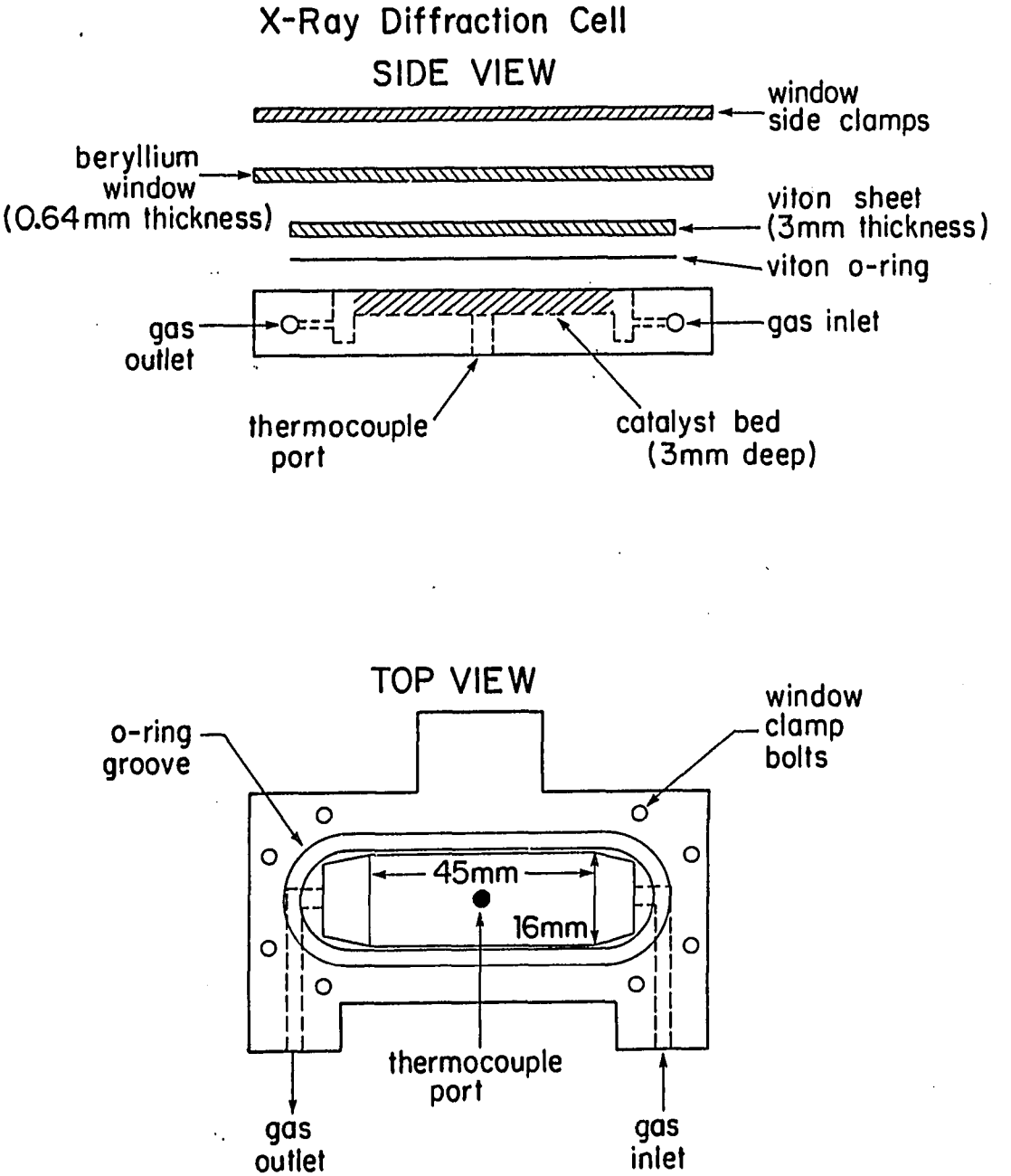

Figure 1. Controlled atmosphere X-ray diffraction cell

to reaction temperatures. To obtain reduced catalyst spectra, 10% H_2 in argon at atmospheric pressure was flowed over the sample for 4 hours. In studies where synthesis gas exposure was performed, the catalyst was first reduced as described above and then a synthesis gas of molar composition $H_2/CO = 2$ was passed over the catalyst at atmospheric pressure for up to 16 hours.

X-ray photoelectron spectra were obtained with an AEI 200B spectrometer using Al Kα radiation. Binding energies of the photoemitted electrons were assigned by referencing the carbon 1s peak of adventitious carbon to 285.0 eV. Samples were prepared by loading the catalyst into soda-lime glass tubing, followed by treatment with a 10% H_2 in argon gas mixture at atmospheric pressure and 523 K for 4 hours, and then evacuating and sealing the tubes. The tubes were then transported to and opened in a helium dry box attached directly to the spectrometer.

RESULTS

Catalytic Behavior of Copper-Alkali Catalyst

The mole fraction of alkali relative to copper incorporated in the catalyst and the resulting catalyst surface areas are given in Table 1. Surface areas are reported for catalysts immediately following hydrogen pretreatment and after synthesis gas reaction. Catalyst surface areas are observed to decrease by a factor of 10 from Li to Cs. In addition, significant sintering occurs while the catalyst is on-stream.

The methanol synthesis activity of the copper-alkali catalysts is summarized in Table 2. Synthesis gas of molar composition $H_2/CO = 2$ was used at 523 K and 5 MPa. As reported previously (1) unpromoted copper catalyst is inactive. For promoted catalysts, the selectivity to methanol was greater than 98 wt % in all cases except for Li where the selectivity was 90 mol %. At these conditions, methane and ethanol were the primary by-products with traces of higher hydrocarbons for all catalysts. When expressed per weight of catalyst, the activity differences do not follow any monotonic trend. Additionally, catalysts are observed to lose activity with time on stream until reaching steady state values. However, when the data are compared on a surface area basis, the initial and steady state activities are nearly the same indicating that sintering is fully responsible for the activity decrease observed with time on stream. An order of magnitude increase in the activity when normalized with respect to surface area was found from Li/Na to K/Rb/Cs.

Apparent activation energies for methanol synthesis were evaluated from the Arrenhius plots shown in Figure 2. There is little change in

Table 1. Composition and surface areas of copper-alkali catalysts

Alkali	Mole fraction alkali[a]	Surface area (m^2/g) Fresh	Used
None	0	---[b]	1.22
Li	.40	1.73	1.04
Na	.38	0.78	1.04
K	.25	0.83	0.33
Rb	.30	0.35	0.17
Cs	.30	0.14	0.10

[a]Defined by mol alkali/(mol alkali + mol Cu).

[b]Not measured.

Table 2. Initial and steady state methanol synthesis rates[a]

Alkali	Activity (kg/g cat/hr) x 10^{-5} Initial	Steady state	Activity (kg/m^2/hr) x 10^{-5} Initial	Steady state
None	0	<0.2	0	<0.2
Li	1.7	1.0	1.0	1.0
Na	1.6	1.4	2.0	2.1
K	9.6	5.1	12	15
Rb	4.9	3.1	14	18
Cs	2.6	1.4	18	14

[a]T = 523 K, P = 5 MPa, H_2/CO = 2, GHSV = 4000 hr^{-1}.

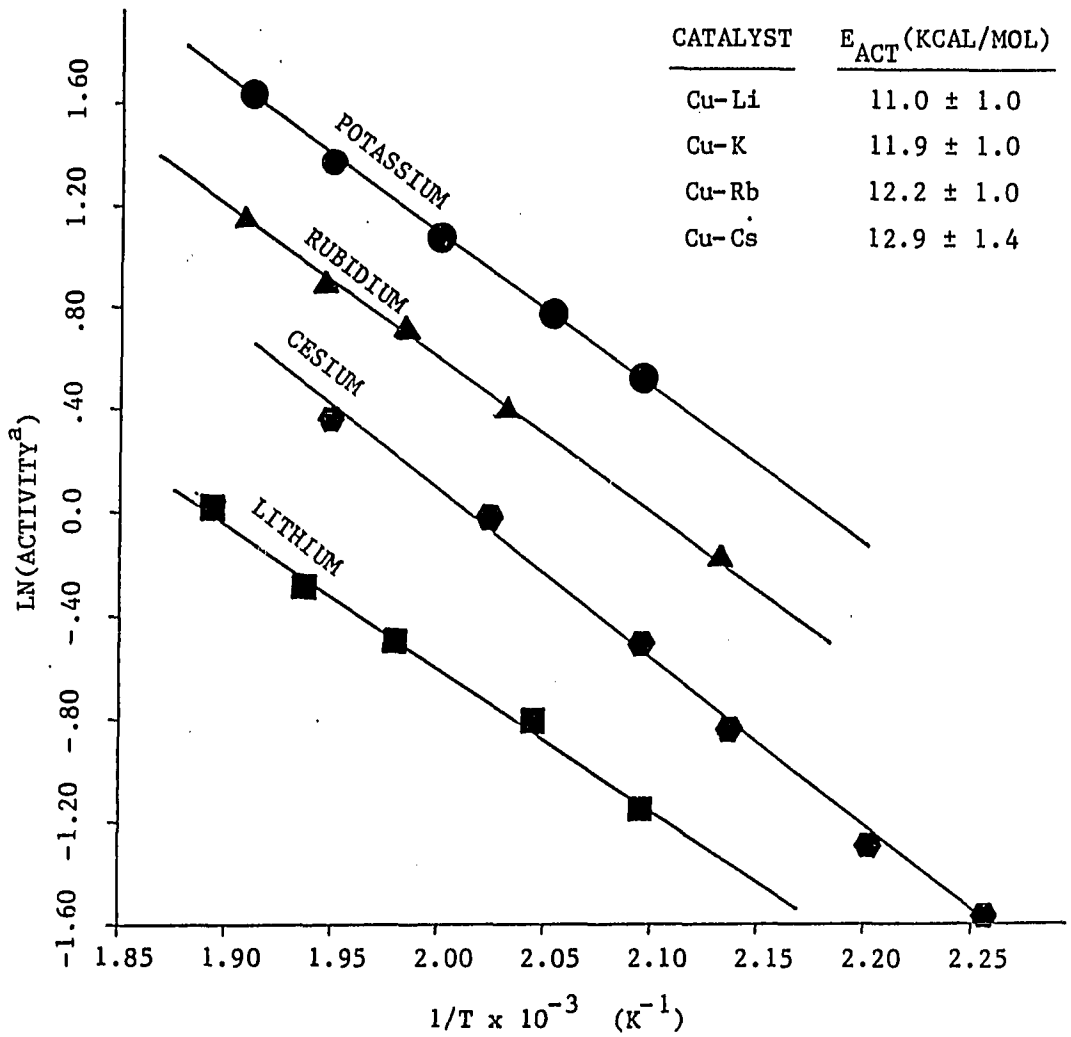

[a]Expressed as KG CH_3OH/G CAT/HR x 10^5.

Figure 2. Arrhenius plots for methanol synthesis on copper-alkali catalysts at 5 MPa and $H_2/CO = 2$

the apparent activation energy from Li, with an apparent activation energy of 11 kcal/mol, to Cs, with an apparent activation energy of kcal/mol. These values are more typical of ones reported for supported Rh (9-11) or Pd (12, 13) catalysts, than of alkali promoted copper-zinc oxides, where a value of 18 kcal/mol has been reported for a cesium promoted catalyst (3).

Increasing the reaction temperature to 573 K and lowering the H_2/CO molar ratio to unity had little effect on the selectivity except in the case of Li where a variety of hydrocarbons and alcohols are observed (see Table 3). Unlike alkali promoted copper-zinc oxide catalysts where significant branching is observed (4), the higher alcohols formed were linear. Moreover, the distribution of both alcohols and hydrocarbons was consistent with Flory theory (see Figure 3). The chain growth probability factors were substantially different with $\alpha = .30$ for alcohols and $\alpha = .53$ for hydrocarbons. When the mole fractions of both functionalities were combined, a chain growth probability factor of .37 was obtained.

Characterization of Copper-Alkali Catalysts

X-ray powder diffraction patterns for the copper-alkali series revealed copper metal to be the only bulk copper phase present. The lattice parameters for the copper metal in the catalyst agreed well with those reported for pure copper metal in the literature (14). A very weak pattern corresponding to the various alkali carbonates was also observed. As we have noted previously for a copper-potassium catalyst (1), the majority of the alkali in the catalyst is invisible to this technique,

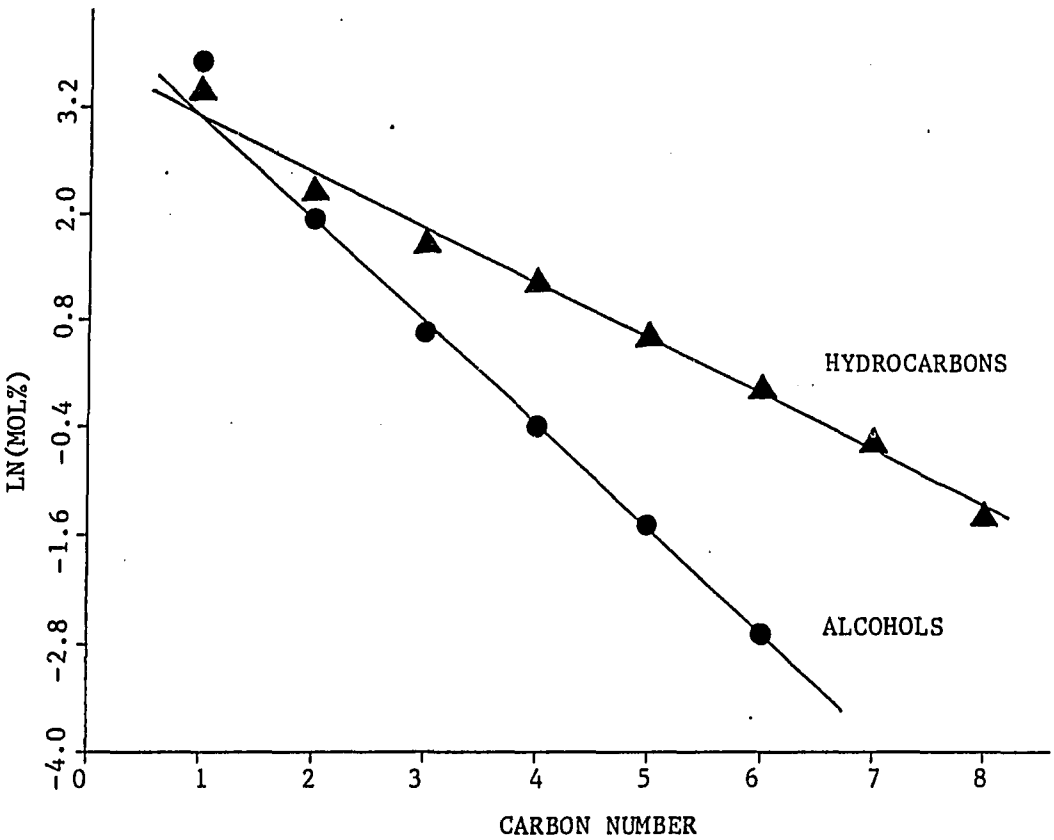

Figure 3. Flory plot of alcohols and hydrocarbons produced on Cu-Li catalyst at 573 K, 5 MPa, and $H_2/CO=1$

Table 3. Activity and selectivity of copper-alkali catalysts under higher alcohol synthesis conditions[a]

Alkali	Activity x 10^{-3} (mol CO/m^2/hr)	Selectivity (mol %) Hydrocarbons		Alcohols		
		C_1	C_2^+	C_1	C_2	C_3^+
Li	0.6	31.1	18.7	40.8	6.9	2.5
Na	0.3	10.6	2.4	87.0	---	---
K	2.3	1.4	---	98.0	0.6	---
Rb	3.5	1.4	0.3	98.2	0.1	---
Cs	9.3	2.2	0.7	96.8	0.4	---

[a] T = 573 K, P = 5 MPa, H_2/CO = 1, GHSV = 4000 hr^{-1}.

indicating that the alkali is in either a micro-crystalline (<20 Å) or an amorphous phase. Scanning electron microscopy coupled with energy dispersive spectroscopy of reduced copper-alkali catalysts revealed no areas of unusually high alkali concentrations such as has been observed with certain preparations of copper-potassium catalysts (1). For each catalyst, the copper to alkali ratio was constant from particle to particle, indicating that good homogeneity of the alkali was accomplished.

In order to evaluate the chemical state of copper at the surface, X-ray photoelectron spectroscopy of reduced catalyst samples was performed. The use of reduced catalysts instead of synthesis gas treated samples is justified by the excellent initial activity of the catalysts. Examination of the Cu $2p_{3/2}$ region revealed only one peak at a binding energy of 931.5 eV for the Na, K, Rb, and Cs catalysts and

at 930.3 eV for the Li promoted catalyst. The Cu $2p_{3/2}$ peak had no satellite structure and was assigned to Cu^+ or Cu^o species. Differentiation of Cu^+ or Cu^o species was performed by examination of the positions of the $L_3M_{4,5}M_{4,5}$ Auger transition relative to the Cu $2p_{3/2}$ position. Figure 4 is a plot of the $L_3M_{4,5}M_{4,5}$ region for the copper-alkali series. The abscissa of Figure 4 is referred to as the modified Auger parameter (15) and is defined by:

$$\alpha + h\nu = KE_{LMM} - BE_{2p_{3/2}}$$

α, the Auger parameter, is the difference of the kinetic energy of the LMM Auger transitions (KE_{LMM}) and the kinetic energy of the $2p_{3/2}$ photoemitted electron ($KE_{2p_{3/2}}$). The addition of $h\nu$, the excitation energy, to α allows for the modified Auger parameter to be independent of the excitation energy since $h\nu - KE_{2p_{3/2}}$ is simply the binding energy of the $2p_{3/2}$ photoemitted electron. The advantage of using Auger parameters is that static charging effects subtract out. The peaks at 1848.8 eV and 1850.6 eV correspond to Cu^+ and Cu^o species, respectively. The extra peak at 1853 eV for the sodium promoted catalyst is the Na KL_1L_1 Auger transition. Qualitatively, the concentration of Cu^+ relative to Cu^o appears to be lower for the Li and Na catalysts than the Cs, Rb, and K catalysts.

The presence of carbonate species was also detected in the C-1s spectra. The binding energies of the C-1s line for the catalysts are listed in Table 4. The 289.7 eV value for the copper-sodium catalyst agrees well with that reported for sodium carbonate (16). The binding

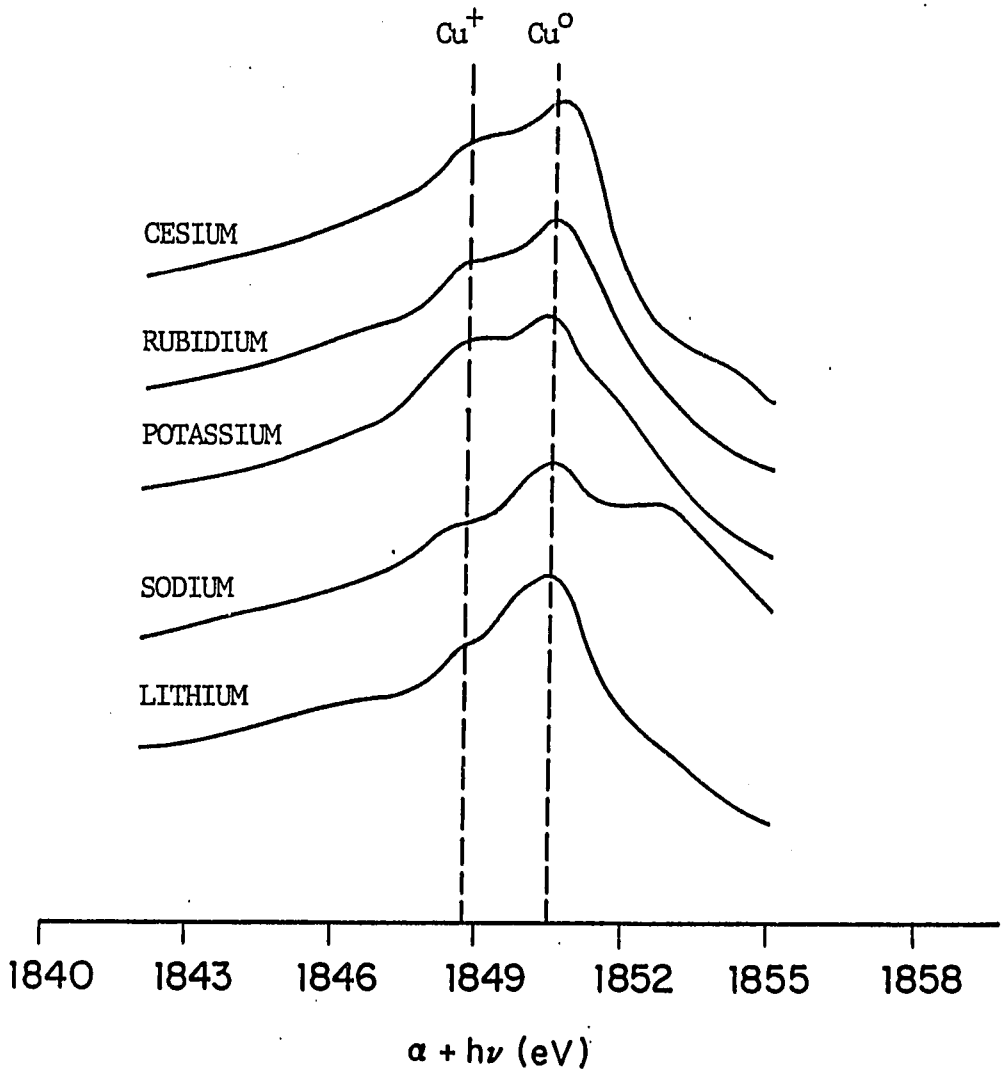

Figure 4. $L_3M_{4,5}M_{4,5}$ X-ray induced Auger transitions for reduced copper-alkali catalysts

Table 4. C-1s binding energies of carbonate species in copper-alkali catalysts

Alkali	C-1s binding energy (eV)
Li	291.4
Na	289.7
K	289.2
Rb	289.0
Cs	288.9

energy of carbon decreased descending from Li to Cs as was expected since the basicity of alkali compounds increases from Li to Cs.

Preparation and Characterization of LiCuO

One possible phase that accounts for the formation of cuprous ions in copper-alkali catalysts is that of alkali-cuprate oxides which have been synthesized and characterized by Hestermann and Höppe (17), Hoppe et al. (18), and Klassen and Hoppe (19). In order to understand what role, if any, these compounds may have in the synthesis of methanol, LiCuO was prepared. LiCuO was chosen over the other alkali-cuprate oxides because of the surprising product distribution observed for the Cu-Li catalyst at higher temperatures and a low H_2/CO ratio.

LiCuO was prepared by heating a mixture of Li_2O (Pfaultz and Bauer, 95%) and Cu_2O (Cerac, 99.9%) in quartz tubing under vacuum at 1113 K for 12 hours (20). Ten mol % excess Li_2O was added to the initial mixture. After heating, unreacted Li_2O was removed by washing the

product with anhydrous methanol. The powder X-ray diffraction pattern revealed only LiCuO to be present. LiCuO is yellow and hydrolyzes in air.

The catalytic behavior of LiCuO at 523 K is summarized in Table 5. The selectivity to methanol was 99 wt %. The steady state activity of LiCuO was comparable to that for the Cu-Li catalyst. However, the initial activity was only 15% of the steady state activity suggesting that LiCuO was modified by synthesis-gas exposure. At 573 K and a H_2/CO ratio of unity, the selectivity to methanol was still approximately 99 wt %. To help elucidate the changes in the chemical nature of LiCuO upon synthesis gas exposure, X-ray diffraction was employed. The diffraction patterns shown in Figure 5 were collected in the sample chamber described earlier. The technique used was to pass synthesis gas over LiCuO for 2 hour intervals at atmospheric pressure and 523 K, purge the cell with helium, and then transfer the cell to the diffractometer. At no time are the contents of the cell exposed to the atmosphere. Before synthesis gas exposure, LiCuO was treated with pure hydrogen for 6 hours at 0.1 MPa and 523 K. The diffraction pattern obtained after hydrogen treatment was identical to that for LiCuO except for the small peaks marked "Cu" which were due to copper metal. Overall, LiCuO was relatively stable under a hydrogen atmosphere at 523 K. After 2 hours of synthesis gas exposure, the amount of copper metal increased dramatically. After 16 hours of syn-gas exposure, only a trace of LiCuO remained. Additionally, a small amount of lithium carbonate, denoted by "LC", was found. It is surprising that despite the presence of an

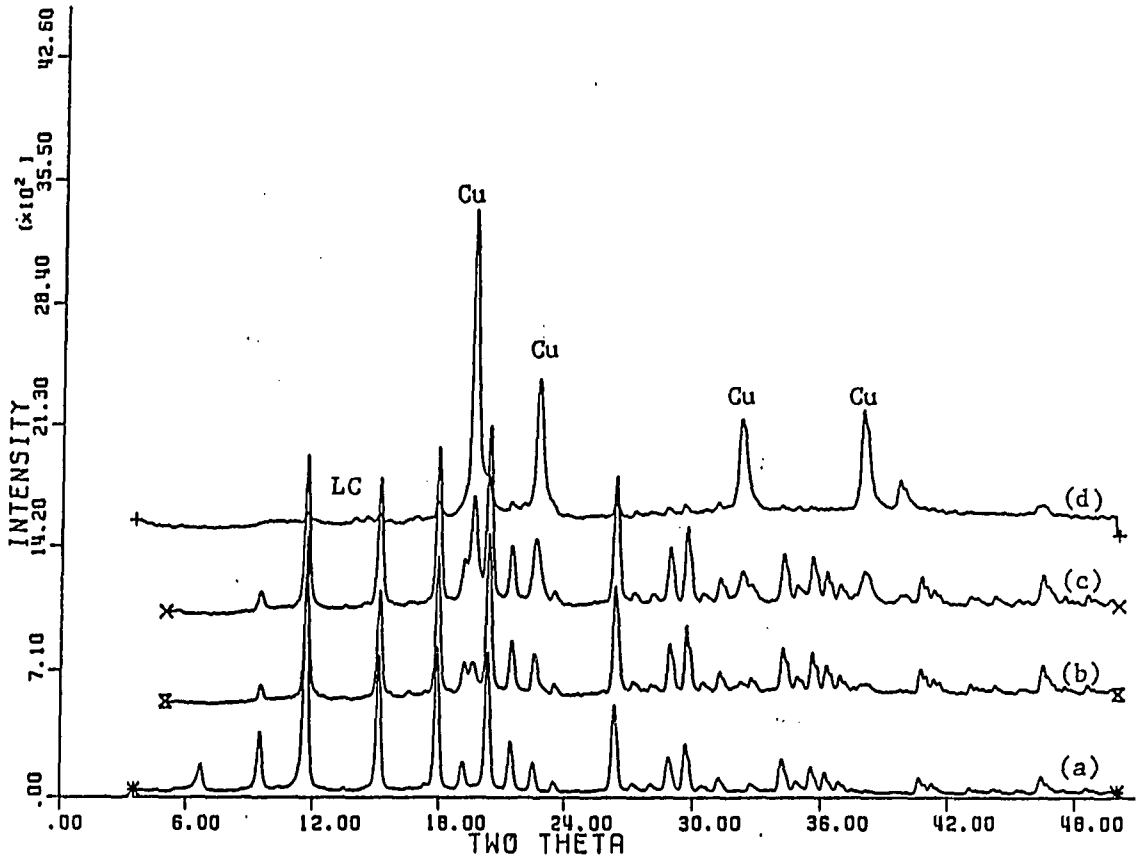

Figure 5. X-ray diffraction patterns of LiCuO after hydrogen and synthesis gas exposure:

(a) no treatment

(b) after 6 hours of hydrogen exposure

(c) after 2 hours of synthesis gas exposure

(d) after 16 hours of synthesis gas exposure

Table 5. Comparison of catalytic behavior of Cu-Li catalysts with CuLiO[a]

Catalyst	Surface area (m^2/g)		Activity ($KgCH_3OH/m^2/hr$)	
	Fresh	Used	Initial	Steady state
Cu-Li	1.73	1.04	1.0×10^{-5}	1.0×10^{-5}
CuLiO	2.32	1.68	0.3×10^{-5}	2.0×10^{-5}

[a] T = 523 K, P = 5 MPa, $H_2/CO = 2$, GHSV = 4000 hr^{-1}.

equimolar amount of lithium to copper, the lithium disappeared from the diffraction pattern in a manner similar to the alkali promoted copper catalysts. The $L_3M_{4,5}M_{4,5}$ X-ray induced Auger spectra of synthesis gas exposed LiCuO was similar to that shown in Figure 4 for the Cu-Li catalyst. The binding energy of the Cu $2p_{3/2}$ emission was 931.7 eV similar to that found for the Na, K, Rb, and Cs promoted catalysts.

DISCUSSION

The methanol synthesis rate on unsupported copper-alkali catalysts was found to increase by an order of magnitude progressively from Li to Cs. Interestingly the majority of this increase occurs from Na to K with the activity of Li and Na promoted catalysts being comparable and that of K, Rb, and Cs promoted catalysts being comparable. The steady state methanol synthesis rate for the K, Rb, and Cs promoted copper catalysts was approximately 15 x 10^{-5} $kg/m^2/hr$ which is a factor of 5 greater than the 3 x 10^{-5} $kg/m^2/hr$ value reported for a Cs promoted copper-zinc oxide catalyst at 523 K, 7.5 MPa, with a synthesis gas of molar composition H_2/CO = 2.3 (3). The apparent activation energies for the catalyst series are only different by 1.9 kcal/mol which is within the limits of experimental error. It is interesting that although the values are within experimental error there is a definite decreasing trend in activation energies from Li to Cs. Vedage et al. (2) have proposed the role of alkali ions in alkali promoted copper-zinc oxide catalysts is to allow for methanol production through hydrogenation of alkali formate intermediates produced by reaction of alkali hydroxide with carbon monoxide. The increase in methanol production from Li to Cs was hypothesized to result from the corresponding increase in basicity. One would expect therefore that if alkali formates were important intermediates in methanol synthesis for the catalysts of interest here, then the activation energy would decrease from Li to Cs. However, if the alkali compounds present in the catalyst were donating electron density to Cu^+ species, presumably the active site in methanol

synthesis (21, 22), to make it more metallic-like than the activation energy would increase. The increasing activation energy found in the work presented here coupled with the presence of Cu^+ species detected via XPS is consistent with this later explanation.

X-ray photoelectron spectroscopy results also indicated that the amount of Cu^+ at the surface is greater for the K, Rb, and Cs promoted catalysts than for the Na and Li promoted catalysts. Since the SEM/EDS results indicated that the alkali is homogeneously distributed throughout the catalyst, the Cu^+/Cu^o ratio is interpreted to be an indication that K, Rb, and Cs are more capable of forming the Cu^+ species than Li and Na. Considering that the increase in activation energy from Li to Cs would decrease the rate of methanol synthesis, the increase in activity from Li to Cs must be attributed to differences in the concentration of active sites and not electronic effects.

The mechanism by which Cu^+ species are stabilized in the catalyst is not known. The poor initial activity and subsequent decomposition of LuCuO upon synthesis gas exposure eliminates alkali-cuprates as possible active phases. The nature of the stabilization of cuprous ions may be suggested by the formation of lithium carbonate as the alkali decomposition product. One could speculate that a mixed metal carbonate, e.g., $LuCuCO_3$, forms. Although literature acknowledgement of alkali-copper carbonates could not be found, the synthesis of alkali-silver carbonates has been reported (23).

The behavior of the Cu-Li catalysts under higher alcohol synthesis conditions (573 K, $H_2/CO = 1$) was quite unexpected. Whereas

alkali-promoted copper-zinc oxide catalysts retain high alcohol selectivity and produce a large fraction of branched alcohols, the Cu-Li catalyst produced a Flory distribution of normal alcohols and normal hydrocarbons more typical of alkali promoted copper-cobalt-chromium oxide catalysts (8). Chen et al. (24) have reported that the activity of copper supported Cr_2O_3 or ZrO_2 for carbon monoxide hydrogenation is a factor of 20-40X greater than that for bulk copper. The withdraw of electron density from copper by the supports, which are p-type semiconductors, was proposed to alter the chemical nature of copper to a state somewhere between Cu^o and Cu^+. In our study, an indication of electron donation to copper from lithium is observed by the 1.2 eV decrease in the Cu $2p_{3/2}$ binding energy. Since alkali carbonates are basic compounds, they would be expected to donate electron density to copper. The increased electron density on copper could increase the chemisorption strength of carbon monoxide resulting in increased carbon monoxide dissociation and Fischer-Tropsch activity. The synthesis of higher alcohols could occur either directly on the electronically modified copper metal sites or by interaction of alkyl chains on those sites with Cu^+ sites stabilized by phase formation.

Two questions become evident from the results reported here. The first is why do the other alkali-copper catalysts not demonstrate the same behavior. One simple explanation is that the increased size of the other alkalis as compared to lithium could lead to increased site blocking. In addition, the other alkalis promote the formation of higher concentrations of Cu^+ species at the surface and consequently the

concentration of copper metal sites is lower. The second question is why was the LiCuO preparation not observed to catalyze the synthesis of higher alcohols and hydrocarbons. Here, the concentration or dispersion of lithium at the surface may play a role especially if the interaction between copper and lithium is localized. Unfortunately lithium is very difficult to observe with XPS and an initial evaluation of surface concentrations could not be obtained.

In any case, the copper-lithium catalyst system will require further investigation to fully understand the interaction of copper with alkali promoters. Initially it would appear that two methods of promotion occur here. The first is phase formation to stabilize Cu^{+} species for methanol synthesis and the second is an electronic interaction resulting in electron donation of copper metal which causes Fischer Tropsch type behavior.

SUMMARY

The rate of methanol synthesis on unsupported copper-alkali catalysts increased by an order of magnitude from Li to Cs with the majority of the increase occurring from Na to K. A 1.9 kcal/mol increase in the apparent activation energy was observed across the series. X-ray photoelectron spectroscopy results indicated the presence of Cu^+ species at the catalyst surface. Activity differences were attributed to differences in the concentration of Cu^+ sites at the surface and not electronic effects.

The alkali-cuprate LiCuO was prepared and investigated with respect to its role as an active phase. The compound exhibited poor initial activity, although steady-state activity was comparable to the Cu-Li catalyst prepared by citrate complexation. X-ray diffraction studies indicated that LiCuO decomposed under synthesis gas to a mixture of copper metal and lithium carbonate. LiCuO as an active phase is discounted and copper-alkali carbonates proposed.

Under higher alcohol synthesis conditions (573 K and $H_2/CO = 1$), the selectivity of the Na, K, Rb, and Cs promoted copper catalysts did not change, but an equimolar mixture of hydrocarbons and alcohols was produced by the Cu-Li catalyst. Both the hydrocarbon and alcohol distributions gave linear Flory plots with $\alpha = .3$ for alcohols and $\alpha = .5$ for hydrocarbons. X-ray photoelectron spectroscopy results indicated that the electron density of copper was greater with lithium as the promoter than the other Group IA elements. Further investigation

will be required to fully understand the interactions between lithium and copper responsible for the synthesis of higher alcohols.

REFERENCES

1. Sheffer, G.; King, T. Submitted for publication in J. Catal.
2. Vedage, F.; Himelfarb, P.; Simmons, G.; Klier, K. In Solid State Chemistry in Catalysis; ACS Symposium Series 279; American Chemical Society: Washington, DC, 1985; pp. 295-312.
3. Nunan, J.; Klier, K.; Young, C.-W.; Himelfarb, P.; Herman, R. J. Chem. Soc., Chem. Commun. 1986, 193.
4. Smith, K.; Anderson, R. Can. J. Chem. Eng. 1983, 61, 40.
5. Quarderer, W.; Cochran, G. European Patent Appl. 0 119 609, 1984.
6. Dianis, W. Appl. Catal. 1987, 30, 99.
7. Sugier, A.; Freind, E. U.S. Patent 4 122 110, 1978.
8. Courty, P.; Durand, D.; Freund, E.; Sugier, A. J. Molec. Catal. 1982, 17, 241.
9. Smith, K.; Jackson, D.; Rigy, S. Appl. Catal. 1984, 85, 428.
10. Chuang, S.; Goodwin, J.; Wender, I. J. Catal. 1985, 95, 435.
11. Gilhooley, K.; Jackson, D.; Rigby, S. Appl. Catal. 1986, 21, 349.
12. Ichikawa, M. Shokubai 1979, 21, 253.
13. Ryndin, Y.; Hicks, R.; Bell, A.; Yermakov, Y. J. Catal. 1981, 70, 287.
14. Joint Committee on Powder Diffraction Standards, file number 4-0838.
15. Gaarenstrom, S.; Winograd, N. J. Chem. Phys. 1977, 67, 3500.
16. Gelius, U.; Heden, P.; Hedman, J.; Lindberg, B.; Manne, R.; Nordberg, R.; Nordling, C.; Siegbahn, K. Phys. Scr. 1970, 2, 70.
17. Hestermann, K.; Hoppe, R. Z. Anorg. Allg. Chem. 1968, 360, 113.
18. Hoppe, R.; Nestermann, K.; Schenk, F. Z. Anorg. Allg. Chem. 1969, 367, 276.
19. Klassen, H.; Hoppe, R. Z. Anorg. Allg. Chem. 1982, 485, 101.
20. Migeon, H.-N.; Zunne, M.; Crleitzer, C.; Courtois, A. J. Solid State Chem. 1976, 16, 325.

21. Herman, R.; Klier, K.; Simmons, G.; Finn, B.; Bulko, J.; Kobylinski, T. J. Catal. 1979, 56, 407.

22. Apai, G.; Monnier, J.; Hanrahan, M. J. Chem. Soc., Chem. Commun. 1984, 212.

23. Papin, G.; Christmann, M.; Sadeghi, N. C. R. Acad. Sci., Ser. C 1977, 284, 791.

24. Chen, H.-W.; White, J.; Ekerdt, J. J. Catal. 1986, 99, 293.

ACKNOWLEDGEMENTS

The authors gratefully acknowledge the receipt of start-up funds from the Shell Faculty Development Fund. One of the authors (GRS) wishes to thank the Amoco Foundation for fellowship support. In addition, we thank Dr. Robert Jacobson (Ames Laboratory) for use of the X-ray diffractometer and James Anderegg (Ames Laboratory) for assistance in the collection of X-ray photoelectron spectra.